UNIVERSITY OF CALIFORNIA SAN DIEGO

Antimalarial Drug Discovery and Target Identification from Phenotypic High-throughput Screening Hits

A dissertation submitted in partial satisfaction of the requirements for the degree Doctor of Philosophy

in

Biomedical Sciences

by

Matthew Abraham

Committee in charge

Professor Elizabeth Winzeler, Chair
Professor Ruben Abagyan
Professor James McKerrow
Professor Victor Nizet
Professor Dionicio Siegel

2020

The Dissertation of Matthew Abraham is approved, and it is acceptable in quality and form for publication on microfilm and electronically:

_____

_____

_____

_____

_____

Chair

University of California San Diego

2020

TABLE OF CONTENTS

LIST OF FIGURES

LIST OF TABLES

LIST OF SUPPLEMENTAL DATASETS

ACKNOWLEDGEMENTS

I would firstly like to thank my thesis advisor Elizabeth Winzeler for providing the opportunity to develop my skills in her lab and for her guidance throughout my career at UCSD. Through those unique opportunities, I was able to combine my passions for biology and high-performance computation to explore a material-field which I found pivotal to my development as a scientist. In this light I must also thank current and former members of the Winzeler lab, namely: Stephan Meister, for a lasting friendship and an introduction to high throughput screening; Gregory LaMonte, for guidance as a mentor and patience with my queries; Annie Cowell and Madeline Luth, for their expertise in genomic sequence analysis; Frances Rocamora, for her molecular biology prowess and encouragement; and the screening members Yevgeniya Antonova-Koch, Korina Eribez, Nimisha Mittal, and Marisa Martino for their weekly support and comradery.

I would also like to thank my colleague Sabine Ottilie, whose wisdom and advice I have found to be invaluable during my graduate training. I am also thankful for the support of several undergraduate research assistants, namely Dylan Hutson and Prianka Kumar, who heightened my efficiency and were a pleasure with whom to work.

I am also deeply grateful for the members of my dissertation committee, including Ruben Abagyan, James McKerrow, Victor Nizet, and Dionicio Siegel. Their patience and generosity with time as well as their constructive feedback about my research has contributed tremendously to my success.

I would also like to thank all of my collaborators for their tremendous contributions which have made this work possible. Thank you to the lab of William Gerwick and his colleague Ariana Remmel for providing the compounds tested in Chapter 1 of this dissertation. Thank you

to Krittikorn Kümpornsin and the lab of Marcus Lee for their expertise in genomic editing which contributed to Chapter 3. Thank you to the lab of David Fidock and in particular Manu Vanaerschot for data in Chapter 2 as well their eagerness to help and prompt contributions both written and experimental. I must also thank Case McNamara and Kerstin Gagaring of Calibr for data contributed to Chapter 2 as well as their willingness to answer my countless questions and for going out of their way to generate or critique the data that is included in Chapter 2.

I am grateful for the various sources of funding that have supported the lab and me. In particular, I would like to thank the Bill and Melinda Gates Foundation for supporting me while I performed work described in Chapter 2, as well as the Medicines for Malaria Venture (MMV) and the National Institutes of Health (NIH) for grants which allowed for the generation and analysis of data included in Chapters 1 and 3.

The often unseen heroes of the UCSD Biomedical Sciences program deserve a special thank you. In particular, Leanne Nordeman and Gina Butcher for their genuine care and willingness to listen to student's concerns.

Finally I would like to thank my family, without whom none of this would be possible. To my parents William and Susan Abraham, thank you for your sacrifice and for risking your lives in the search for freedom so that my brothers and I would be blessed with opportunity. Thank you to my older brothers, Ferdi and George Abraham, for instilling the passion for science and engineering that has led me to this career, and for showing me the beauty and power of brotherhood. To my best friend Bryant Alfaro, your presence was the remedy to much pain, and I cannot thank you enough for spending years with me in San Diego during the course of my PhD training. Lastly, to my dearest love, Deborah, I thank you for your ability to endure, for your

willingness to sacrifice, and for your undying love. Without you, no degree or accolade is worth having.

Chapter 1, in part, contains material that may be prepared for publication at a future time with co-authors including Matthew Abraham, Sabine Ottilie, Stephan Meister, Prianka Kumar, Madeline R. Luth, Ariana Remmel, William H. Gerwick, and Elizabeth A. Winzeler. The dissertation author is the primary investigator and author of the pending manuscript.

Chapter 2, in full, has been accepted for publication for the material as it may appear in the *American Chemical Society Infectious Diseases*, 2020. Matthew Abraham, Kerstin Gagaring, Marisa L. Martino, Manu Vanaerschot, David M. Plouffe, Jaeson Calla, Karla P. Godinez-Macias, Alan Y. Du, Melanie Wree, Yevgeniya Antonova-Koch, Korina Eribez, Madeline R. Luth, Sabine Ottilie, David A. Fidock, Case W. McNamara, Elizabeth A. Winzeler "Probing the Open Global Health Chemical Diversity Library for Multistage-Active Starting Points for Next-Generation Antimalarials" The dissertation author was the primary investigator and author of this manuscript.

Chapter 3, in part, contains material that may be prepared for publication at a future time with co-authors including Annie N. Cowell, Frances Rocamora, Sabine Ottilie, Dylan Hutson, Marcus C.S. Lee, and Elizabeth A. Winzeler. The dissertation author was the primary investigator and author of this manuscript.

VITA

2012 Bachelor of Science, California State University Los Angeles

2020 Doctor of Philosophy, University of California San Diego

2021 (Expected) Pharmacology Doctor, University of California San Diego

PUBLICATIONS

1. Abraham M, Gagaring K, …Winzeler EA. (2020). Probing the open Global Health Chemical Diversity Library for multistage-active starting points for next-generation antimalarials. ACS Infect Dis. 2020 Apr 10;6(4):613-628. doi: 10.1021/acsinfecdis.9b00482

2. Antonova-Koch Y, Meister S, Abraham M, …Winzeler EA. (2018). Open-source discovery of chemical leads for next-generation chemoprotective antimalarials. *Science*. 2018 Dec 7;362(6419). doi:10.1126/science.aat9446

3. Cowell AN, …Abraham M, …Winzeler EA. (2018). Mapping the malaria parasite druggable genome by using in vitro evolution and chemogenomics. *Science*. 2018 Jan 12;359(6372):191-199. doi:10.1126/science.aan4472

4. Delves MJ, Miguel-Blanco C, …Abraham M, et al. (2018). A high throughput screen for next-generation leads targeting malaria parasite transmission. *Nat Commun.* 2018 Sep 18;9(1):3805 doi:10.1038/s41467-018-0577-2

5. Flannery EL, …Abraham M, …Winzeler EA. (2015). Next-generation sequencing of Plasmodium vivax patient samples shows evidence of direct evolution in drug-resistance genes. ACS Infect Dis. 2015 Aug 14;1(8):367-79. doi: 10.1021/acsinfecdis.5b00049

FIELDS OF STUDY

Major Field: Biomedical Sciences, specialization in molecular biology and high throughput drug screening

Studies in Drug Discovery
Professor Elizabeth Winzeler

ABSTRACT OF THE DISSERTATION

Antimalarial Drug Discovery and Target Identification from Phenotypic High-throughput Screening Hits

by

Matthew Abraham

Doctor of Philosophy in Biomedical Sciences

University of California San Diego 2020

Professor Elizabeth Winzeler, Chair

The drive to propagate a species genes is among the strongest biological forces, shared by humans and pathogens alike. For pathogens like *Plasmodium* parasites, the etiological agent of human malaria, self-preservation comes at the cost of hundreds of thousands of human lives annually (WHO R, 2018). Between 2000 and 2016, worldwide cases of malaria were progressively declining (WHO R, 2017). Although there are many causes for the recent increase in global malaria cases, parasite drug resistance is a likely contributor. Thus, research is desperately needed to identify druggable targets and develop novel therapeutics capable of more than symptom alleviation. This dissertation highlights the use of key strategies that have resulted in new preclinical drug candidates, namely the systematic investigation of vast small molecule libraries. In Chapter 1, the investigation of more than 100 marine derived natural products identified six compounds with promising antiparasitic activity and selectivity relative to the host cell. Additionally, this chapter describes the successful target identification of choice screening hits, such as hectochlorin and its newly validated target, actin. In Chapter 2 high throughput screening methods are embraced to explore the activity of nearly 70,000 small molecules, testing them, with collaborators, against all malaria parasite stages that dwell in the human host. Hundreds of these molecules are discovered to have activity against one or more of these stages. Studies in collaboration with Manu Vanaerschot show the target of one such molecule acting within the mitochondrial electron transport chain, against cytochrome bc1. Despite affecting a well-characterized drug target in *Plasmodium*, this target rediscovery legitimizes our strategy for antimalarial hit selection from untested chemical libraries. Because drug target discovery is vital to the development of novel therapeutics, and can guide drug design to minimize the likelihood of off target effects, Chapter 3 describes the search for the target of a potent asexual blood stage (ABS) inhibitor. Here, the protein cytoplasmic isoleucyl-tRNA synthetase (PF3D7_1332900) is

shown as the target of a drug-like scaffold, TCMDC-124553. This protein was previously shown to be critical in *P. falciparum* ABS (Istvan ES et al., 2011), and our data also suggest it is essential in the liver stage of infection as well.

1. Identifying novel chemoprotective antimalarials through phenotypic screening of marine natural products

Abstract

Modern high-throughput phenotypic screens aimed to discover new antimalarials are typically conducted with extensive small molecule libraries designed with iterative synthetic chemistry. This strategy builds an impressive quantity of test molecules, often at the cost of unique structural diversity. Given the prevalence of naturally derived antimalarials and their innate chemical complexity, we tested a 145 compound marine natural product library against the malaria liver stage of infection to identify scaffolds with prophylactic capabilities and limited hepatic cytotoxicity. Three compounds reconfirmed with potent (IC_{50} range 0.308 – 3.05 μM) liver stage activity, and cytotoxicity above the highest tested concentration. Directed evolution and reverse genetic engineering was used to show one of these compounds, hectochlorin, inhibits *S. cerevisiae* and *Plasmodium* by targeting actin. In addition, hectochlorin showed potent ABS (IC_{50} = $1.44x10^{-5}$ μM) activity, but was not effective against mature gametocytes (IC_{50} > 12.5 μM) where actin is least expressed. Although actin is highly conserved across eukaryotes, *Plasmodium* isoforms are among the most different from humans, suggesting refinement of the hectochlorin structure may further limit off-target effects and expose a novel antimalarial pathway.

Introduction

Over the last 37 years, natural products (NP) and their synthetic derivatives have accounted for over half of the newly approved drugs (Newman DJ and Cragg GM, 2016). The ratio of naturally-derived to completely-synthetic antimalarials is even more dramatic, with approximately

2/3 of the clinically recommended therapies having natural origins (Wells TN, 2011). Quinine is a natural product and is the first drug specifically marketed (Achan J et al., 2011) for the treatment of malaria. This natural product was isolated from the cinchona tree, from which indigenous people have made remedies for centuries (Gachelin G et al., 2017). The current gold standard for treating severe or chloroquine-resistant malaria belongs to an endoperoxide family of natural products that includes artemisinin (Guidelines WHOT, 2015). However, since artemisinin (along with derivatives such as artemether and artesunate) was first introduced in the 1980s (Faurant C, 2011), there have been reports of increased parasite clearance time in areas of Southeast Asia (Ashley EA et al., 2014). Thus, new drugs are desperately needed to slow the resurgence of global malaria infection rates (WHO R, 2018), and the success of NP in this field make them a valid starting point.

The therapeutic emphasis of most current antimalarials target the symptomatic ABS of infection. While the treatments directed against this stage undoubtedly save lives, they embody a reactive approach to disease management. This generates a race between the development of new antimalarials and the emergence of drug resistance. Alternatively, prophylactic medicine aimed to prevent malaria liver stage growth in a mammalian host could negate disease progression altogether. The use of high throughput screening techniques has been effective to saturate the pre-clinical pipeline with novel antimalarials, (Hovlid ML and Winzeler EA, 2016), but these methods typically require thousands of individual starting molecules. The current antimalarial drug discovery pipeline contains compounds with activity throughout the parasitic life-cycle (Hooft van Huijsduijnen R and Wells TN, 2018); however, since the introduction of atovaquone in 1992 (Baggish AL and Hill DR, 2002), only derivatives of previously-known antimalarial compounds have been clinically approved.

Marine natural products (MNP) were screened against the malaria liver stage of infection to explore their often overlooked chemoprotective potential. Following a bloodmeal from an infected mosquito, the malaria parasite uses its motility to burrow between epithelial layers to enter the blood stream, then again through channels in the liver before ultimately invading and forming a vacuole within a hepatocyte, where replication can ultimately occur (Frevert U et al., 2005). The mechanism by which sporozoites select their final hepatocellular home is unknown, but during this selection process the parasites forcibly traverse some hepatocytes, killing them in the process (Mota MM et al., 2001). We identify several new natural products which are active in the liver stage, and have limited off-target effects. Further investigation of the lead screening hit, hectochlorin, shows potent liver and ABS activity, the former stemming from an interruption of canonical sporozoite motility. Finally, in collaboration with Sabine Ottilie, Prianka Kumar, Madeline R. Luth, Ariana Remmel, and Wiliam H. Gerwick, we identify ACT 1 as a resistance gene and potentially the target of hectochlorin in *S. cerevisiae.* Genome sequencing and CRISPR/Cas9 editing shows a single amino acid substitution is sufficient to generate measurable resistance.

Results

Marine natural product primary screen

To investigate the causal prophylactic potential of marine natural products, we began by testing 145 compounds against a previously established liver stage malaria model (Swann J et al., 2016). For these studies we utilized the murine species, *P. berghei*. This was selected because of its commercial availability (New York University insectary) and innate safety when contrasted to human-infecting *P. falciparum* sporozoites. Furthermore, luciferase-expressing *P. berghei*

(PbLuc) offers a fast and sensitive endpoint measurement compared to other antibody-dependent high content imaging detection assays (Meister S et al., 2011). With a relatively small compound library, and because our *in vitro* screening assay is optimized for high throughput, inhibition values for the primary screen were averaged across four test wells for each compound in biological duplicate. Potency was normalized to positive and negative controls via atovaquone (5 μM) and DMSO (0.5%), respectively. This yielded a total of 21 compounds with > 70% PbLuc inhibition across both replicates (Supplemental Dataset 1). Natural products that are released by one organism have evolved to indiscriminately harm nearby, competing organisms as there is a constant struggle for limited nutrients (Cutler S et al.;Zhang H et al., 2017). Thus, a large number of these inhibitors were likely to be cytotoxic; preventing *P. berghei* liver stage proliferation by means of host cell injury. In order to identify such false-positive compounds, we concurrently tested the library against uninfected HepG2 cells with otherwise identical methods to the PbLuc assay, whereby hepatocyte viability inhibitors (> 50% signal perturbation) were identified so they could be deprioritized. Unsurprisingly, many of the most potent natural products also negatively affected the hepatocytes, with 18 of the 21 prospective hits inhibiting HepG2 growth by 50% (Supplemental Dataset 1). Those remaining included two compounds proposed to be voltage-gated sodium channel modulators, palmyramide A (Na^+ inhibitor) (Taniguchi M et al., 2010) and hoiamide B (Na^+ activator) (Choi H et al., 2010), and as well as a putative actin filament stabilizer hectochlorin (Marquez BL et al., 2002).

Hit reconfirmation

In order to quantify the potency of our primary screen hits, six hits were picked from the original library plates and diluted in a 12-point titration series (concentrations varied due to molecular mass and compounds originally supplied at 1 mg/mL; see Supplemental Dataset 1).

These included compounds with the highest ratio of PbLuc to HepG2 activity, and which maintained at least 70% PbLuc inhibition. All six of the selected compounds reconfirmed with a PbLuc IC_{50} < 3.05 μM and 3 showed submicromolar potency (Figure 1.1). From these hits, only kalkitoxin, which showed significant HepG2 viability inhibition in the primary screen, reconfirmed cytotoxicity in dose response (HepG2 IC_{50} 0.494 μM). These data show that MNP can kill organisms that their producers would not encounter under normal circumstances.

Hectochlorin multistage activity profile

With the success of compounds like hectochlorin in our liver stage model, we sought to explore the activity of this lipopeptide in other stages of host malaria infection. Hectochlorin was chosen in part for having the highest selectivity index (Supplemental Dataset 1: SI range 2.4 – 22.8) of all the reconfirmed compounds. Here, the SI ratio describes the ratio of PbLuc potency to HepG2 cytotoxicity. Thus, the higher a SI value one compound has, the greater its theoretical safety profile and effect will be, especially for *in vivo* studies (Muller PY and Milton MN, 2012). Like many naturally-derived antibiotics (for example azithromycin and daptomycin), hectochlorin and the other PbLuc hits are large molecules (366.3 – 939.4 Da), assembled with complex chemical linkages. However, in addition to having a published method for hectochlorin synthesis (Cetusic JR et al., 2002), the cyanobacterium (*Lyngbya majuscula*) from which it was discovered can be grown in the lab and used to isolate the active molecule (Marquez BL et al., 2002). The latter source was selected as the most efficient and cost-effective solution, which ultimately produced 21 mg of ≥ 98% pure hectochlorin for future experiments.

In order to determine the effect of hectochlorin on actin-mediated sporozoite motility, we used rhodamine dextran (RD)-containing media and GFP-expressing *P. berghei* sporozoites to measure the degree of hepatocyte traversal and overall infection rate. When added to the

extracellular media, RD cannot enter cells with intact outer membranes, due to its size (Balda MS and Matter K, 2007). Therefore, the proportion of RD+ hepatocytes found under infected conditions correlates with the motility of invading sporozoites. Furthermore, to effectively normalize for those sporozoites which traversed few or zero hepatocytes before invading and replicating, the overall infection rate was measured. The well-known alkaloid and gold standard for actin-dependent motility inhibition assays, cytochalasin D (10 μM) (Stracke ML et al., 1993), was used as a positive control for these studies, with DMSO acting as our negative control. The assay was conducted in duplicate using a 96-well format, with each condition (cytochalasin D 10 μM, hectochlorin 1 μM, DMSO, uninfected) allotted eight wells per plate. Overall, the infected negative control wells showed the highest quantity of RD+ hepatocytes (9.0±0.27%) and the highest GFP+ infection rate (0.57±0.02%) (Figure 1.2). Interestingly, however, hectochlorin outperformed cytochalasin D by a 1.2-fold reduction in infection rate, and by a 10.6-fold reduction in RD+ cell frequency. Furthermore, our data show no meaningful difference between the GFP+ signal in hectochlorin treated (0.26±0.01%) and non-infected (0.25±0.05%) wells, but the 2.6-fold greater RD+ frequency in non-infected wells suggests that actin filament stabilization may contribute to cell integrity.

While sporozoites require motility to navigate through tissues before infecting a hepatocyte, the asexual and mature sexual stages of malaria are intraerythrocytic and can float throughout the bloodstream (Alano P, 2007). The rapid turnover of asexual forms and the intracellular segregation of merozoites during maturation suggests increased susceptibility to cytoskeletal interference over the metabolically lax sexual stage counterparts. In order to test the effect of hectochlorin on *P. falciparum* Dd2 ABS parasites, we first conducted a 12-point dose response (10 – 5.65 $x10^{-5}$ μM) assay using a previously described SYBR Green I fluorescent

readout (Plouffe D et al., 2008). However, even at the lowest concentration, the average maximum growth measured over three replicates was < 25% (data not shown). The dose response titration was then expanded to 24-points (10 – $5.65x10^{-10}$ µM) and run again, this time yielding an average IC_{50} of $1.44x10^{-5} \pm 3.63x10^{-6}$ µM over three replicates (Figure 1.3). In order to ensure hectochlorin had no innate fluorescent properties at an excitation wavelength similar to SYBR Green I (485nm), we measured the signal intensity in red blood cells (RBC) using DMSO as the vehicle. On average, the SYBR Green I (1x concentration) treated wells amplified signal intensity by ~3-fold, but there was no appreciable difference in fluorescence between DMSO (0.5%) and hectochlorin (10 µM) conditions (Figure 1.4).

The preparation of mature sexual stage malaria from asexual cultures requires consistent attention over a period of two weeks. We start with an in-house generated clone of *P. falciparum* (NF54-G3), which was found to produce an abundance of gametocytes when nutritionally stressed. Following this starved state, cultures were treated with N-acetyl glucosamine (50 mM) to prevent reinvasion of undifferentiated asexual parasites. Daily blood smears along with Giemsa staining were used to track gametocytes during their maturation into the later, stage V, forms. Similar to the previous dose response assays, a serial titration was prepared with hectochlorin (12.5 – $7.06x10^{-5}$ µM), puromycin (positive control; 12.5 – $7.06x10^{-5}$ µM), and DMSO (negative control; fixed 0.5%). Even at the highest tested concentration, hectochlorin could only inhibit viability in ~45% of stage V gametocytes when compared to puromycin after 72 hrs (Figure 1.5).

Hectochlorin target identification and validation

Fluorescence microscopy has shown that hectochlorin-treated cells stabilize filamentous actin (F-actin), but the mechanism by which this occurs is unclear. In order to identify the gene target of hectochlorin, we planned to treat *P. falciparum* ABS parasites with increasing doses of

the compound until resistance was generated. The DNA isolated from these mutants and their wild-type parents could then be sequenced and compared for base pair, and ultimately protein residue, changes. However, similar to the effects discussed in other cell types from hectochlorin exposure, the morphology of red blood cells *in vitro* became misshapen, which could impact the parasite's ability to invade and replicate. For this reason, we began selecting for resistant mutants in a drug sensitized strain of *S. cerevisiae* (*Sc*), "Green Monster" (Suzuki Y et al., 2011), using the same principles as those in ABS evolutions (Corey VC et al., 2016). The Green Monster (GM) strain was previously used to validate these methods with antimalarials like KAE609, whereby the resistant yeast protein was homologous to the known malaria target (Goldgof GM et al., 2016). After two rounds of hectochlorin pressure at 1 and 2 μM, the polyclonal IC_{50} shifted over 7.5-fold, from 0.20 μM to > 1.5 μM (Figure 1.6A). Rather than extracting DNA from these polyclonal mutants, we reconfirmed the resistant phenotype was present in monoclonal colonies streaked from the bulk culture. Whole genome sequencing of clones from two independently reared resistant lineages identified a mutation in Act1, resulting in a R116K amino acid substitution. Using a CRISPR/Cas9 system, this single substitution was successfully incorporated into our parental Green Monster cells, which recapitulated the resistance shift observed in our selected lines (Figure 1.6B).

Discussion

The use of natural products as effective antimicrobial therapeutics predates our knowledge of the germ theory of disease (Dias DA et al., 2012). This was true for one of the first antimalarials, quinine, and echoes in the current standard-of-care treatment in severe malaria, artemisinin combination therapies (ACTs). However, most present day antimalarials target the symptomatic

blood stage of infection (Delves M et al., 2012), which highlights the value of disease preventing therapeutics that act earlier in the parasitic life-cycle. Furthermore, the current list of approved drugs for prophylactic use or eradication of dormant liver stage forms from species like *P. vivax*, is limited (Schwartz E, 2012). Here we evaluated a compound library of 145 marine natural products against the liver stage of malaria. Our work identified five liver stage active scaffolds, that demonstrate no significant hepatocellular cytotoxicity at tested concentrations. Furthermore, the target of our screening lead (hectochlorin) was identified in *Sc* by WGS and validated by reverse genetics. This suggested a relationship between hectochlorin and the modulation of F-actin stability through contact with actin itself, rather than a dependent cofactor.

Phenotypic screening in malaria has successfully introduced new scaffolds into the clinical trial pipeline (Wells TN et al., 2015). However, unlike a number of previous screens (Avery VM et al., 2014;Guiguemde WA et al., 2010), our focus on the liver stage of infection has helped to identify potential prophylactic agents. The fallout of prospective hits from our primary screen due to cytotoxicity was unsurprising, given the hostile marine environments of their producing organisms (Marris E, 2006). It remains possible that with extended incubation time in our HepG2 counterscreen (or in other host cell lines), compounds like hectochlorin could be regarded as toxic. However, an exceptionally toxic proteasome inhibitor from our library, carmaphycin B, was previously rectified of its antiproliferative traits with systematic side-chain modifications (LaMonte GM et al., 2017). This result is encouraging, and suggests that with their large size, natural products come with the ability to selectively enhance target specificity.

One effective method of halting the threat of malaria progression is to block the sporozoite's ability to invade or replicate within hepatocytes; the role of current prophylactic agents such as Malarone (Looareesuwan S et al., 1999). By restricting canonical actin

depolymerization, thus blocking sporozoite motility, hectochlorin is capable of reducing infection rates *in vitro* to levels comparable with uninfected negative controls (Figure 1.2). Interestingly, others groups have shown increased intercellular distances in endothelial and mesenteric tissues from 10 µM cytochalasin D treatment (Waschke J et al., 2005), while no change was reported when using low concentrations (0.1 µM) of the actin hyperpolymerizing agent Jasplakinolide. While these studies focused on intercellular distances, they established a relationship between F-actin organization and cell integrity. We noticed a similar trend through decreased RD+ signal from hectochlorin treated versus uninfected cells. When compared to our own and previously reported cytochalasin D data (Swann J et al., 2016), hectochlorin was similarly efficacious but at one-tenth the concentration. These data empirically validate the liver stage activity of hectochlorin in lieu of a biochemical luciferase inhibition counterscreen.

P. falciparum ABS merozoites are reliant on canonical actin turnover to invade new red blood cells post egress (Baum J et al., 2006;Das S et al., 2017). Conversely, while mature gametocytes express and utilize actin (specifically isoforms I and II) extensively within the mosquito midgut during sexual reproduction (Vahokoski J et al., 2014), the non-replicating intraerythrocytic forms predictably survive longer with hectochlorin-mediated cytoskeletal restraints. *In vitro* this translated to picomolar inhibition of the ABS (Figure 1.3), with incomplete killing of mature gametocytes even at 12.5 µM (Figure 1.5). Because our sexual stage assay focuses on the effect of hectochlorin on erythrocyte bound gametocytes, we concede that measuring male gametocyte exflagellation --which naturally occurs inside the mosquito midgut following a bloodmeal (Deligianni E et al., 2011)-- could reasonably show potent transmission blocking properties. However, the motile podia from male gametocytes in these conditions function predominantly with the actin 2 isoform, and the mutated residue (R116K) in our *S.*

cerevisiae lines share homology with both *Plasmodium* actins. In addition, because the antiproliferative properties of hectochlorin have been established against several different cancer cell lines from the National Cancer Institute's *in vitro* panel (Marquez BL et al., 2002), we predict this would follow against fully differentiated male gametocytes.

If a compound's target is known, medicinal chemistry techniques can be leveraged to enhance potency and reduce toxicity. A previous example was given with carmaphycin B, where a series of side chain modifications generated analogs with 98-fold less toxicity to HepG2 cells than the parent compound (LaMonte GM et al., 2017). By using a drug-sensitive *S. cerevisiae* strain, we rapidly generated hectochlorin-resistant clones with identifiable mutations in the ACT1 gene. The validation of this resistance-causing mutation suggests a direct effect on the assembling protein, rather than inhibition of those actin-binding proteins that facilitate depolymerization.

Translating a compound which targets a widely conserved protein like actin into a safe therapeutic presents unique future challenges. Even subtle changes in actin proteins can have profound effects, as is evident by the six functionally distinct human isoforms varying in sequence identity by a maximum of 6%. Conversely, both actin isoforms in *Plasmodium* confer < 80% sequence identity to other eukaryotes, and each other. While chemical modification of hectochlorin to maximize *Plasmodium* selectivity is beyond the scope of this study, we remain optimistic of its potential given the variability of *Plasmodium spp* actin to that of humans.

Figure 1.1 Dose response analysis of primary screen PbLuc MNP hits. Parasite luminescent signal measured after 48hr incubation in the presence of compounds in titration. Curves represent mean inhibition across two independent replicates (error bars = SD).

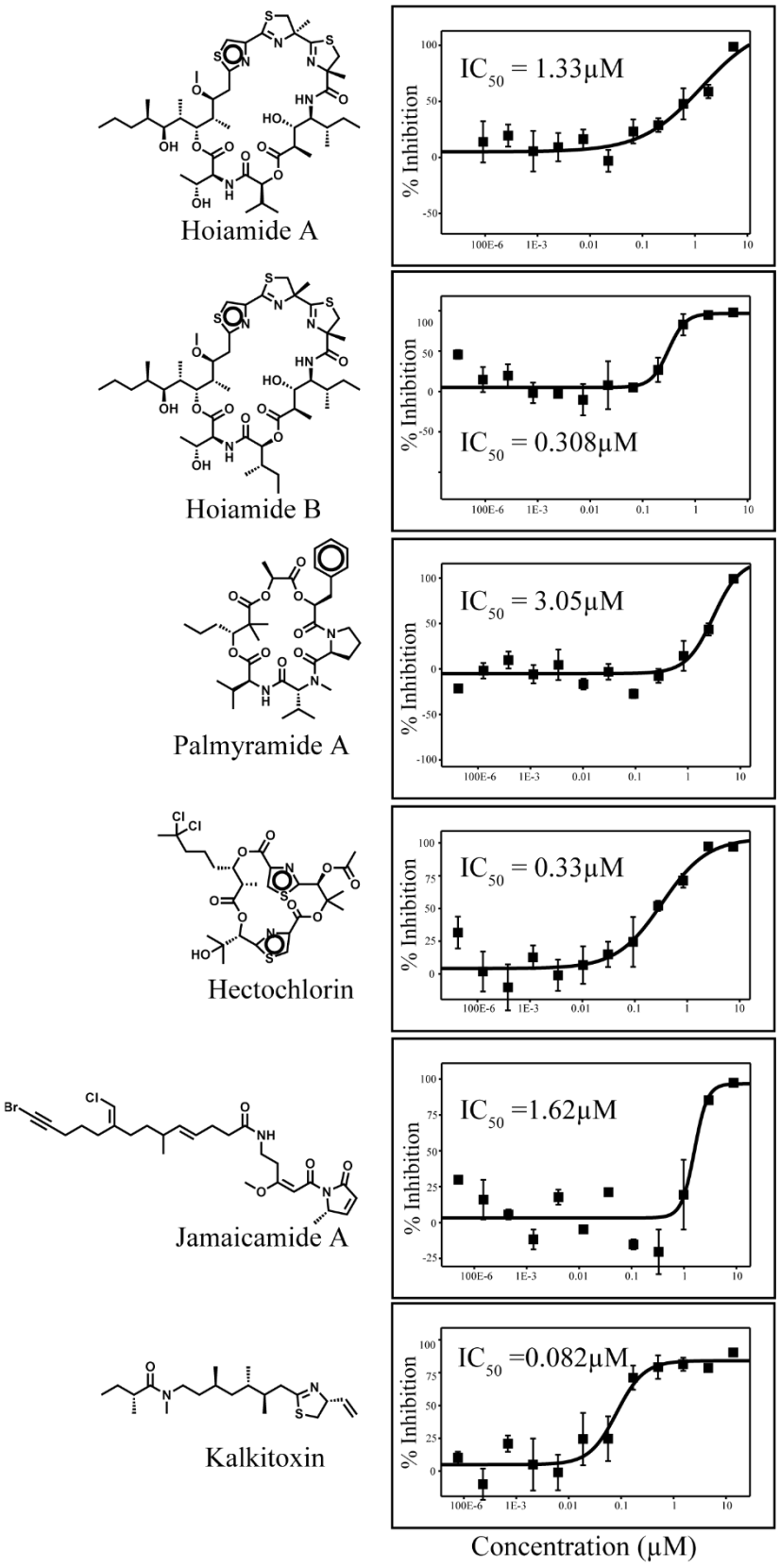

Figure 1.1 Dose response analysis of primary screen PbLuc MNP hits, Continued

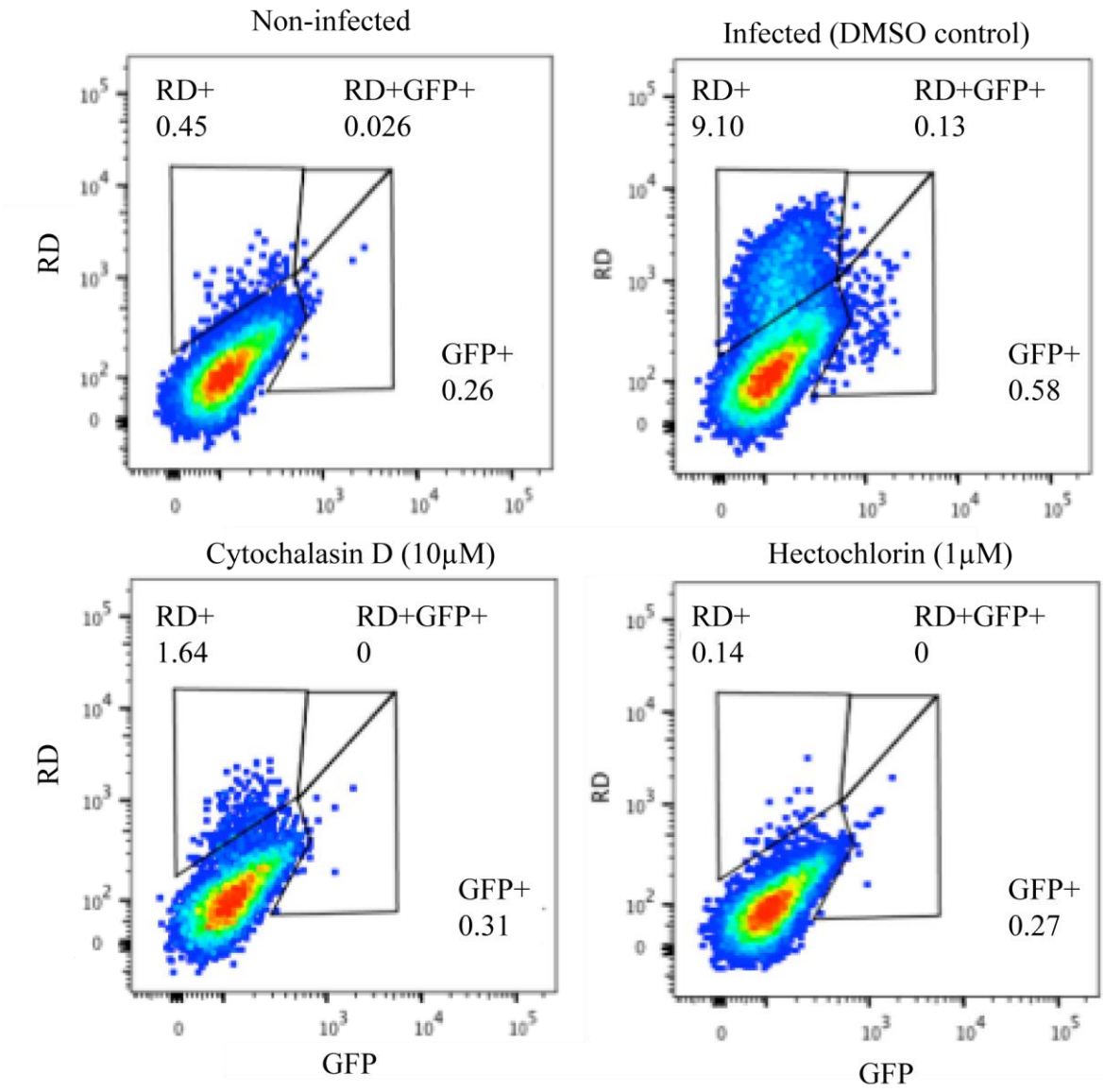

Figure 1.2 Evaluation of hepatocellular traversal by *P. berghei* sporozoites using an established flow cytometry-based assay. Flow cytometry plots show traversal and invasion of host cells at 2 hours post invasion by exoerythrocytic forms in Huh7.5.1 cells. Percent of rhodamine-dextran positive single cells was used to determine overall traversal frequency, controlled against cytochalasin D (positive) at 1µM and infected untreated conditions, while invasion was evaluated by exclusive GFP+ signal.

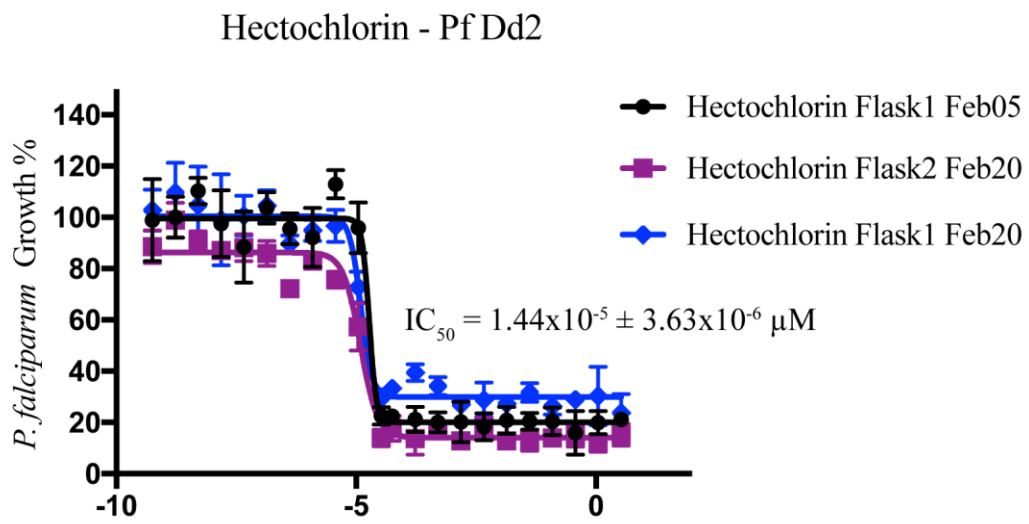

Figure 1.3 *P. falciparum* dose response inhibition by hectochlorin in the ABS. Two independent clones of Pf Dd2 were tested in biological triplicate using a 24-point titration to capture the unusually potent ABS profile of hectochlorin in a 72-hour SYBR Green I assay. Curves represent multiple lanes within each test plate (error bars = SD).

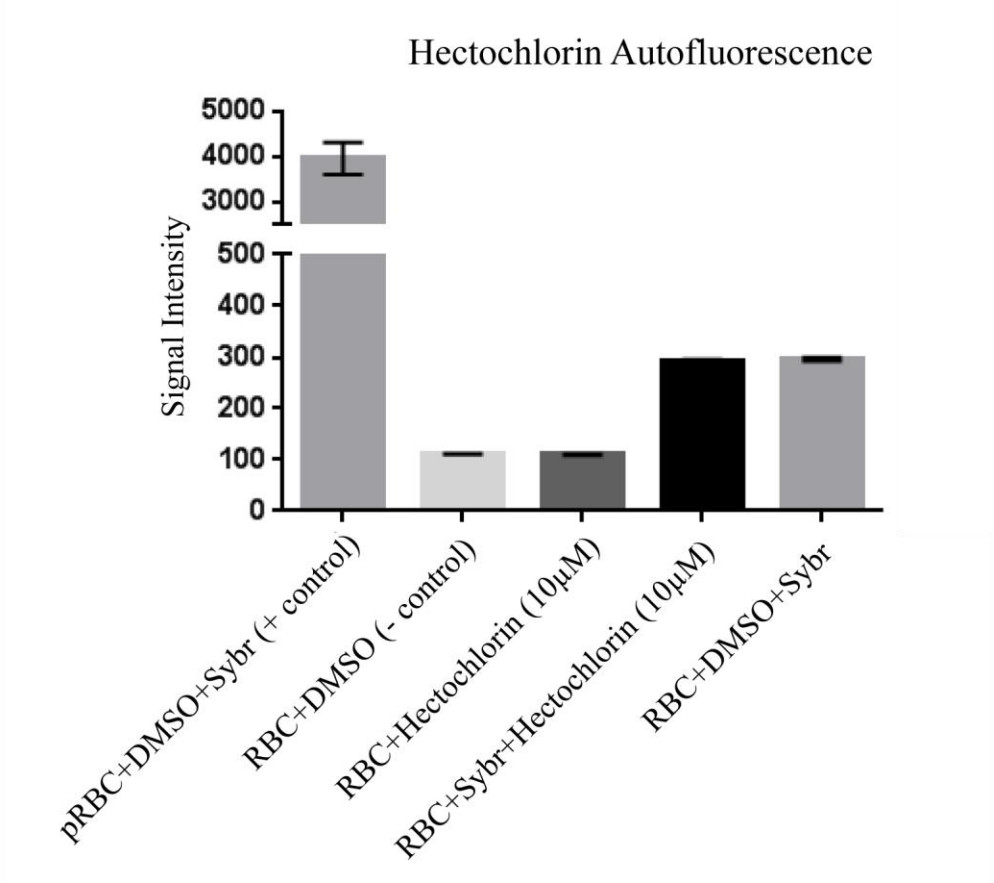

Figure 1.4 Validation of non-interference from hectochlorin on SYBR Green I fluorescence. SYBR Green I signal compared between hectochlorin (single 10µM concentration) and the standard vehicle, DMSO (0.5%), used in ABS dose response assays after 72hr incubation at 37°C. Represented data were collected in duplicate (error bars = SD).

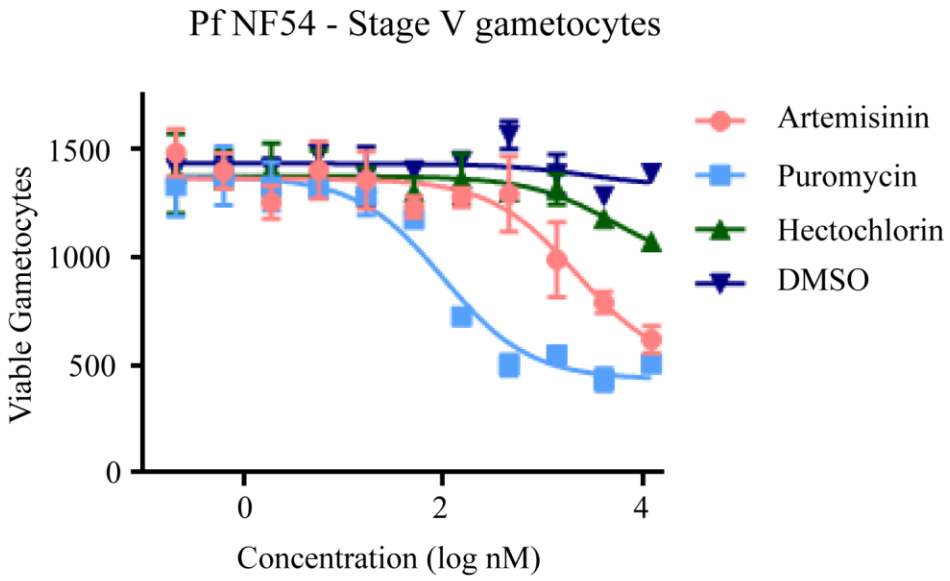

	IC_{50} nM (95% CI)
Artemisinin	2195 (952 - 5065)
Puromycin	101.2 (66 - 156)
Hectochlorin	> 12.5 µM

Data generated by: David Plouffe
Data analyzed by: Matthew Abraham

Figure 1.5 Mature *P. falciparum* sexual stage inhibition using an established high-content imaging assay. Stage V gametocytes were used to evaluate the transmission blocking capability of test compound hectochlorin (12.5 – $7.06x10^{-5}$µM) versus puromycin (positive control) and DMSO (negative control).

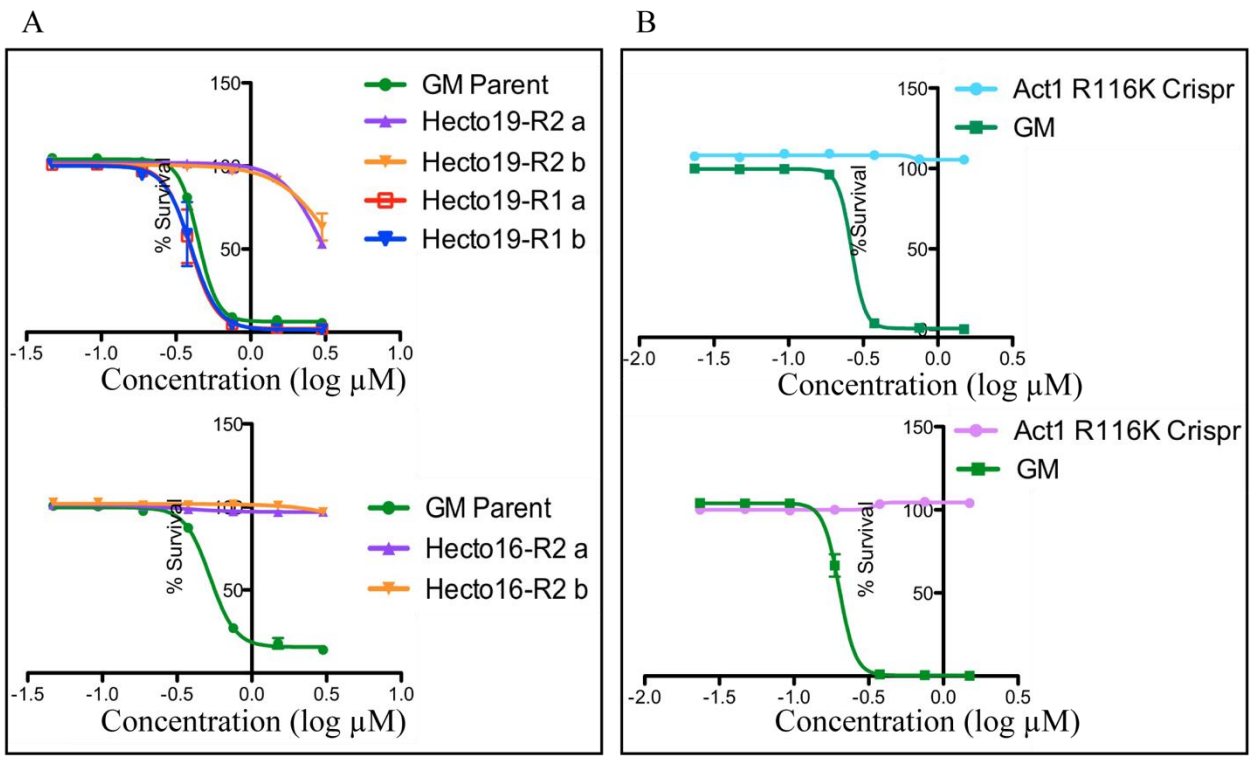

Data generated and analyzed by Prianka Kumar and Sabine Ottilie

Figure 1.6 Hectochlorin mutant selections in *S. cerevisiae* Green Monster. (A) Resistance develops after two rounds of compound selection in separates lineages 19 (top) and 16 (bottom). (B) The resistance phenotype is recapitulated in wild-type Green Monster from the single amino acid change (R116K) determined by WGS of resistant clones.

Acknowledgements

Matthew Abraham (M.A.) designed experiments and wrote the manuscript draft. Sabine Ottilie (S.O.) designed experiments and analyzed data. Prianka Kumar (P.K.) designed and performed directed evolution experiments and CRISPR/Cas9 genome editing in Green Monster with hectochlorin. Stephan Meister (S.M.) and M.A. performed liver stage and cytotoxicity screens for the natural product library. Madeline R. Luth (M.R.L.) performed whole genome sequencing analysis of the hectochlorin resistant Green Monster strains. Ariana Remmel (A.R.) and William H. Gerwick (W.H.G.) generously provided the entire natural products library and extracted hectochlorin for subsequent experiments from a lab grown biomass. Elizabeth A. Winzeler (E.A.W.) analyzed data and wrote the manuscript draft.

Chapter 1, in part, contains material that may be prepared for publication at a future time with co-authors including Matthew Abraham, Sabine Ottilie, Stephan Meister, Prianka Kumar, Madeline R. Luth, Ariana Remmel, William H. Gerwick, and Elizabeth A. Winzeler. The dissertation author is the primary investigator and author of the pending manuscript.

2. Discovery of stage specific and multistage active next-generation antimalarials

Abstract

In conjunction with providing relief from symptomatic disease states, targeting transmission-blocking pathways and prophylactic intervention are key to malaria prevention. The lack of current antimalarials with preventive activity profiles likely contributes to the stagnant rate of malaria related deaths, globally. To help find the next generation of antimalarials with activity against the exoerythrocytic, asexual, and sexual blood stages of the *Plasmodium* life cycle, we conducted the largest, single-library, phenotypic screen against all stages of vertebrate host infection. Nearly 70,000 small molecules were tested systematically for activity against the liver stage, mature sexual stage, and asexual blood stage infections. Cheminformatic analysis of active compounds identified scaffold families similar to known antimalarials, as well as hitherto unknown scaffolds with potent multistage activity. Among those active scaffolds, 10 novel delayed-death inhibitors were identified with submicromolar activity against the asexual blood stage. All together we observed that 158 of 164 bioactive scaffolds (96% IC_{50} < 1 μM) had stage-specific activity and six potent (half-maximal inhibitory concentration < 1 μM) multistage scaffolds were also identified. We further showed that at least one of these multistage inhibitors targets essential *Plasmodium* proteins like the cytochrome bc1 complex. In total, this dataset presents fresh starting points for drug development of preventative medicines, which are essential to realize continued global reduction of malaria infections and eventual eradication.

Introduction

Malaria parasites remain a lethal threat for nearly half the world's population, and claimed 445,000 lives in 2016 (WHO R, 2017). Until now, efforts to successfully combat this disease have come primarily through vector control measures, such as the use of insecticide-treated bednets (Killeen GF et al., 2017;Shanks GD and Mohrle JJ, 2017) as well as small molecule therapeutics. Despite a multifaceted approach, progress has recently stalled, and the WHO malaria reported an increase in cases in 2017 after years of decline (WHO R, 2018). Although there are many possible reasons, including population growth, insecticide-resistance, political conflict and parasite artemisinin-combination therapy resistance (Mills A et al., 2008) the fact remains that current treatment options are suboptimal. Importantly, current therapies that are widely used either allow continued disease transmission (artemisinin-derivatives, 4-aminoquinolines), or are associated with high rates of resistance (artemisinin-derivatives, 4-aminoquinolines, antifolates and cytochrome bc1 inhibitors), limiting their widespread use. In addition, few widely used-therapies prevent malaria.

The problems with the current set of treatments is historical. The active chemical scaffolds of many current antimalarial treatments were identified decades or even millennia ago, often well before much was known about the complicated lifecycle of the malaria parasite. It is now known that asymptomatic host infection starts in the liver, following the delivery of about 100 sporozoites by the bite of a female *Anopheles* mosquito (Medica DL and Sinnis P, 2005;Rosenberg R et al., 1990). Early disease symptoms only occur following the egress of asexually-replicating blood stages from invaded hepatocytes, 1-2 weeks later (Amino R et al., 2006;Blackman MJ, 2008). Finally, 1-5% of ABS parasites will differentiate into gametocytes (GAMs), the cells that can immediately differentiate into male and female gametes once the cells sense that they have left the

vertebrate host. While earlier stages (I-IV) continue developing within the host, mature gametocytes (stage V) are the only parasite forms able to survive in the mosquito midgut and are responsible for the disease's transmission (Eichner M et al., 2001;Saliba KS and Jacobs-Lorena M, 2013;Talman AM et al., 2004). Most current therapies, many derived from historical folk remedies, only kill the asexual blood stage of the parasites, as this is the only stage that is associated with clear symptoms in humans and animal models of the disease (Antony HA and Parija SC, 2016). For this reason, and because it is sometimes easier to make an new drug out of an old drug (Raju TN, 2000), 15 different ABS-targeting drugs are indicated for the treatment of malaria, including artemisinin combination therapies (ACTs), which are the current standard of care for severe and chloroquine resistant malaria (Guidelines WHOT, 2015). Patients who take a drug that only targets the ABS may continue to transmit malaria to their neighbors.

Another problem with targeting only the ABS is that by the time an infection is symptomatic, the patient may harbor billions of parasites, which increases the probability that these genetically-pliable parasites will have evolved resistance (Lu F et al., 2017;Noedl H et al., 2008). To escape the inevitable cycle of resistance and fulfill the goal of global malaria eradication, next generation antimalarials should inhibit the liver stage (exoerythrocytic forms; EEFs) or sexual stage in addition to providing symptomatic relief (Diagana TT, 2015). Furthermore, interruption of the lifecycle at these points is ideal for their innate population bottleneck, which can be targeted at lower risk of developing resistance than in the ABS due to relatively fewer parasites.

Armed with our knowledge of the parasite's lifecycle, the field has come to the recognition that better drugs might be possible (Diagana TT, 2015). This has spurred the search for potent scaffolds that act throughput the parasite's complex life-cycle (Okombo J and Chibale K, 2018), primarily using phenotypic screening of different stages in cell culture models (Sinha S et al.,

2017). Although no licensed therapies are available yet, multistage-active compounds have been identified by iteratively screening libraries through successive life-cycle stages (Almela MJ et al., 2015;Meister S et al., 2011;Swann J et al., 2016). For example, one million compounds might be screened through the asexual blood-stage, followed by testing of 5,000 in the liver stage and testing 100 in a transmission-blocking assay. Several promising antimalarial drug candidates are currently wading through clinical trials following the chemotype's discovery in such screens (Coteron JM et al., 2011;Kuhen KL et al., 2014;Paquet T et al., 2017;Rottmann M et al., 2010). However, stepwise filtering fails to identify all multistage active scaffolds, since hits from only one stage are carried forward. Furthermore, many stage-specific compounds, which could be formulated into combination therapies for a multistage drug, are ignored by these methods.

Here we describe a pan-lifecycle screen of the Global Health Chemical Diversity Library. This library, consisting of ~70,000 compounds, was screened in parallel against *P. falciparum* (Pf) ABS, *P. falciparum* Stage V GAMs, and *P. berghei* (PbLuc) liver-stages. These efforts have identified potent stage specific and multistage active chemical scaffolds. Together, our findings highlight new chemical space to fill the current void surrounding radical cure, transmission blocking, and causal prophylactic antimalarials.

Results

High-throughput Screening Workflow.

In order to find new compounds capable of inhibiting the diverse lifecycle stages of malaria, a library was designed with unique physiochemical properties. Care was taken to maximize the library's value by excluding scaffolds that were similar to those in the Medicines for

Malaria Venture Drug Development Portfolio (Olliaro P and Wells TN, 2009). The resulting commercially available Global Health Chemical Diversity Library (GHCDL), is comprised of 68,614 compounds, that were selected for their diversity and adherence to lead-like physiochemical properties. All but 30 compounds obey the standard Lipinski Rule of Five (Lipinski CA et al., 2001), with an average molecular weight of 320.7 Da (184.20 to 492.23 Da), mean logP of 2.0 (-3.27 to 6.35), mean hydrogen bond donor count of 0.9 (0 to 5), and mean hydrogen bond acceptor count of 5.6 (1 to 10). While adherence to these chemical guidelines have inspired drug development efforts for decades, in their acclaimed review the authors exonerate several antibiotics, fungicides, and protozoacides from the "rules" (McKerrow JH and Lipinski CA, 2017), suggesting exploration of curative agents for neglected diseases outweighs straightforward drug design. In addition, because ideal antimalarials should be orally bioavailable, the library was constructed to give an ideal topological polar surface area (TPSA) average of 64.2 Å (16.13 to 160.88 Å), with an average rotatable bond count of 4.5 (0 to 10) (Hou T et al., 2007). The degree of carbon saturation as a surrogate for successful clinical testing outcome has been previously described (Lovering F et al., 2009), and was emphasized in the GHCDL with an average fraction of sp^3 hybridized carbon count (Fsp3) of 0.48 (0 to 1.0). This same library has been used on other pathogens including *Cryptosporidium*, in which 31 compounds were shown to inhibit *C. parvum* development in HCT-8 cells (Love MS et al., 2017).

ABS screen for fast-acting and delayed-death inhibitors.

To interrogate the library, we first performed a screen for activity against the ABS; compounds active here are expected to provide symptomatic relief from malaria. Previous exploratory screens to detect such compounds have used the DNA intercalating dye, SYBR Green I, which gives a readout on the amount of parasite DNA replication after compound treatment for

72 hours (Plouffe D et al., 2008). This method is effective, but may give a low signal to noise ratio if a compound does not act quickly to kill the parasite as some DNA replication will have occurred before death. SYBR Green I screening has been used to discover a number of fast-killing compounds, such as the spironoindolone, KAE609. Fast acting ABS inhibitors are necessary to quickly mitigate symptoms of malaria, but these can be combined with slower acting "delayed-death" inhibitors such as clindamycin which can compensate for the rapid pharmacokinetic turnover of some compounds, like artesunate (Burkhardt D et al., 2007).

Slow-acting, or delayed death inhibitors, typically act against the parasite apicoplast, a unique organelle needed for fatty acid biosynthesis. Interference with canonical apicoplast function is thought to cause the latent killing of the untreated daughter-generation parasites, resulting in a delayed-death phenotype (Dahl EL and Rosenthal PJ, 2007). Known antimalarials, such as doxycycline, work by this mechanism and are used as prophylactic treatments. Such inhibitors have been commonly overlooked during previous large-scale screens that have used a 72-hour incubation period (Gamo FJ et al., 2010).

To cast a wider net and potentially acquire slower-acting or "delayed-death" compounds, all primary screening and preliminary reconfirmation studies in the ABS, were performed on the GHCDL against a *P. falciparum* Dd2 (PfLuc) line expressing firefly luciferase (Ekland EH et al., 2011) under the control of the *pfhrp3* (5' UTR)/*pfhrp2* (3' UTR) promoter. In the presence of luciferin, healthy parasites emit light in proportion to the infection rate per well. This bioluminescence is normalized to DMSO (negative control) and artemisinin (positive control)-treated wells for the single point screens, with the addition of clindamycin in dose response as the standard for delayed-death inhibition. In order to capture more compounds, the primary screen also used a 96hr-incubation time to further help identify delayed-death inhibitors.

To run the primary screening assay, 8 µL of ABS parasites in screening media (see methods) were dispensed into 1536-well plates previously spotted with the 64,811 GHCDL compounds at 5 µM. The remaining library compounds arrived later and were evaluated separately. After a 96-hour incubation, 2 µL of BrightGlo was added and luciferase signal was measured. For this primary screen, assay fidelity was determined on a per plate basis using both the Z'-factor and potency variance of the positive (artemisinin) and negative (DMSO) controls. The mean Z' value was 0.60 (range 0.43 – 0.75), with only one plate falling below our ideal 0.5 threshold (Figure 2.1). Both controls were consistent, with a mean inhibition for artemisinin and DMSO equaling 99.6 ± 1.03% and -3.91 ± 29.2%, respectively.

The ABS primary screen yielded 950 compounds with >70% parasitic bioluminescence inhibition, relative to controls (Figure 2.2, Supplemental Dataset 2). Because single replicate screening will have more false positives and negatives (especially in low volume HTS formats where instrument tolerance impacts the accuracy of compound and culture dispensing), reconfirmation of the available 924 single point hits was performed against ABS parasites in single point triplicate at 1.25 µM. Even at this reduced concentration, 359 compounds averaged ≥ 50% inhibition and 176 compounds maintained ≥ 70% inhibition, across three replicates (Supplemental Dataset 3; List 1). Because the GHCDL was specifically curated to avoid known antimalarial chemotypes, the overlap of our hits with known scaffolds was minimal. However, with relaxed similarity criteria (Tanimoto similarity > 60%), we recovered analogs of several classes, including 4-aminoquinolines (for example chloroquine -- DDD01078433) and triazolopyrimidines (for example DSM265 – DDD01063654) in this screen. Altogether, 363 compounds (≥ 43% inhibition at 1.25 µM) were chosen to refine the list of ABS inhibitors through an 8-point (5 µM – 0.00232 µM; 96 hr) dose response series against PfLuc Dd2. With commercial compound availability

remaining a constant hurdle, and because all 363 compounds maintained an IC_{50} < 3μM, this series of ABS hits (List 1) was deemed eligible for powder reconfirmation. Following the primary screen and subsequent reconfirmation assays, another 3,642 library compounds arrived (Supplemental Dataset 3; List 2) and were funneled directly into single point triplicate testing at 1.25 μM. In total, 16 compounds which averaged > 50% inhibition across all three replicates were advanced to 11-point dose response testing, along with the hits from List 1.

To measure for latent killing profiles of active scaffolds, we evaluated the parasitic luminescence inhibition of 300 commercially available primary screen hits (Set 1 and 2) using fresh powder stocks in 11-point dose response at 48 and 96-hour time points (PfLuc; n=2). As a counter screen for luciferase inhibitors, these compounds were also tested in an identical format at 96 hrs except SYBR Green I was used. In total, 30 compounds maintained a PfLuc IC_{50} of ≤ 1 μM at 48hrs with 87 others showing the same level of activity (< 1 uM) in the 96 hr PfLuc assay only. The prevalence of activity in our extended duration (96 hr) assay highlights the effect of prolonged chemical exposure rather than a delayed-death phenotype, as the majority (> 90%) had a PfLuc IC_{50} of less than 12.5 μM at 48hr. Conversely, among these 87 compounds, a lack of measurable inhibition in the 96hr SYBR Green I assay (for example having an IC_{50} > 12.5 μM) revealed a higher proportion of delayed-death inhibitors rather than the intended false positive luciferase inhibitors. This may stem from a general lack of luciferase inhibitors in the ABS hits, but also showed the modest resolution of SYBR Green I for distinguishing parasite growth over one generation (Figure 2.3). The average potency of our delayed-death control, clindamycin (Dahl EL and Rosenthal PJ, 2007), at 96 hrs was 0.00520 ± 0.001253 μM (n=4) and > 10 μM (n=4) in the luciferase and SYBR Green I assays, respectively. Doxycycline, another delayed-death control, behaved similarly at 96 hrs, but conveyed some activity (IC_{50} 7.18 ± 1.59 μM) in the 48 hr PfLuc

assay. For our test compounds, a delayed-death phenotype was considered if the 48 hr to 96 hr PfLuc IC_{50} ratio was > 10, which we observed in nine of the 87 aforementioned hits (Figure 2.4). These nine inhibitors preserve no structural similarity to previously-reported antibiotics with a delayed death phenotype in the *P. falciparum* ABS (Dahl EL and Rosenthal PJ, 2007;Ramya TN et al., 2007). However, a familiar quinoline substructure is present in DDD01057375 and DDD01057225, with the former exhibiting the highest potency ($7.14x10^{-3}$ μM; 95% CI 0.004 – 0.01 μM) against 96 hr ABS parasites in our overall set.

To explore their potential chemoprotective profile, three of the nine delayed-death inhibitors were repurchased (Figure 2.4) based on commercial availability. They were run in our suit of exoerythrocytic stage assays (see methods) including a counterscreen against host cells and recombinant firefly luciferase. DDD01057375 and DDD01073393 both showed dose dependent inhibition of *P. berghei* liver stages over two replicates and neither compound interfered with recombinant luciferase; however, DDD01073393 was moderately cytotoxic (9.86 μM; 95% CI 9.9 – 12.4 μM) toward the host HepG2 hepatocytes.

Causal prophylaxis screen.

The need to alleviate malaria symptoms can be bypassed with prophylactic liver stage inhibitors, which prevent infection, acting either against sporozoite invasion or during the early stages of parasite development. To identify compounds with potential prophylactic activity, we used a *P. berghei* rodent malaria liver-stage model (Janse CJ et al., 2006) and HepG2-A16-CD81 hepatocytes (Yalaoui S et al., 2008). The advantage of this model is that it has a 48-hour incubation period, which prevents hepatoma cell overgrowth. In addition, the luciferase expressing sporozoites of this murine *Plasmodium* species model represent a more abundant and safer alternative to human-infecting species. Furthermore, the use of hepatoma cells provides day to day

consistency, making them ideal for high throughput screening. We simultaneously conducted a library-wide cytotoxicity counter screen against uninfected hepatocytes to ensure that a loss of signal was not from host cell death.

For the screen, 5 µL of HepG2-A16-CD81 hepatocytes containing $3x10^3$ cells were seeded into 1536-well plates, prespotted with 10 nL of library compound (2 µM final assay concentration (Figure 2.2)). For PbLuc infected plates, approximately 750 purified sporozoites in 5 µL of screening media were added to each well. Compounds were tested for toxicity in parallel (see methods) by measuring uninfected-hepatocyte viability using CellTiter-Glo. In total, 151 compounds inhibited > 75% of parasite bioluminescence at 2 µM, while only 67 compounds inhibited uninfected hepatocyte growth by more than 50%. This hit rate was much lower than expected for an agnostic library, which prompted us to rescreen the entire library at 10 µM. The PbLuc and cytotoxicity assay plates for this second replicate would be stamped in-house with 50 nL per well, using the same compound plates as the sexual stage screen. Excluding the change in concentration and shortening of time the compounds spent in each well prior to infection, all other assay parameters were kept similar. This yielded 1440 compounds with > 75% PbLuc inhibition, of which 103 were found to be cytotoxic (> 50% HepG2 inhibition). All toxic and potential false positive effectors were filtered from subsequent studies (Supplemental Dataset 2). Commercially available primary screen hits which inhibited PbLuc at > 60% in both replicates were resourced (mean HepG2 inhibition < 50%). The resulting 41 compounds were acquired as DMSO stocks and retested in dose-response (50 – $2.82x10^{-4}$ µM or 25 – $141.13x10^{-6}$ µM) against PbLuc and uninfected hepatocytes (Supplemental Dataset 4). Liver stage activity reconfirmed for 23 molecules with an IC_{50} < 10 µM, nine of which averaged submicromolar efficacy across two or more replicates. Because our priority was to find liver stage potent molecules, we could not ignore

the excess number of prospective hits from the 10 µM primary screen replicate. Despite the likelihood of a much lower reconfirmation rate from the reliance on a single replicate, we evaluated 405 compounds with > 70% inhibition from the second PbLuc screen. The majority of these proved inactive; however, 18 submicromolar hits were found and added to Supplemental Dataset 4. For these reconfirmation studies, compounds were considered non-toxic if the PbLuc to HepG2 IC_{50} ratio was ≥ 10 fold, or if maximum hepatocyte inhibition was ≤ 60% at the highest tested concentration (25 or 50 µM). This included all but three of the compounds retested in dose response.

While bioluminescent reporter systems allow for high-throughput screening endeavors like ours, the challenge of teasing out true hits from interference compounds remains (Thorne N et al., 2010). To counter screen for such inhibitors, the most potent dose response hits were also tested for bioluminescence interference of recombinant firefly luciferase (rLuci) (*Photinus pyralis*) in the presence of luciferin. Compounds with a 10-fold or greater difference in PbLuc versus rLuci IC_{50} were considered physiologically-relevant hits. We identified eight previously unreported luciferase inhibitors with submicromolar IC_{50} against rLuc, in two independent replicates (Figure 2.5). A cluster of four analogs (cluster ID: 3452) contained the most potent inhibitors and was significantly overrepresented in the set ($p\text{-value}_{rLUCi} = 4.16 \times 10^{-12}$). The remaining compounds were structurally distinct from one another; however, DDD01252313 closely resembles PTC124 (Ataluren), a drug used to treat Duchenne muscular dystrophy. The 3,5-aryl-oxadiazole core of these analogs can reversibly inhibit firefly luciferase, but not *Renilla reniformis* luciferase (Auld DS et al., 2009).

Stage V gametocyte screen.

Gametocytes are responsible for malaria transmission and killing them is expected to block progression of the disease. To identify possible transmission-blocking inhibitors, we screened the GHCDL against a pure population of stage V gametocytes (Plouffe DM et al., 2016). A prolific gametocyte generating clone of *P. falciparum* (NF54-G3) was used to culture mature sexual stages for these studies. Stage V gametocytes were specifically favored for screening due to their intrinsic chemical resilience over immature forms (D'Alessandro S et al., 2016), and their pharmacodynamically favorable circulation within the bloodstream. This strategy mimics *in vivo* conditions felt by these parasites, thus providing an ideal model for malaria sexual-stage drug discovery.

To induce a sufficient quantity of mature gametocytes for screening, tightly synchronized asexual blood stages at 6-8% parasitemia were stressed for 24 hrs with 50% spent media and followed by daily blood smear to track their morphology. The addition of N-acetyl glucosamine (NAG) 0-9 days post induction prevented reinfection of undifferentiated asexual stages. For the primary screen, 1536-well assay plates were stamped in duplicate with 10 nL of library compounds for a 2 µM final testing concentration. Infected cultures were added at 0.75% gametocytemia in 10 µL of screening media and 1.25% hematocrit. Viability of gametocytes was measured after 72 hrs of compound treatment using the dye MitoTracker Red CMXRos, which selectively labels parasites with intact mitochondrial membrane potential (Pendergrass W et al., 2004). This yielded 71 hits with an average gametocyte count reduction of > 50% relative to the DMSO negative control. To reconfirm these hits, all 71 compounds were retested against stage V gametocytes in triplicate 10-point dose response (10 µM to 5.08×10^{-4} µM). Taken together, 44 compounds established an IC_{50} of < 2 µM, of which 26 compounds had submicromolar IC_{50}s (Supplemental Dataset 5).

Chemical scaffold clustering.

In order to assess the quality of our selected hits and identify scaffolds amenable to future drug discovery efforts, we clustered the GHCDL by scaffold similarity using ECFP4 fingerprints and a Dice similarity coefficient (DSC) of 0.7. This generated an extensive similarity network, with scaffold families segregated into discrete clusters. We then calculated the enrichment of potent clusters for each biological screen (ABS, EEF, and stage V GAM) to identify scaffolds that had overrepresented bioactivity compared to rates expected by chance (hypergeometric p-value < 0.005). Taken together, we identified 35 clusters across all malaria life-cycle stages, eight of which contain compounds with potent dual stage activity (Figure 2-3). It should be noted that 13 ABS, 3 liver-stage, and 2 gametocyte active compounds with an $IC_{50} \leq 1$ μM produced clusters of 1-2 (singletons or doublets) members, and were excluded from enrichment analysis (Figure 2.6).

We observed the greatest overlap of potent clusters between ABS and GAM stages (Figure 2.7 cluster ID 223, 2587, 4193, and 8128) versus either with EEFs. The most enriched set of dual blood stage inhibitors (cluster ID 8128) contains a pyrimidoazepine substructure previously described as a serotonin receptor antagonist, but not implicated with antimalarial effect (Yang HY et al., 2013). A thiophene heterocycle adjacent to the tertiary amine was potent under 1 μM in both blood stages (DDD01243664), with imidazole (DDD01254777; $p\text{-value}_{ABS}$ $6.31x10^{-8}$) and thiazole/pyrazole (DDD01258014/DDD01255965; $p\text{-value}_{GAM}$ $9.65x10^{-10}$) substitutions favoring potency in ABS and GAMs, respectively. Another GAM inhibitory cluster with at least one potent ABS member (cluster ID 2587) boasts a pyridine-thiazole core, similar to previously known ABS potent scaffolds MMV007907, MMV001246, and MMV665909 (Hain AU et al., 2014). However, the pyridine substitutions in our inhibitors lay opposite to those previously described. This linkage independent blood-stage selectivity highlights the dual stage potential of this cluster's core

substructure. In contrast to the abundant overlap of blood stage inhibitors, simultaneous asexual and liver-stage potency was confined to cluster 3452. All aryl modifications were dual active in both primary screens, while a 5-(pyridine-3-yl)pyrimidine linkage (DDD01060831; 24.8% PbLuc inhibition at 10 μM) lost meaningful efficacy. One cluster representative, DDD01061024, was tested in dose response for both stages and yielded submicromolar potency in both (Figure 2.7 brown; p-value$_{EEF}$ $9.50x10^{-14}$). This scaffold was evaluated for target identification studies, indicating an affinity for the mitochondrial electron transport chain which we elaborate below.

With the exception of gametocyte-enriched clusters, of which five of nine share some ABS activity, most of the potent chemical space within the GHCDL is stage-specific. Among the 170 library-wide submicromolar inhibitors, 148 affected only one respective life-cycle stage. To explore the distribution of stage-specific inhibitors, the previously-generated cluster network was vetted for enriched, unique, scaffold families (Figure 2.8). Of the 87 submicromolar potent ABS inhibitors (96 hr PfLuc), 45 belonged to enriched scaffold families (Figure 2.7 and 2.8 red), 13 were structurally unique (singletons/doublets), and the remaining inhibitors were members of non-enriched clusters.

Subsequent cheminformatic analysis of PbLuc inhibitors validated their data: Of the 27 submicromolar compounds 12 were members of 9 distinct clusters (58 total nodes with 4 to 11 nodes per cluster (Figure 2.7 and 2.8 green). In total, 9 of 10 enriched compound clusters with activity against *P. berghei* were stage-specific (excluding multistage EEF cluster 3452). All alkyl derivatives of cluster 756 qualified for dose response testing, with two representatives, DDD01027733 and DDD01027481 (p-values$_{EEF}$ $8.94x10^{-7}$) yielding an IC_{50} of 0.096 μM and 0.138 μM, respectively. An analog of the aforementioned substructure has shown inhibition of the human dihydroorotate dehydrogenase (DHOD), the *Plasmodium* homolog of which being a well

characterized target (Phillips MA and Rathod PK, 2010). Importantly, cytotoxicity in both DDD01027733 and DDD01027481 were > 25 μM in HepG2 hepatocytes.

Among the 26 submicromolar potent gametocyte inhibitors, 18 reside in 8 significantly enriched scaffold clusters (45 total nodes with 3 to 12 nodes per cluster) (Figure 2.7 blue line). Four of those scaffold families were unique to gametocyte inhibition, while five others contained at least one member with potency < 1 μM against the ABS. The enriched gametocyte-specific inhibitors comprise four distinct substructure families highlighted in Figure 2.8 (blue). Cluster 3033 echoes a similar substructure to the dual blood-stage active DDD01057018 from Figure 2.7 (cluster ID 2587). However, the nitrogen rich substitutions in DDD01058843 ($p\text{-value}_{GAM}$ $8.28x10^{-7}$) seemingly absolve its ABS potency, while retaining potent gametocytocidal activity (Figure 2.8 blue). The core hexahydrobenzo[4,5]thieno[2,3-d]pyrimidine of cluster 2247 (Figure 2.7) has reported *Plasmodium* dihydrofolate reductase (PfDHFR) inhibition (Leeza Zaidi S et al.), although our library analogs contain a unique dihydropyrimidine substructure which may account for the lack of ABS activity seen in other DHFR inhibitors.

Gene Target Identification of Multistage Inhibitor.

A previously-noted, potent luciferase inhibitor, DDD01061024, also maintained activity against *Pf* ABS. In addition to reconfirming in our SYBR Green I assay (IC_{50}: 0.344 μM (Supplemental Dataset 3; List 1)), these blood-stage results were further validated by measuring its efficacy in a non-transgenic *Pf* Dd2-B2 line. Here, a lactate dehydrogenase (LDH) assay was used to assess the metabolic activity of treated and untreated parasites, yielding an IC_{50} of 0.521 μM (Figure 2.9b).

In order to identify the gene target of DDD01061024, we started by selecting resistant mutants from a wild-type population of *Pf* Dd2-B2. Three independent cultures containing roughly

$1.0x10^9$ parasites were treated with 10 times the IC_{50} concentration for 24 hrs. The few remaining viable parasites were allowed to recrudesce and were cloned by limiting dilution to generate a consistent genetic background. These mutant lines were considered resistant if their IC_{50} shifted 3-fold or more following the *in vitro* selection pressure. Altogether, we identified three resistant clones from two independently treated flasks, which maintained a 7.9 to 10.8-fold shift in potency relative to wild-type Pf Dd2-B2 (Figure 2.9b). Whole genome sequencing of these clones versus the parent line revealed a non-synonymous mutation in cytochrome b (PfCYTB; mal_mito_3). The resulting V259L substitution seemingly alters the Q_0 binding pocket shape within the cytochrome bc1 complex. Molecular docking studies against a *Pf* CYTB homology model suggest DDD01061024 occupies this quinone binding site in its lowest free energy state (Figure 2.9a). Several druggable targets within the *Plasmodium* mitochondrial electron transport chain have been previously described, including *PF*DHODH and *Pf*CYTB (Akhoon BA et al., 2014;Phillips MA and Rathod PK, 2010). For example, a commonly used prophylactic drug, atovaquone (in conjunction with proguanil), is known to target the Q_0 binding site of cytochrome bc1 (Siregar JE et al., 2015). Mutations within this site, and indeed at our V259L residue, were previously reported using other known cytochrome B inhibitors (Stickles AM et al., 2015). Atovaquone cross-resistance was also tested against wild-type Dd2-B2 and one mutant clone (2-G6). The IC_{50} against wild-type parasites was 0.377 nM, which jumped 11-fold to 4.19 nM in DDD01061024 mutants (Figure 2.9c).

Discussion

Previous efforts to identify multistage active antimalarials employed a stepwise screening approach where non-overlapping hits from latter tested stages would be lost. This approach, while

sometimes fruitful (Wu T et al., 2011), fixates on the few inhibitors with life-cycle spanning efficacy in a given library, and ignores the value of highly potent stage specific scaffolds. Given the rarity of multistage *Plasmodium* inhibitors found in small molecule libraries (Kato N et al., 2016), greater emphasis should be placed on combination therapies comprised of complementary inhibitors. This strategy is already used in the field with drugs like Malarone (atovaquone/proguanil), and several different artemisinin combination therapies (for example artemether/lumefantrine). However, except in a few cases like primaquine—ACT and atovaquone—proguanil, clinically approved combination therapies lack a gametocytocidal or liver stage component. To this end, we generated a panoramic view of bioactivity in the Global Health Chemical Diversity Library, marking the largest lifecycle-wide screening efforts in *Plasmodium* to date. Overall our data suggest the advantage in throughput using a luminescent reporter for ABS and liver stage screening outweighs the risk of detecting false positive luciferase inhibitors, despite reliance on repetitive counterscreening. This is evident by our consistent rediscovery of analogs to known antimalarials and emphasizes the predictive nature of our screening models. This work provides dozens of potential new starting points for development of symptomatic relief, transmission blocking, and prophylactic drugs; the latter two being critical components highlighted by the Medicine for Malaria Venture's call to new therapies (Burrows JN et al., 2017). It remains unclear if the lack of pan-active inhibitors here is a function of the chemical space explored by the GHCDL, or if the probability of finding such inhibitors is exceptionally low. With an abundance of hits throughout the parasitic life-cycle, cheminformatic analysis allowed for a probabilistic determination of scaffold activity. Nearly half of these hits belonged to enriched bioactive clusters, thus establishing a structure activity profile which can be leveraged by groups in lead development.

While we continue focusing on these enriched sets, we acknowledge that many potent singletons remain. Thus, all screening data will remain open access as tools for future investigation.

The overall prevalence of ABS inhibitors versus that of stage V GAMs is perhaps unsurprising given the relatively few essential pathways known to exclusively disrupt sexual stage function (such as translation repression (Mair GR et al., 2006), autophagy (Cervantes S et al., 2014), or meiosis (Delves MJ et al., 2013)). Nonetheless, with conserved blood stage targets including protein translation (targeted by puromycin), protein secretion (KAF156), or protein degradation (carmaphycin B and epoxomycin), a higher incidence of dual blood-stage inhibitors (versus either with exoerythrocytic forms) is more likely. Still, numerous structurally distinct scaffolds with concurrent liver and ABS activity have been linked to mitochondrial electron transport chain disruption (Antonova-Koch Y et al., 2018). This is in-line with our findings of DDD01061024 and its proposed target, cytochrome-bc1.

By exclusively testing against stage V GAMs in our sexual-stage screens, we likely missed inhibitors that act on fully differentiated forms occurring within the mosquito midgut. However, compounds which effect mature intraerythrocytic sexual stages have shown contraceptive effect in mosquitos by standard membrane feeding assays (SMFA) (Plouffe DM et al., 2016). While SMFAs remain the gold standard for testing a compound's transmission blocking capabilities, their overall throughput makes large scale screening impractical. Furthermore, as stage V gametocytes persist in the host's bloodstream for days, interventions there present a pharmacodynamic advantage to the fertilization window occurring over minutes within the mosquito midgut.

Despite potentially missing some liver stage inhibitors by using a murine malaria species, the practical advantages of *P. berghei* as a surrogate of liver stage infection are noteworthy. In addition to the safer handling characteristics of murine malaria, the acquisition of human malaria

species is more expensive and produces less sporozoites per mosquito, decreasing screening efficiency. This limitation to throughput is compounded by a decreased *in vitro* infection rate of human infecting malaria parasites. Furthermore, prophylactic drugs like Malarone (specifically the atovaquone component) show significant potency against our model, while the liver stage activity of other clinical candidates (Meister S et al., 2011) were identified by similar methods.

In conjunction with limited access to clinics and an abundance of counterfeit pharmaceuticals (Ambroise-Thomas P, 2012), the lack of patient adherence to scheduled therapy is a consistent problem which drives selection pressure in favor of drug resistance. While the search for a single dose radical cure therapy continues, the fact remains that all ABS treatments to date have varying degrees of resistant malaria parasites in the field (McClure NS and Day T, 2014). Thus, there is intrinsic value in the pursuit of prophylactic and transmission blocking therapies as a means of global malaria eradication; starting points for which could be contained in this work.

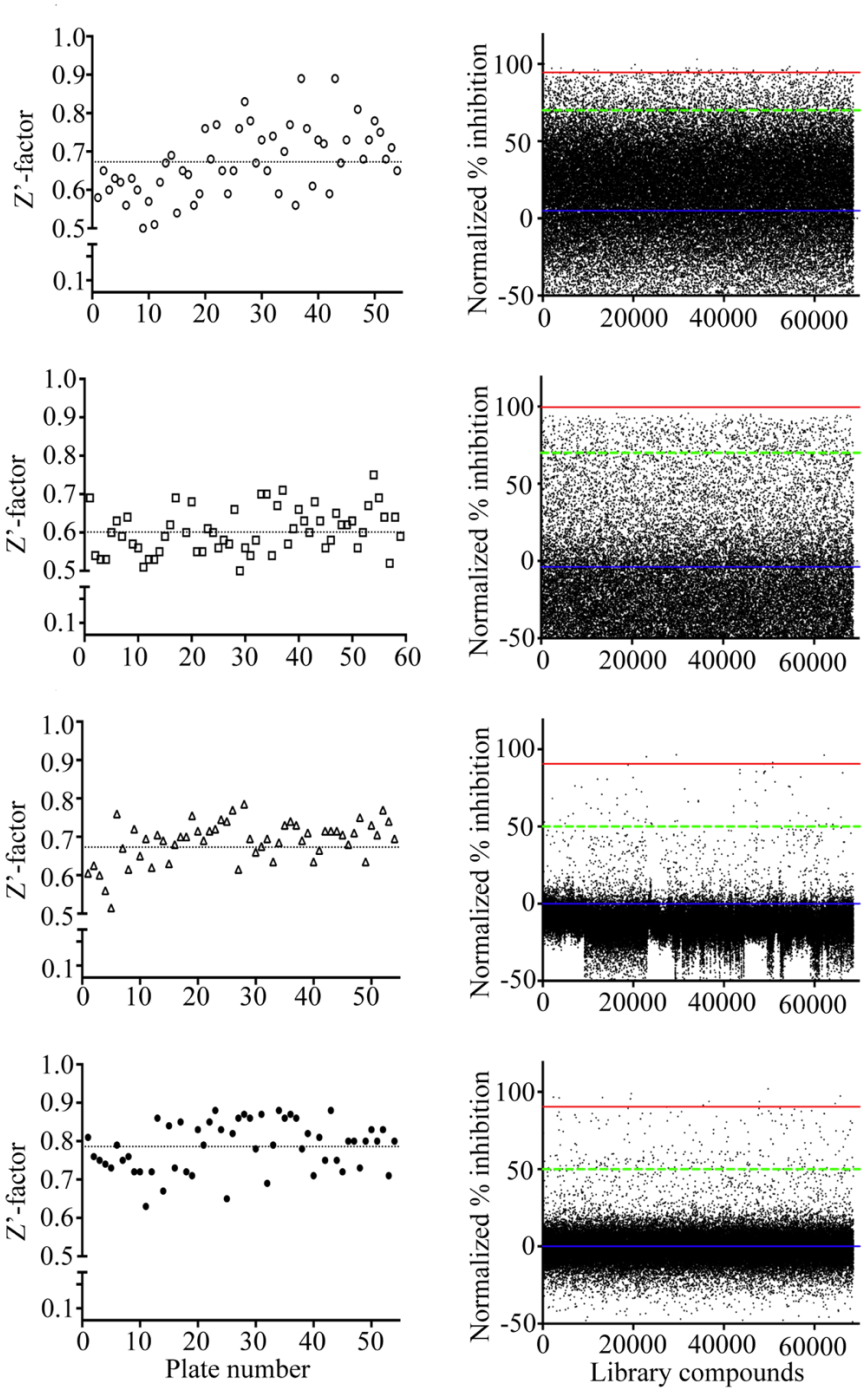

Figure 2.1. Primary screen assay statistics. The Z'-factor was calculated per plate throughout the GHCDL HTS campaign. Screen averages (± SD) included **a,** 0.67±0.089 PbLuc (○), **b**, 0.60±0.062 ABS (•), **c**, 0.69±0.054 stage V GAMs (Δ), and **d**, 0.79±0.065 HepG2 cytotoxicity (●). Averages are depicted for each screen by the dotted line, and plates with a Z'-factor below 0.5 were repeated. Library-wide inhibition plots (column 2) show compound activity (black spots) with mean negative control (blue line), mean positive control (red line), and cutoff criteria for subsequent screening (green dashed line).

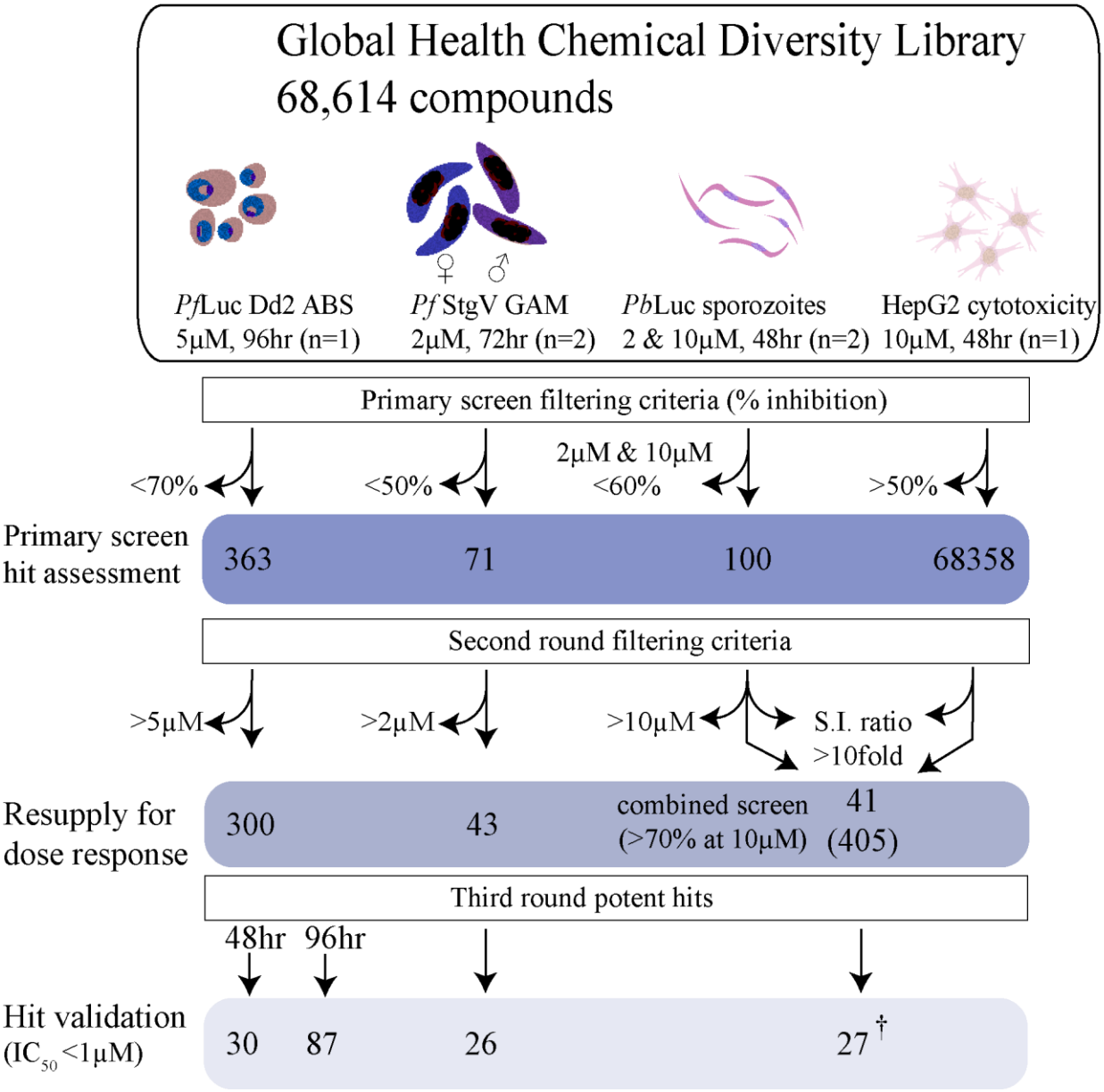

Figure 2.2 Global Health Chemical Diversity Library screening workflow. A set of 68,614 small molecules was sequentially screened across the *Plasmodium* life-cycle. Horizontal arrows indicate the removal of unqualified compounds at a given criterion while vertical arrows track the progress of desirable ones. Primary screening data were filtered by inhibition to generate a list of reconfirmation worthy hits. Commercially-available compounds were resupplied and reconfirmed in dose-response to round off a series of potent leads.
† total includes future designated rLuc inhibitors

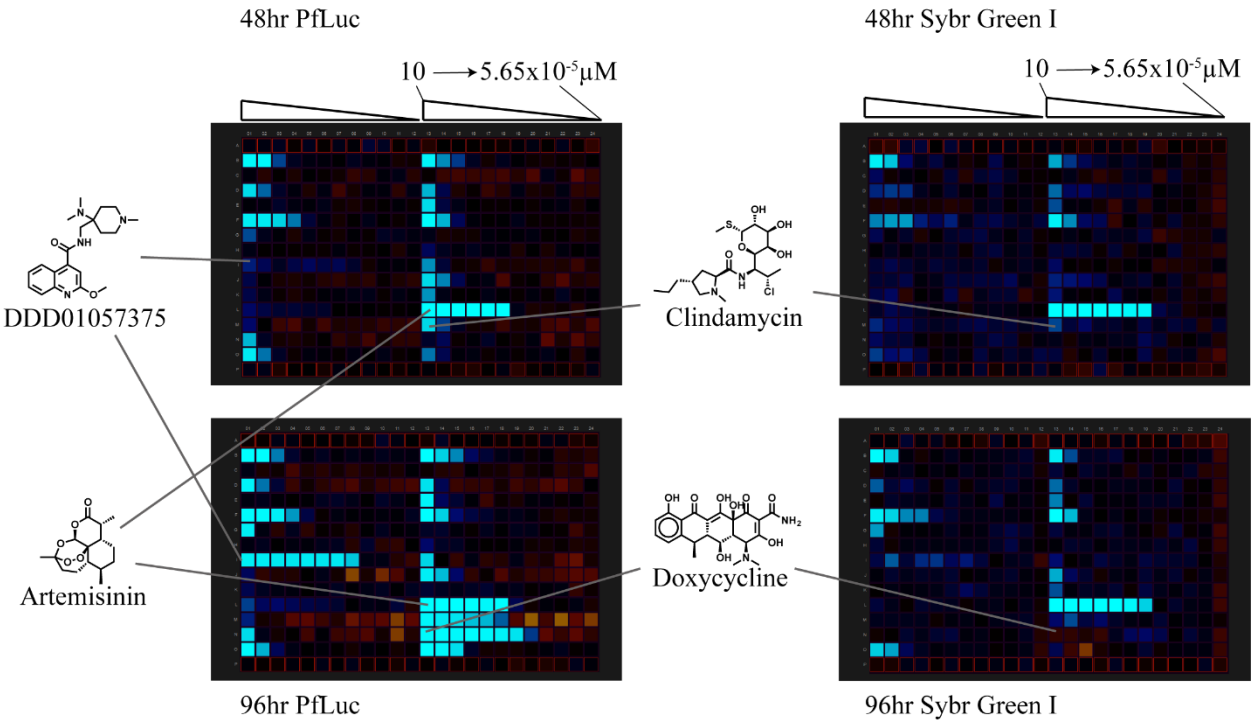

Figure 2.3 A comparison of ABS assay sensitivity for detection of delayed-death inhibitors. Compounds were titrated in dose response and in identical patterns across all four representative plates shown. Artemisinin controls are positive for parasite death (turquoise) at all time points, and in both readouts. Delayed-death controls, clindamycin and doxycycline, give a sharp inhibitory contrast between 48 hr and 96 hr PfLuc, but look equally inactive with a SYBR Green I endpoint. Our highest potency ABS inhibitor, DDD01057375, shows a similar trend to the delayed-death controls.

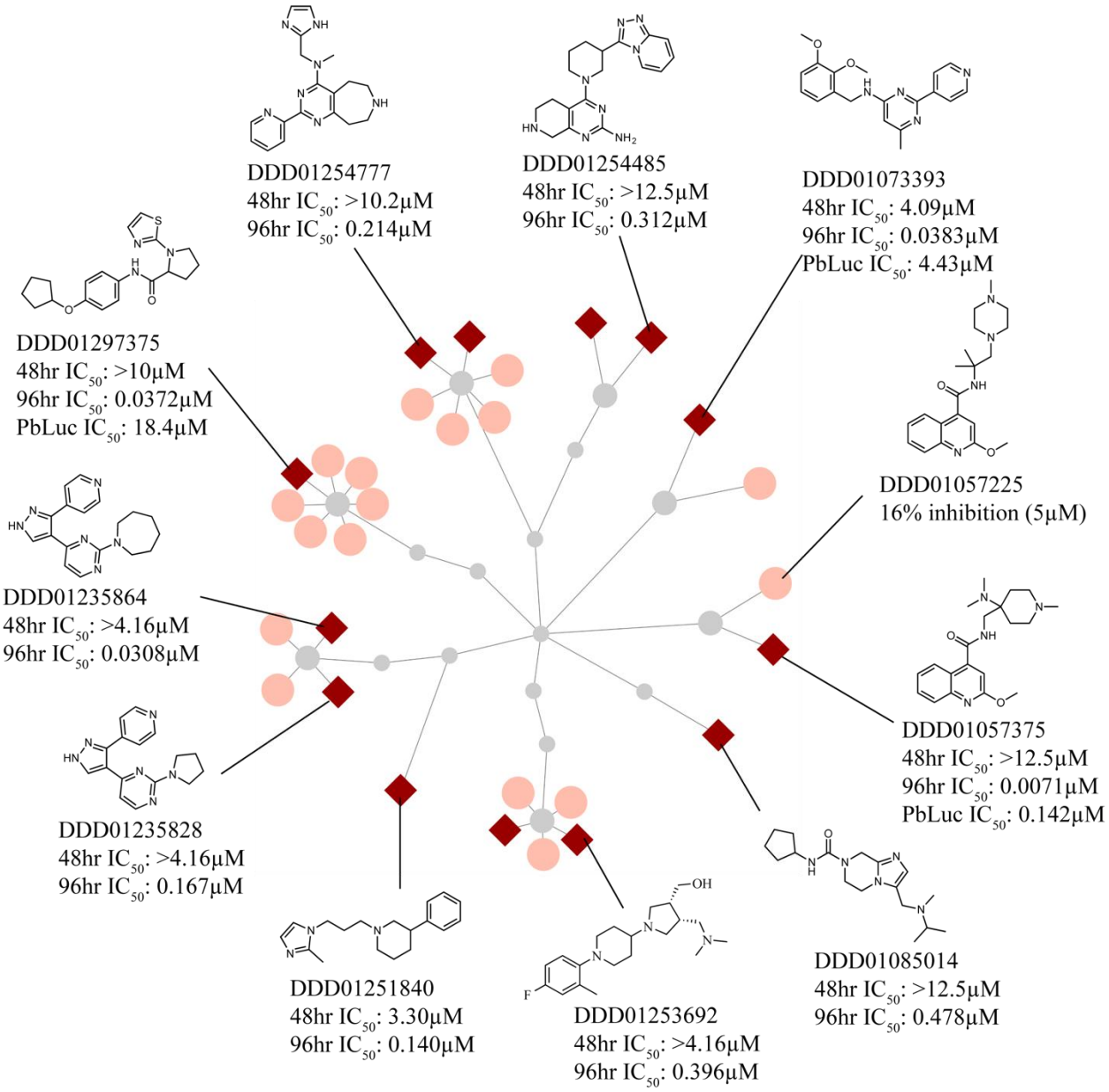

Figure 2.4 *P. falciparum* ABS delayed-death inhibitors.
Compounds with preferential activity on the second generation of ABS are shown clustered with their structural nearest neighbors (DSC > 0.7) from the GHCDL. Perimeter nodes have an IC_{50} < 1 µM (◆), or had no activity (●). The central node of perimeter clusters represents the maximum common substructure (MCS), while each layer within the scaffold tree represents overall ring count, starting from 1 at the figure center.

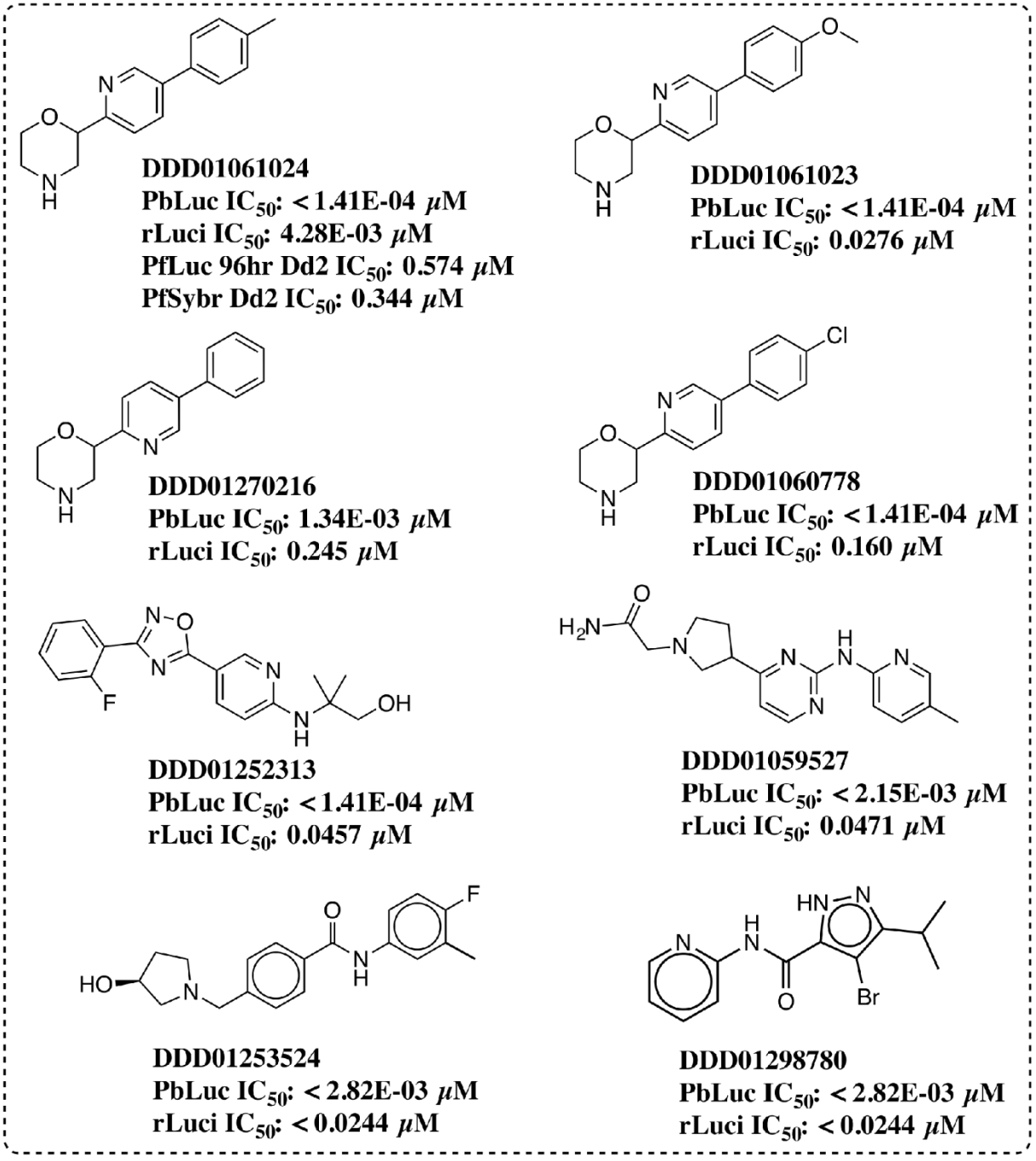

Figure 2.5 Recombinant luciferase inhibitors. Compounds tested against firefly luciferase in dose response produced potent inhibition of overall bioluminescence. A cluster of four closely related analogs is heavily enriched in an otherwise diverse pool of molecules

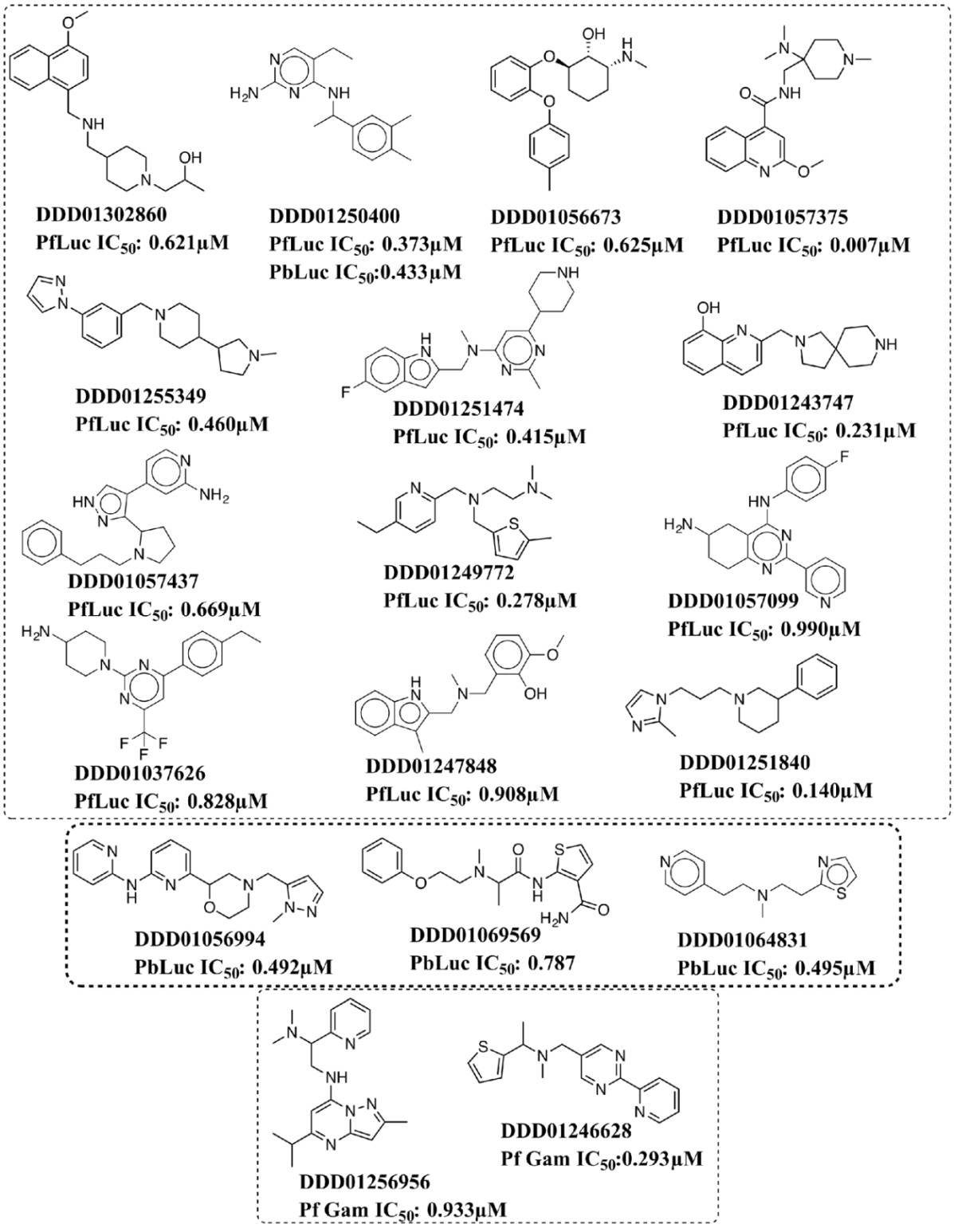

Figure 2.6 Potent low structural similarity hits (top=ABS, middle=EEF, bottom=GAM). Structurally distinct scaffolds with two or fewer members following chemical clustering. *P. falciparum* Dd2 dose response values are shown for the 96 hr time point.

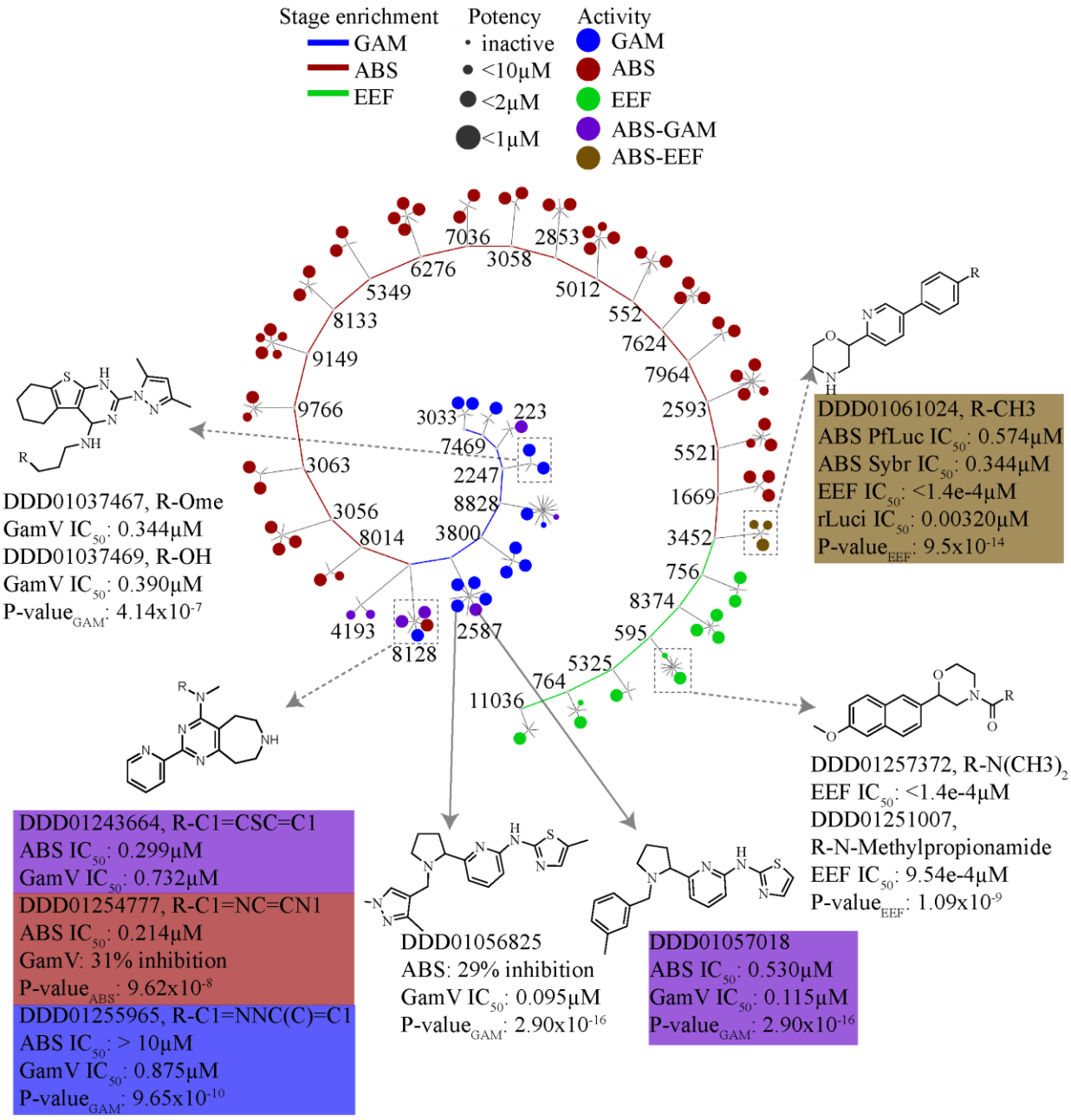

Figure 2.7 Potent multistage and stage-specific enriched clusters. The GHCDL was clustered by chemical fingerprint similarity, whereby edges connect nodes with a Dice similarity coefficient of > 0.7. The hypergeometric mean was calculated for each cluster, and only those enriched for bioactivity are shown (P-value < 0.005). Each perimeter node represents one compound whereby potency increases with size, while the central node of each cluster represents the maximum common substructure (MCS). Clusters are anchored to each other based on their affinity for a given life-cycle stage, while multistage active compounds are further differentiated by color.

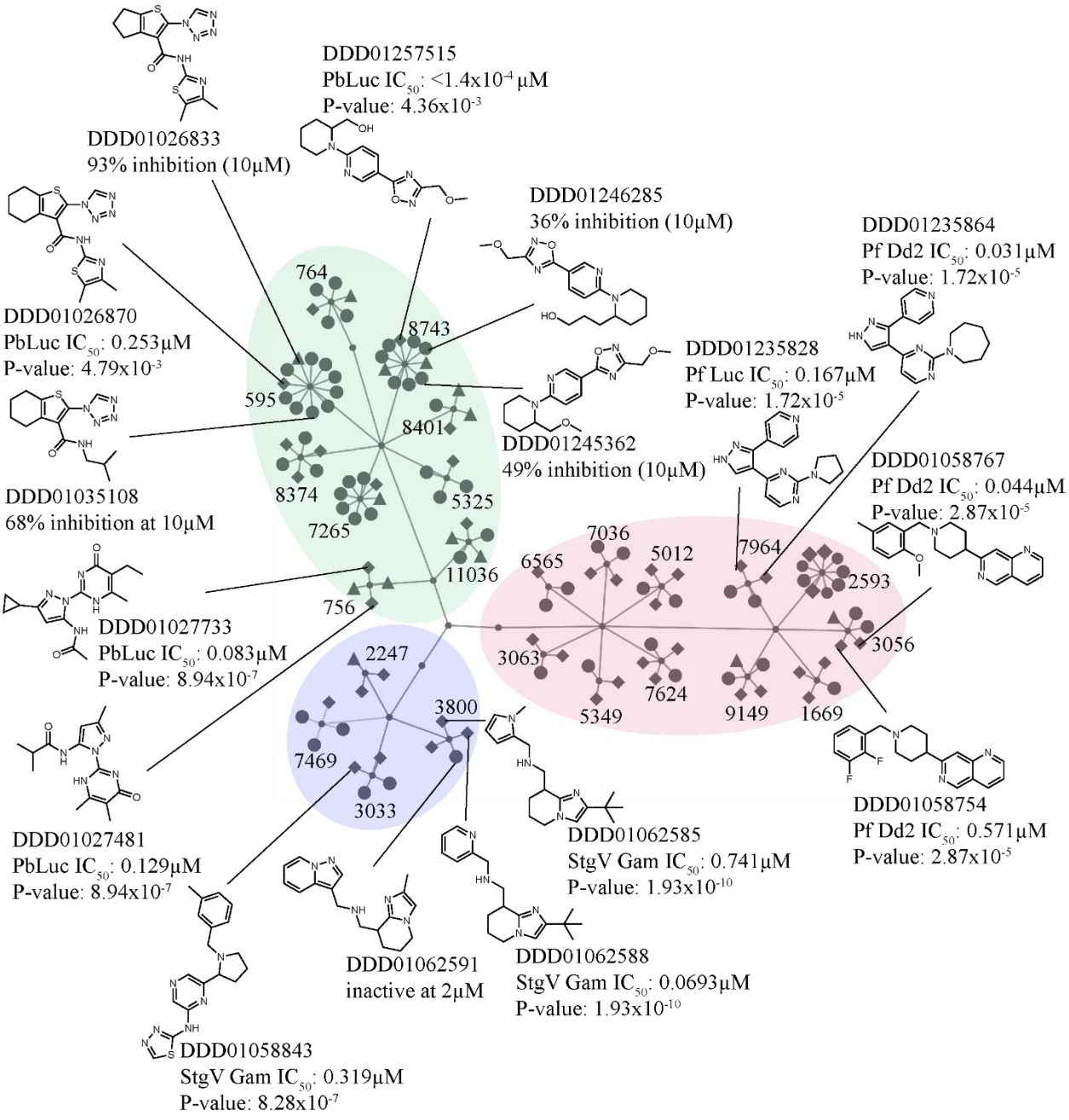

Figure 2.8 Bioactive enrichment of stage specific inhibitors. The intrinsic library-wide structure activity relationships highlight differences in cluster efficacy. Only nodes with single stage activity and their inactive but structurally similar neighbors are shown. Compound nodes with dose response potency < 1 µM (◆), primary screen hit selection (▲) or inactivity (●), are separated between the ABS (red), stage V gametocytes (blue), or liver stages (green). All clusters have an enrichment score of $p < 0.005$ for their respective stage of activity.

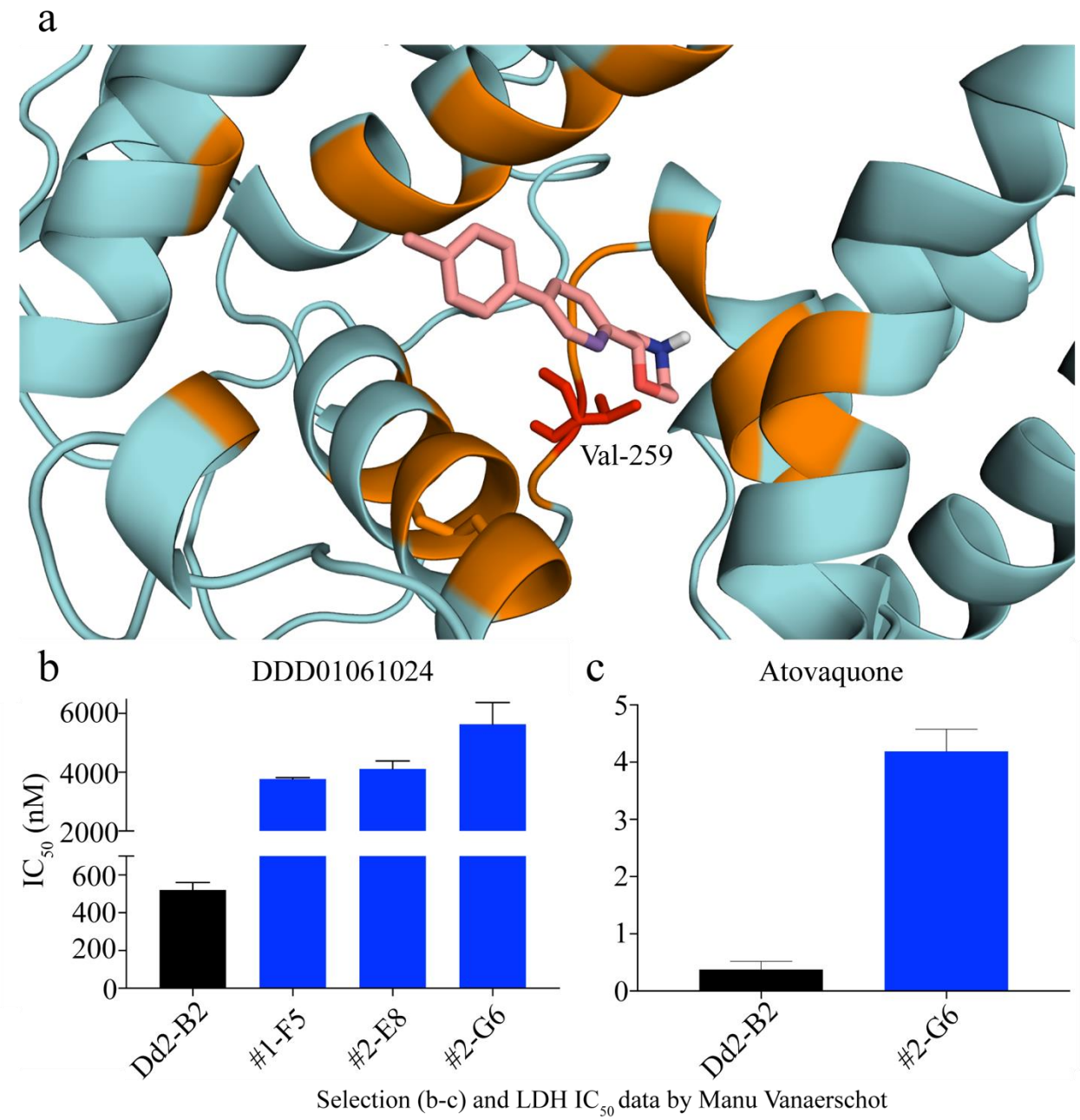

Figure 2.9 *P. falciparum* cytochrome b homology model molecular docking profile. The affinity of dual stage inhibitor, DDD01061024, is shown occupying the Q_0 site of a Pf Cyt Bc1 homology model (from PDB: 1BE3) (a). A local V259L substitution (red) in mutant clones may destabilize the interactions within this pocket, helping resistant clones tolerate higher doses of the inhibitor (b). This effect is exemplified by cross resistance to atovaquone (c), another multistage active antimalarial which targets the Q_0 binding site.

Acknowledgements

Matthew Abraham (M.A.) designed experiments, performed PbLuc and ABS reconfirmation HTS assays, analyzed data, and wrote the manuscript. David M. Plouffe (D.M.P.), Melanie Wree (M.W.), and Alan Y. Du (A.Y.D.) performed the sexual stage HTS assays and analyzed data. Kerstin Gagaring (K.G.) and Marisa L. Martino (M.L.M.) performed ABS HTS assays and analyzed data. Yevgeniya Antonova-Koch (Y.A.-K.) and Korina Eribez (K.E.) performed liver stage HTS assays. Manu Vanaerschot (M.V.) selected for compound resistant parasites in the ABS. Madeline R. Luth (M.R.L.) performed whole genome sequencing analysis of resistant ABS parasites. Sabine Ottilie (S.O.) procured and managed compounds. David A. Fidock (D.A.F.) and Case W. McNamara (C.W.M.) provided advice and wrote the manuscript. Elizabeth A. Winzeler (E.A.W.) analyzed data and wrote the manuscript.

Chapter 2, in full, has been accepted for publication for the material as it may appear in the *American Chemical Society Infectious Diseases*, 2020. Matthew Abraham, Kerstin Gagaring, Marisa L. Martino, Manu Vanaerschot, David M. Plouffe, Jaeson Calla, Karla P. Godinez-Macias, Alan Y. Du, Melanie Wree, Yevgeniya Antonova-Koch, Korina Eribez, Madeline R. Luth, Sabine Ottilie, David A. Fidock, Case W. McNamara, Elizabeth A. Winzeler “Probing the Open Global Health Chemical Diversity Library for Multistage-Active Starting Points for Next-Generation Antimalarials” The dissertation author was the primary investigator and author of this manuscript.

3. Selective inhibition of cytoplasmic isoleucyl-tRNA synthetase with a dual stage active scaffold in *Plasmodium*

Abstract

Aminoacyl-tRNA synthetases are essential protein-building precursors with evolutionarily conserved functions in most organisms including *Plasmodium* and humans. Using *in vitro* evolution and whole genome analysis (IVIEWGA) in *P. falciparum*, confirmed by CRISPR-Cas9-based gene editing, we show that cytoplasmic isoleucyl-tRNA synthetase is the gene target of a thienopyrimidine-derived antimalarial scaffold identified by a GSK phenotypic screen. This activity decreases the rate of protein translation, as shown by a concentration-dependent reduction of radiolabeled methionine/cysteine within ABS parasite proteins. Furthermore, this scaffold confers submicromolar inhibition of both the ABS and liver stage, with no significant hepatotoxicity (IC_{50} > 10 μM). These data highlight a clinically unutilized target in *Plasmodium* that is essential in multiple stages of development, and provide starting points for future drug design.

Introduction

For diseases like malaria that primarily affect the poor, rapid advancement toward new therapies has the potential to save tens of thousands of lives annually. Global efforts toward this common goal have produced expansive, open access, datasets that can catalyze drug development. One example includes the Tres Cantos Antimalarial Compound Set (TCAMS) (Gamo FJ et al., 2010), whereby GlaxoSmithKline (GSK) disclosed 13,533 compounds which reproducibly inhibited *P. falciparum* ABS. Among this set were scaffolds theorized to affect many different

targets including dihydrofolate reductase (DHFR), dihydroorotate dehydrogenase (DHOD), and several different aminoacyl-tRNA synthetases (aaRS). Both DHFR (Schweitzer BI et al., 1990;Yuthavong Y et al., 2012) and DHOD (Ittarat I et al., 1994;Phillips MA and Rathod PK, 2010) have been extensively studied, and compounds which target these proteins are currently undergoing clinical trials (Abbat S et al., 2015;Phillips MA et al., 2015). Although aaRS have been reported as promising antimalarial targets (Baragaña B et al., 2019;Herman JD et al., 2015;Nyamai DW and Tastan Bishop O, 2019), inhibitors of these proteins have not yet translated into first-line, clinically viable, drugs. In contrast, aaRS-targeting antibacterials like mupirocin (Nakama T et al., 2001) have been clinically utilized for decades (McCarthy M and MacCulloch D, 1987), and others continue through clinical trials (Koon HB et al., 2011). Mupirocin was also shown to target the apicoplast form of isoleucyl-tRNA synthetase in *P. falciparum* (Istvan ES et al., 2011). Two forms of isoleucyl-tRNA synthetase exist in *Plasmodium* (Bhatt TK et al., 2009), one of which is bound to the apicoplast and the other is located within the cytoplasm. Targeting either form is lethal, albeit a delayed-death is observed for the apicoplast effecting compound.

In general, organisms that undergo rapid cellular turnover, for example during the liver stage of *Plasmodium* development (Vaughan AM et al., 2012), would predictably show sensitivity to protein translation inhibitors like cycloheximide (Schneider-Poetsch T et al., 2010). However, in the liver stage of malaria, compounds targeting the aaRS have not been extensively studied. Here we show that the target of an ABS-active scaffold from the TCAM set is *P. falciparum* cytoplasmic isoleucyl-tRNA synthetase (cIRS). Point mutations, identified by whole genome sequencing of resistant parasites, were edited into parasites and shown to confer resistance. We further show that this compound rapidly blocks the incorporation of radiolabeled methionine/cysteine (^{35}S-Met/Cys) into protein. Finally, while lysyl-tRNA synthetase has

previously shown activity against the malaria liver stage (Hoepfner D et al., 2012), this is to our knowledge the first example of cIRS effecting compounds with submicromolar potency against exoerythrocytic forms of malaria, effectively broadening the scope of action for this target.

Results

TCMDC_124553 reconfirmation and multistage activity profile

Complete blood stage activity (mature gametocytes and asexual stages) has previously been established for TCAMs compounds (Almela MJ et al., 2015); however, causal prophylactic efficacy remains largely missing, in particular for our choice scaffold. In order to round out the life-cycle activity profile of this scaffold, fresh powders of two analogs TCMDC-123835 (MMV019266) and TCMDC-124553 were purchased from commercial sources. These analogs were part of a 6-member compound cluster (ID: 473) within the TCAM set, each with a submicromolar XC_{50} against *P. falciparum* ABS (range 0.19 – 0.88 μM) (Gamo FJ et al., 2010). Powders were reconstituted in DMSO for reconfirmation of ABS activity. Using a drug resistant *P. falciparum* Dd2 strain, potency for both compounds was reconfirmed < 1μM in 12-point dose response ($10 – 5.64x10^{-5}$ μM) over three biological replicates (Figure 3.2A) (see methods). These data reassured the quality of our new stocks, allowing for confident liver stage evaluation. Both analogs were tested in duplicate at 12-point dilutions ($50 – 2.82x10^{-4}$ μM) in 1536-well format using our standard *P. berghei* liver stage infection model discussed in previous chapters of this dissertation (see methods). While these compounds behaved similarly in the ABS, TCMDC-123835 with an IC_{50} of 0.0263 ± 0.007 μM (mean ± SD) showed greater potency for the liver stage than TCMDC-124553 at 2.48 ± 0.52 μM (Figure 3.1).

To ensure these effects were specific to the parasites and not the result of off-target host cell inhibition or interference of the bioluminescent luciferase readout, both analogs were counterscreened in assays which isolate each variable. As previously noted, the cytotoxicity counterscreen evaluates hepatocyte viability post compound incubation through the indirect measurement of available intracellular ATP. When compared to the DMSO (0.5%) negative control signal, neither of our compounds exceeded 41% (TCMDC-123835) HepG2 inhibition up to 50 µM across two independent replicates (Figure 3.1). To account for potential bioluminescent interference, we incubated our test compounds in dose response titrations (50 – $2.82x10^{-4}$ µM) with recombinant firefly luciferase (rLuc) for 30 minutes prior to the addition of luciferin. Because the components in each well are freely available to interact (independent of diffusion or shuttling of molecules across membranes), this assay was run in technical quadruplicate to maximize degrees of freedom. For the rLuc counterscreen, variance between the test plates for both positive (Luciferase Inhibitor II) and negative (DMSO) controls as calculated by the Z'-factor never fell below 0.63 (data not shown), suggesting a highly reproducible assay and supporting our favor of multiple technical replicates. The rLuc inhibition IC_{50} of TCMDC-123835 was lower overall than that of TCMDC-124553 at 12.9 µM (95% CI: 4.7 – 35.8 µM) and 19.5 µM (95% CI: 6 – 64 µM), respectively (Figure 3.1).

TCMDC_124553 target identification and validation

In order to determine the target of this scaffold, we selected resistant *P. falciparum* Dd2 parasites using a ramp-up method described elsewhere (Corey VC et al., 2016). TCMDC-124553 was used exclusively for these selections because the ABS potency is comparable with TCMDC-123835, they are structurally similar compounds (87% Tanimoto similarity), and an abundance of powder was commercially available for resupply. Because such selections can take many weeks

or even months to generate resistant parasites, having excess compound is favored over constantly reordering fresh supplies. Furthermore, potency can vary between commercially sourced batches, or the compound can become outright unavailable. To maintain a common starting genetic background, selections were run in three independent flasks originating from a single parental clone. Over a period of 217 days, each flask was subjected to increasing concentrations of compound starting from 2x IC_{50}, with daily tracking of culture health by Giemsa-stained blood smears. The resistance selections were stopped after the bulk, polyclonal, cultures yielded a 3-5x shift in IC_{50} compared to wild-type Dd2. During this process, all three cultures undergoing selections remained sensitive to our positive control, artemisinin. Clones from each replicate flask were isolated by limiting dilution and tested against our two analogs, revealing a common resistance pattern across all replicates (Figure 3.2B). Isolating individual clones was necessary to ensure DNA was only sequenced for parasites that maintained a resistant phenotype and that both compounds share a similar target (or resistance mechanism), which we observed by the prevalence of cross-resistance in clone G7.

With the confirmation of resistance in our selected lines, DNA from two clones per replicate flask (six clones total) was extracted and prepared for whole genome sequencing (WGS). Single nucleotide variants between these resistant clones and the wild-type Dd2 parent were called using our inhouse bioinformatics pipeline. To narrow the list of possible gene targets, filters were applied to remove regions of hypervariability (for example rifin and stevor genes (Lavazec C et al., 2006)). This yielded a total of 12 SNVs across all 6 flasks (Table 3.1). Only one gene, isoleucine tRNA synthetase (annotated: PF3D7_1332900), was common to all sequenced clones, although four different mutations were identified within. All identified mutations in our resistant lines were exclusive to the cytoplasmic isoleucyl-tRNA synthetase (cIRS) form. Only one of the

four independent mutations (amino acid change: E180D) was in the catalytic domain (Rossman fold) of cIRS (Rao ST and Rossmann MG, 1973); however, this variant conferred the most significant resistance shift (10-fold (Table 3.1)). The remaining three mutations (C502Y, V500A, S288I) maintained a 3-5 fold IC_{50} shift, and were all localized to the editing domain of cIRS.

To confirm that cIRS is the target of our scaffold and not a resistance mechanism, several mutations from our WGS data were introduced into an otherwise wild-type *P. falciparum* Dd2 background, using the CRISPR/Cas9 system. Specifically, one mutation was chosen from the catalytic (E180D) and editing domains (V500A) of our work, in addition to a tertiary L810F substitution previously shown to confer resistance in cIRS to the isoleucine analog thiaisoleucine (Istvan ES et al., 2011). The potency of TCMDC-124553 against our CRISPR/Cas9 engineered lines followed the same trend as the selected clones, with the E180D mutants producing a fold change greater (5.5x IC_{50}) than the V500A lines (3.4x IC_{50}) (Figure 3.3). In general, however, this shift was stunted when compared to the selected clones, suggesting a potential resistance contribution from mutations outside the cIRS gene. Conversely, the L810F engineered line which generated a ~2-fold resistant shift to thiaisoleucine became sensitized to TCMDC-124553.

Protein incorporation under compound pressure

Inhibition of canonical aminoacyl-tRNA synthetase function is expected to cause a decrease in protein translation (Vondenhoff GHM and Van Aerschot A, 2011). In order to further validate cIRS as the target of our scaffold, we measured the quantity of radioactively labeled ^{35}S-methionene/cysteine incorporated into newly synthesized parasite proteins, at various compound concentration. An effect would be most easily quantifiable during peak protein translation (Caro F et al., 2014); thus, experiments were conducted using synchronized trophozoites. When treated with 100x the IC_{50} concentration, TCMDC-124553 showed a similar decrease in amino acid

incorporation to cycloheximide (positive control) at the same concentration, while chloroquine (negative control) had no effect across all concentrations (Figure 3.4).

Discussion

The abundance of data generated from HTS campaigns can quickly over saturate the means for in-depth analysis of promising hits. In some cases, these expansive data sets contain attractive chemical starting points that, when made broadly available, can be leveraged to expand the field of druggable antimalarial targets. Our objective was to use WGS and reverse genetic engineering to identify and validate the target of an ABS potent scaffold cluster (ID: 473) from the GSK TCAM set. Furthermore, to illustrate the chemoprophylactic potential of this scaffold, cluster members were evaluated in a *P. berghei* liver stage model. This approached highlighted cytoplasmic isoleucyl-tRNA synthetase as the common gene target in compound resistant clones, with SNVs that maintained comparable resistance profiles when introduced into otherwise wild-type parasites.

Liver stage efficacy of our scaffold was reproducibly shown independent from host cell damage. Additionally, recombinant luciferase inhibition over 50% was only recorded at 50uM for both analogs and neither regression curve contained a top end plateau. This suggests that the true rLuc IC_{50} is closer to the upper end of the reported 95% confidence interval, and likely did not interfere with the PbLuc readout. Notably, TCMDC-123835 showed significantly greater liver stage potency than TCMDC-124553, despite their similar behavior in the *P. falciparum* ABS. This may result from decreased steric hindrance when accessing the *P. berghei* active site by the methyl substituted thienopyrimidine in TCMDC-123835. For example, another cluster member (TCMDC-124514) with an identical substructure, but missing any alkyl substitutions on the thienopyrimidine ring, was reported to be the most potent in ABS parasites (Gamo FJ et al., 2010).

Importantly, while the *P. berghei* cIRS protein shares limited sequence similarity (76.6%) to that of *P. falciparum*, all four residues highlighted by WGS in our resistant lines were conserved across species. A change in the binding pocket shape from the overall difference in protein sequence could however provide favorable access or interactions to TCMDC-123835.

Previous experience selecting for compound resistant mutants suggested that the time intensive ramp up method yielded greater success. However, an increase in culture time raises the likelihood that superfluous mutations will appear. Despite this risk, two key features in our sequencing data highlighted cIRS as the gene target of TCMDC-124553. Firstly, each independently treated flask and their respective clones have one mutant gene in common (PF3D7_1332900). Given the rate of mutation in *P. falciparum* (1-9.7x10^{-9} mutations/bp/generation) (Bopp SE et al., 2013) and the overall genome size (22.9MB (Gardner MJ et al., 2002)), the probability of these events occurring randomly in an essential gene is infinitesimally small. Secondly, the fear of cross-contamination is nullified by the presence of differing mutations represented across clones from each flask. Interestingly, TCMDC-124553 generated mutations in both the catalytic and editing domains of cIRS (Table 3.1), suggesting the compound has access to both binding pockets. Given the function of the editing domain, which is to remove or temporarily retain mischarged valine from IRS (Fukunaga R and Yokoyama S, 2006), we presume an inhibitor with favorable properties for one active site could reasonably access the other.

P. falciparum parasites resistant to the isoleucine analog, thiaisoleucine, were previously reported only to contain a mutation (L810F) in the synthetic site (Rossman fold) (Istvan ES et al., 2011). Our clones with editing site mutations are predictably more sensitive to TCMDC-124553 and TCMDC-123835 than the E180D Rossman fold mutants. This is because the inability to

successfully charge tRNAs will likely have a greater penalty than an increase in mis-synthesized valyl-adenylate frequency. Surprisingly, however, the thiaisoleucine resistance conferring mutation L810F showed increased sensitivity to TCMDC-124553. The reason for this is unclear, but the influence of a larger phenylalanine could favorably alter the binding pocket for access by our scaffold. We successfully recapitulated the resistance phenotype in wild-type Dd2 parasites by introducing single amino acid changes from clones 1-A5 (E180D) and 2-G7 (V500A); thus, validating the interaction between our scaffold and cIRS. This relationship was further validated by the predicted impact of TCMDC-124553 on protein translation.

Leveraging previously reconfirmed hits provided a head start in our pursuit of new antimalarial targets. With our scaffold generating mutations along both ligand binding domains in the protein target, a clear mechanism of action is presently unknown. Further evaluation is required to differentiate the relative impact on parasite viability from perturbances in translational editing versus tRNA charging. Importantly, our results suggest that cIRS is a worthy target in *Plasmodium*, and that the activity profile precedes the erythrocytic stage of disease.

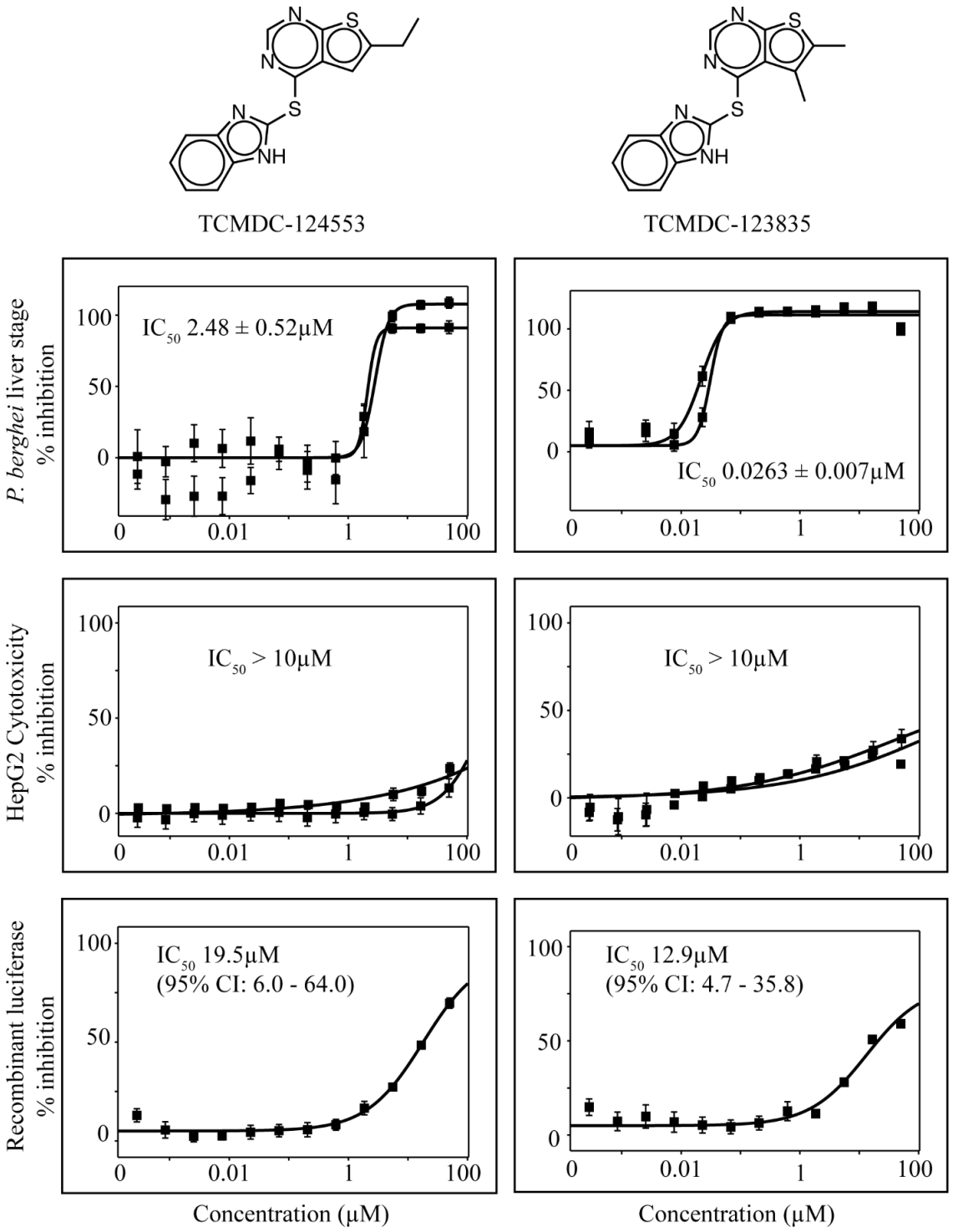

Figure 3.1 Efficacy of potent ABS compounds TCMDC-124553 and TCMDC-123835 against PbLuc liver stages and counterscreens. Both analogs generate sigmoidal dose response curves against EEF when normalized to atovaquone (positive controls) and DMSO (negative control), but showed no significant cytotoxicity up to the highest tested concentration (10μM). PbLuc and HepG2 screens were run in biological duplicate, while recombinant luciferase screen was tested in technical quadruplicate (error bars = SD).

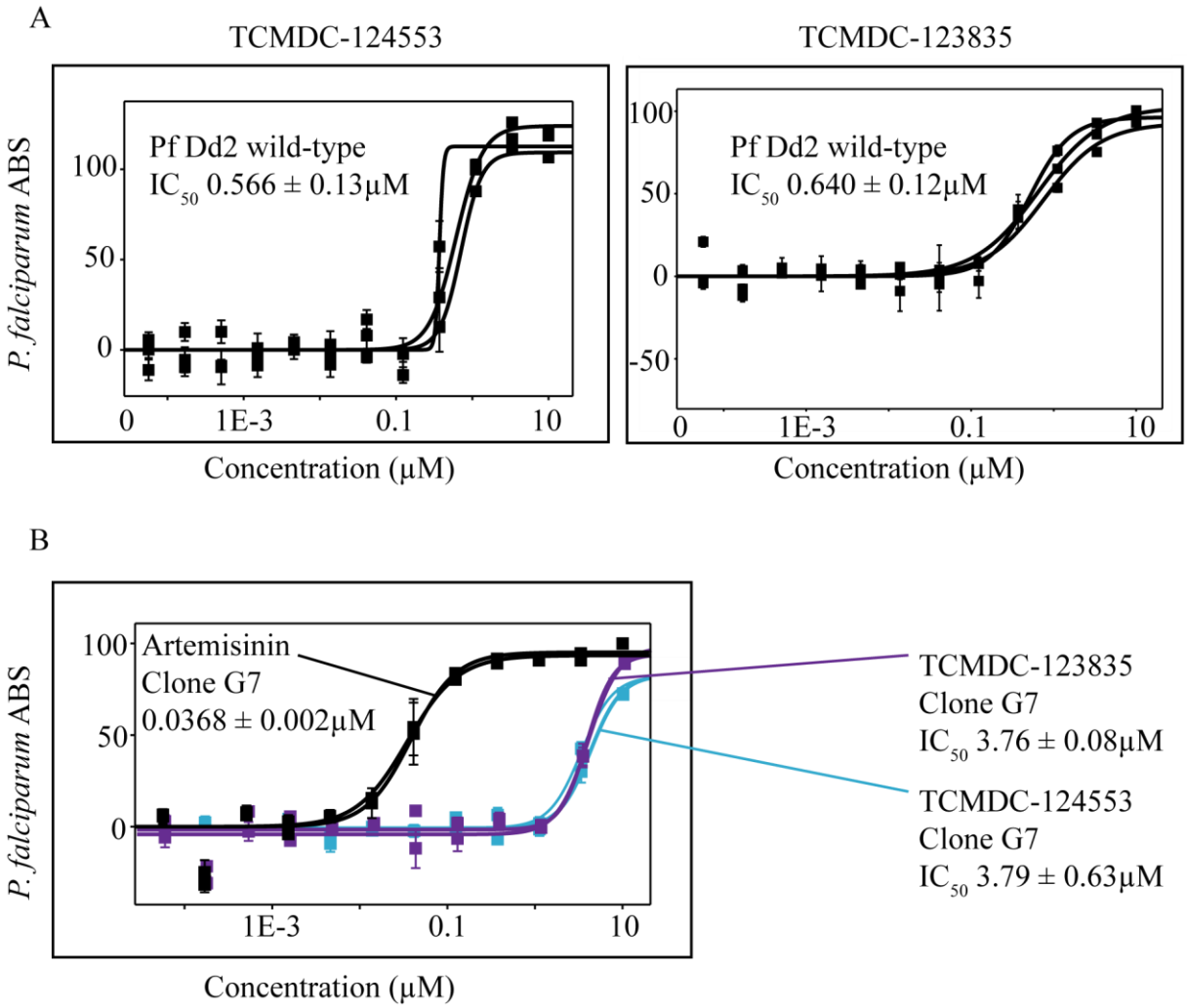

Figure 3.2 ABS potency of analogs TCMDC-124553 and TCMDC-123835 in wild-type and resistant *P. falciparum* Dd2. (a) Fresh stocks of both analogs generated repeatable submicromolar inhibition of wild-type Dd2 (shown as biological triplicate mean IC_{50} ± SD). (b) Mutant clone G7 selected for resistance against TCMDC-124553 showed cross resistance to analog TCMDC-123835, while remaining sensitive to the positive control artemisinin (IC_{50} mean in biological duplicate ± SD).

Table 3.1 Whole genome sequencing calls from TCMDC-124553 resistance parasites. DNA from six resistant clones of three independently selected flasks were comparted to a wild-type *P. falciparum* Dd2 parent. A single common gene across all clones (cytoplasmic tRNA synthetase: PF3D7_1332900) contained 4 distinct mutations, with those residing in the catalytically relevant Rossman fold (E180D) contributing the greatest resistance shift.

Flask-Clone	Gene Description	a.a. change	IC50 fold change
1-A5	**isoleucine tRNA synthetase (PF3D7_1332900)**	E180D	10.8
1-C3	transcription factor with AP2 domain (PF3D7_1222600)	K2207N	8.7
	isoleucine tRNA synthetase (PF3D7_1332900)	E180D	
2-A9	zinc finger protein 2C putative (PF3D7_1205500)	H689P	4.3
	isoleucine tRNA synthetase (PF3D7_1332900)	C502Y	
2-G7	**isoleucine tRNA synthetase (PF3D7_1332900)**	V500A	5
	Pf conserved membrane protein (PF3D7_0903300)	Y14*	
3-E3	translocation protein SEC63 (PF3D7_1318800)	R284G	3
	isoleucine tRNA synthetase (PF3D7_1332900)	S288I	
3-A1	**isoleucine tRNA synthetase (PF3D7_1332900)**	S288I	3.7
	Pf conserved protein (PF3D7_1027000)	D126E	
	Pf conserved protein (PF3D7_0811700)	E605D	

Sequencing data analyzed by Annie Cowell

Table 3.1 Whole genome sequencing calls from TCMDC-124553 resistance parasites, Continued

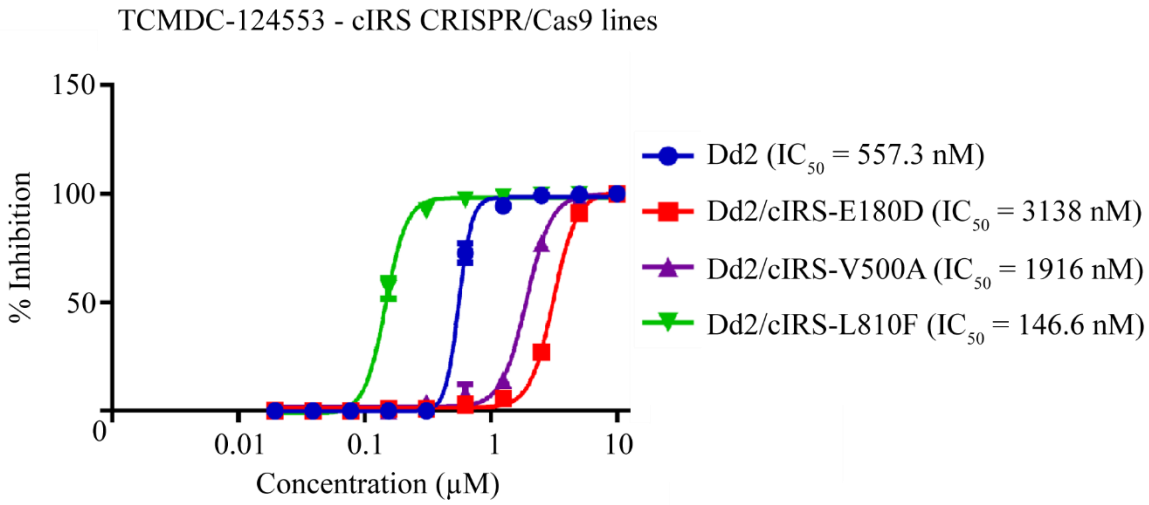

	Resistant selections (Dd2)	CRISPR edited (Dd2)
	IC_{50} (µM)	
Dd2 wild-type	0.566	0.577
Dd2/cIRS-E180D	6.12 (fold change = 10.8)	3.14 (fold change = 5.5)
Dd2/cIRS-V500A	2.83 (fold change = 5)	1.92 (fold change = 3.4)

Data generated by Krittikorn Kümpornsin

Figure 3.3 CRISPR/Cas9 engineering of compound selected resistance mutations into wild-type *P. falciparum* Dd2. Single amino acid changes in the editing (V500A) and tRNA charging (E180D) domain of cIRS resulted in a resistance shift consistent with selected lines. Dose response assays were normalized against artemisinin (positive control) and DMSO (negative control) in duplicate (error bars = SD).

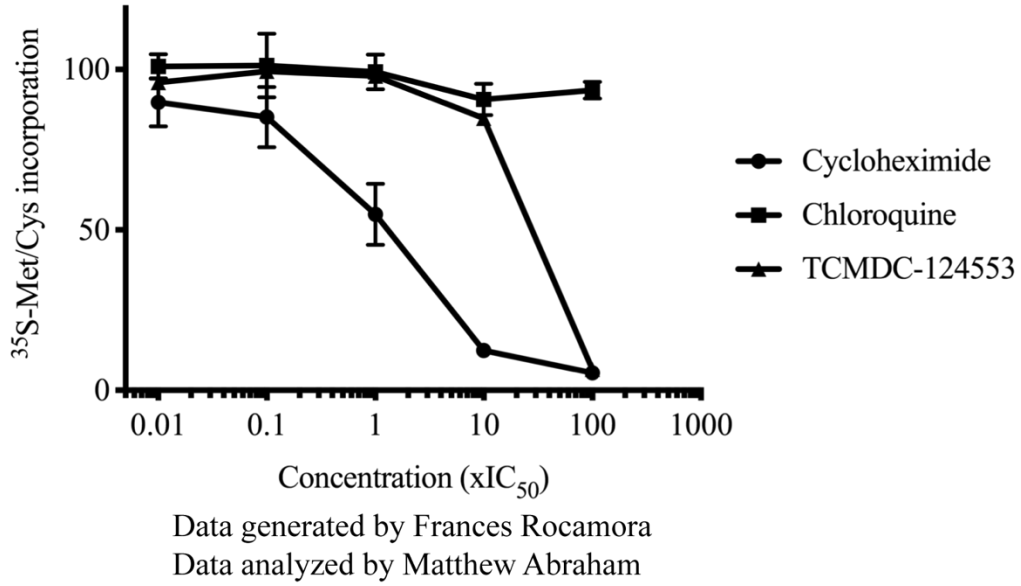

Figure 3.4 TCMDC-124553 diminishes protein synthesis in *P. falciparum* ABS. Protein synthesis was evaluated using ^{35}S radiolabeled methionine and cysteine in trophozoite synchronized parasites. *P. falciparum* samples were treated at 5 concentrations (increasing by a factor of 10 from 0.01 – 100 times the IC_{50}) for 1 hour before their extraction, whereby percent incorporation was normalized to the signal measured in untreated parasites. Data points represent average counts over three biological replicates ± standard deviation.

Acknowledgments

Matthew Abraham (M.A.) designed experiments and wrote the manuscript draft. Compound resistant parasites were selected by M.A., and IC_{50} experiments performed in conjunction with Dylan Hutson (D.H.). Whole-genome sequencing (WGS) was performed by Annie N. Cowell (A.N.C.) and the UCSD Institute for Genomic Medicine Core Facility. WGS analysis was performed by A.N.C. CRISPR/Cas9 editing and resistance IC_{50} experiments were performed by Krittikorn Kümpornsin (K.K.) and Marcus Lee (M.L.). Radiolabeled methionine/cysteine experiments were performed by Frances Rocamora (F.R.) and analyzed with M.A. Sabine Ottilie (S.O.) sources compounds and facilitated collaborations. Elizabeth A. Winzeler (E.A.W.) analyzed data and wrote the manuscript draft.

Chapter 3, in part, contains material that may be prepared for publication at a future time with co-authors including Annie N. Cowell, Frances Rocamora, Sabine Ottilie, Dylan Hutson, Marcus C.S. Lee, and Elizabeth A. Winzeler. The dissertation author was the primary investigator and author of this manuscript.

Methods

Compound libraries

Marine Natural Product Library. In total, 145 marine natural products were provided courtesy of the Gerwick lab from the Scripps Institute of Oceanography, UC San Diego. All screening compounds were provided with a minimum of 15µL and a concentration of 1 mg/mL. Compound purities varied from 60% to > 98% due to their extracted nature.

Global Health Chemical Diversity Library. This collection of 68,614 compounds was compiled by University of Dundee, Scotland and generously provided for screening against the Bill and Melinda Gates Foundation priority pathogens. Compounds were sourced from commercial vendors following the filtration of undesirable chemotypes. These include structural alert filters from Eli Lilly, University of Dundee, and Pan-Assay Interference Compounds (PAINS)(Baell JB and Holloway GA, 2010;Bruns RF and Watson IA, 2012).The library was curated to interact with a diverse range of biological targets and is available for 25 screens over 3 years.

Evolution of hectochlorin resistant *S. cerevisiae*

To generate hectochlorin-resistant *S. cerevisiae,* sub-lethal concentrations of hectochlorin were added to a conical tube containing 25 µl of saturated ABC_{16}-Monster cells, and 20 ml YPD media. Each culture was grown to saturation under shaking incubation, diluted into fresh YPD media and subjected to increasing concentrations of hectochlorin. Multiple rounds of selection were performed until resistance was confirmed by a two-fold dilution IC_{50} assay comparing resistant cells to the parental cell line. Cultures identified as resistant were streaked out onto YPD agar plates containing Hectochlorin to select for single colonies. Subsequent IC_{50} assays determined the degree of evolved resistance in single colonies compared to the parent strain.

Evolution of compound resistant *P. falciparum* Dd2

Step-wise selections (TCMDC-124553): Approximately $1x10^9$ parasites were treated at 2-3x IC_{50} concentration to determine culture tolerance. Compound concentration was increased incrementally based on daily examination of parasite health, aiming for a reduction in growth rate of 50%. Compound pressure was maintained until cultures achieved a reproducible IC_{50} shift of 3 to 5-fold. The maximum culture tolerated concentration of TCMDC-124553 before this shift occurred was ~5x IC_{50}.

High-pressure selections (DDD01061024): Approximately $1x10^9$ parasites were treated at 5-10x IC_{50} concentration for 2-3 days, or until no visible parasites remained by Giemsa blood smear. Following compound treatment, cultures were washed with complete daily and allowed to recrudesce. Using the selecting compound, bulk cultures were tested in dose response to measure for a 3 to 5-fold shift in IC_{50}. If necessary, treatment was reinstated.

Whole genome sequencing

Using the YeaStar Genomic DNA Kit (Zymo Research), genomic DNA was isolated from resistant clones for whole genome sequencing. The Illumina Nextera XT kit was used to prepare sequencing libraries following a standard dual indexing protocol. One hundred base pair paired-end reads were generated using the Illumina HiSeq 2500 in RapidRun mode. Reads were aligned to the *S. cerevisiae* 288C reference genome using BWA-mem and processed with Picard Tools (http://broadinstitute.github.io/picard/). GATK HaplotypeCaller was used to call SNVs and INDELs, which were further filtered based on GATK recommendations and annotated with SnpEff. Mutations that were present in both resistant strains and the parent strain were removed, so that only mutations which arose during the resistance evolution process were retained.

Parasite pellets were extracted from infected red blood cells using 0.05% saponin. Genomic DNA was either extracted immediately, or the parasite pellet was stored at -80C until needed. To extract the gDNA, a DNeasy Blood and Tissue Kit (Qiagen) was utilized by following the included protocol. Samples were provided to UC San Diego Screening Core to prepare the sequencing libraries. The Illumina HiSeq 2500 was used to sequence 100 base pair fragments. The in-house Platypus pipeline was utilized as previously described (Manary MJ et al., 2014) following read alignment to the P. falciparum 3D7 reference genome v13 (PlasmoDB). Single nucleotide variants were called using HaplotypeCaller from GATK, and the recommended filters were applied.

CRISPR/Cas9 allelic exchange in *S. cerevisiae*

CRISPR/Cas9 mediated single base-pair substitution was conducted on the *S. cerevisiae* ABC_{16}-Monster strain to obtain cells with a mutation in Act1. Cas9-expressing ABC_{16}-Monster cells were produced via standard lithium acetate transformation with vector p414 obtained from the Church lab, modified with a *met15* selection marker (Addgene). To generate gene-specific guide RNA (gRNA), 45bp oligonucleotide primers were designed to match the target sequence and contain a 24bp overlap with a p426 vector backbone (Church lab, Addgene) and synthesized by Integrated DNA Technologies. Subsequent amplification of gRNA via PCR was followed by transformation into XL10-Gold Ultracompetent *E. coli* cells (Agilent), which were plated on LB-Ampicillin plates. Act1 gRNAs were isolated and purified from bacterial cells using the QiaQuick Miniprep kit (Qiagen), and quantified with Qubit technology (Thermofisher). A standardized lithium acetate method was implemented to transform Cas9-expressing ABC_{16}-Monster cells with 400ng purified gRNA and 1.2 nmole of a 90bp synthesized donor template containing the desired base-pair substitution. Transformed cells were selected on methionine and

leucine deficient CM glucose plates, and mutations were confirmed via colony PCR followed by Sanger Sequencing (EtonBioscience).

Parasite and cell culturing

ABS parasites. P. falciparum intraerythrocytic parasites were continuously grown in complete media, but assayed in screening media, the latter being devoid of human serum. All ABS experiments were conducted using similar strains of *P. falciparum*, and as such culturing requirements remained largely the same. Strains utilized included *P.falciparum* Dd2-B2, and *P. falciparum* Dd2-luciferase (the luciferase marker was selected for by WR9910 and blasticidin as described in (Ekland EH,Schneider J and Fidock DA, 2011). The Dd2-B2 line was formerly derived from a limiting dilution of Dd2 originally obtained from T. Wellems (NIAID, NIH), making them genetically homologous parasites. Complete media is composed of RPMI Medium 1640 (Thermo Fischer Cat#11835-030) supplemented with 0.05 mg/mL gentamicin, 0.015 mg/mL hypoxanthine, 3.4mM NaOH, 38.5mM HEPES, 0.19% sodium bicarbonate, 0.21% glucose, 0.21% albumax, and 4.3% human serum (O^+). The lack of human serum in screening media is offset by an increased albumax (0.44%) and HEPES (39.8 mM) concentration, while remaining similar otherwise.

Gametocyte production. Mature gametocytes were generated using previously described methods (Plouffe DM et al., 2016). Briefly, asexual *P. falciparum* parasites (NF54) were grown to 7-10% parasitemia after triple synchronization with 5% (w/v) D-sorbitol, in T225 (100 mL) culture flasks. Gametocyte induction was performed by adding 50% spent media to cultures for 24 hours, followed by daily media changes supplemented with 50mM NAG. Culture progression was monitored daily by blood smear and NAG was excluded from media after 10 days.

EEF sporozoites. P. berghei GFP-Luc-SM_{con} (reference clone 15cy1) sporozoites were freshly obtained by salivary gland dissection of *A. stephensi* mosquitoes (New York University Insectary) (Janse CJ et al., 2006). Salivary glands were suspended in cold DMEM (Invitrogen, Carlsbad, USA), and kept on ice until time of infection. A 15 mL glass Dounce tissue grinder (Wheaton Industries) was used to free sporozoites from salivary glands. Sporozoites were sequentially vacuum-filtered through 20 µm (Millipore SCNY00020) and 11 µm (Millipore NY1104700) nylon net filters. Parasite concentration was determined by manual counting using a Neubauer hemocytometer.

Hepatocyte line. The immortalized HepG2-A16-$CD81^{EGFP}$ line (Yalaoui S et al., 2008) was used for all liver stage infection screening. Culture maintenance was performed with phenol red containing DMEM (Invitrogen cat# 11965-092), 10% FBS (Corning cat# 35-011-CV) and 1x Pen Strep Glutamine (100 Units/mL Penicillin, 100µg/mL Streptomycin, and 0.292mg/mL L-glutamine) (Invitrogen cat# 10378-016). Conversely, screening conditions require phenol-free DMEM (Invitrogen cat# 31053-028), 5% FBS (Corning), and 5x Pen Strep Glutamine (Invitrogen). Culture maintenance and screening conditions were performed at 37°C and 5% CO_2.

ABS Screening.

A transgenic line of *Plasmodium falciparum* (Dd2) constitutively expressing firefly luciferase was used for primary and reconfirmation screening. Cultures were maintained in complete media at 5% hematocrit (Human Whole Blood O+), and incubated at 37°C in a low oxygen environment (3% O_2, 5% CO_2, and 92% N_2). Culture health and parasitemia was tracked by Giemsa staining and bright field microscopy. Prior to dispensing parasites for primary screening, 20 nL of test compounds and 10 nL of control compounds (artemisinin and DMSO) were seeded per well using an Echo 550 acoustic dispenser (Labcyte) for a final assay

concentration of 5 µM and 10 µM, respectively. When parasite cultures reached 3% to 8% parasitemia, as determined by blood smear, infected blood was centrifuged at 800g for 5 minutes. A predetermined volume was taken from the resulting pellet and transferred to generate a mixture of 0.1% parasitemia and 2.5% hematocrit in screening media. From this blood mixture, 8 µL was dispensed per well in 1536-well, white, solid bottom plates (789173-F, Greiner) using a MultiFlo FX Multi-Mode dispenser (BioTek). Plates were covered with a porous metal lid and incubated at 37°C inside large plastic Ziploc bags filled with a blood gas mixture (3% O_2, 5% CO_2, and 92% N_2) for 96 hrs. To prevent evaporation, a clean tray of water was included within each bag. Following incubation, BrightGlo was prepared by manufacturer specifications and dispensed at 2 µL per well using the MultiFlo dispenser. Plates were left for 20 minutes before being read with the ViewLux uHTS microplate imager (PerkinElmer) with a 90 second exposure time at the High Sensitivity Luminescence setting. Raw data were processed using GeneData (v12.0.5), whereby activity was normalized to negative minus positive controls. The correction of Runwise Pattern (Multiplicative) was applied and compounds were considered hits when activity was reduced by ≥ 70%. The procedure for dose response testing was similar, except compounds were diluted 1:3 for both 8-point (5 µM peak assay concentration) and 11-point (12.5 µM peak assay concentration) titrations. Also, plates tested in 11-point dose response format were incubated at both 48 hrs and 96 hrs for delayed-death studies.

Stage V Gametocyte Screening.

Prior to parasite addition, 10 nL (final concentration of 2 µM) of each compound was dispensed using an Echo 550 acoustic dispenser (Labcyte) in 1536-well, black, clear-bottom plates (ref# 789866-691-2B, Greiner Bio-One). High-content imaging experiments were performed on Stage V gametocytes as previously described (Plouffe DM et al., 2016). Briefly, mature

gametocytes were diluted to 0.5-0.75% gametocytemia and 1.25% hematocrit in serum free screening media. Cultures were dispensed at 10 µL per well using a MultiFlo dispenser (BioTek), and incubated at 37°C for 72 hr (3% O_2, 5% CO_2, and 92% N_2). A solution of 2.5 µM MitoTracker Red CMXRos and 0.13% saponin (w/v) was made in screening media and added to each well for 1-2hr at 37°C to allow for complete red blood cell lysis. The Operetta (Perkin Elmer) high content imaging platform was used to read all 1536-well plates with analysis performed by the accompanying Harmony software.

$$\text{Viability Index 1° Screen} = \frac{\text{Compound treated well particle count}}{\text{DMSO average particle count per plate}}$$

Compounds with >50% inhibition were resourced from younger stocks and plated in 10-point dose-response format. All screening and analysis steps were then repeated as previously described.

EEF Liver stage Screening.

The *P. berghei* sporozoite (PbLuc) infection and maturation assay was conducted as previously described with some modifications (Swann J et al., 2016). Using the Gen 4 Plus Acoustic Transfer System (Biosero, San Diego, USA) 50nL of compounds diluted in DMSO (final concentration of 10µM) were dispensed into 1536-well, white, opaque-bottom plates (ref# 789173-F, Greiner Bio-One). Similarly, atovaquone (final concentration of 5µM/well) and DMSO (final concentration of 0.5%/well) were added as positive and negative controls, respectively. HepG2-A16-CD81^{EGFP} cells (3 x 10^3/5µL/well) are added within 12 hr of compound dispense. Within 20-24 hr, day 23 PbLuc sporozoites (10^3/5uL/well) were dissected, purified, and dispensed using a bottle valve liquid handler (GNF). Plates were centrifuged (Eppendorf 5810R) for 3 min (RT) at 330g and incubated for 48 hr at 37°C and 5% CO_2. A combination of high incubator humidity and custom ventilated metal lids (Wako Automation, San Diego, USA) with tight sealing

rubber gaskets were used to mitigate edge effect. All other methods were as previously described. bioluminescence

$$PbLuc\ inhibition = \frac{Bioluminescence\ (avg\ Compound\ -\ avg\ atovaquone)}{Bioluminescence\ (avg\ DMSO\ -\ avg\ atovaquone)}$$

HepG2 Cytotoxicity Screening.

At the same time hepatocytes were dispensed for PbLuc infection, HepG2-A16-CD81^{EGFP} cells (3 x 10^3/5µL/well) were dispensed into compound treated, uninfected, 1536-well plates. An additional 5µL of parasite-free screening media was added to match the infected plates final volume (V_f = 10 µL). Cytotoxicity plates were stamped with identical concentrations of compounds earmarked for infection, with the inclusion of puromycin (final concentration 10µM) (Cayman Chemical, Ann Arbor, USA) as a positive control. All other methods were as previously described (Swann J et al., 2016).

$$HepG2\ inhibition = \frac{Bioluminescence\ (avg\ Compound - avg\ puromycin)}{Bioluminescence\ (avg\ DMSO - avg\ puromycin)}$$

FireFly Luciferase Inhibition.

To quantify the rate of false positives reported during the PbLuc liver stage reconfirmation screen, hits selected for tertiary round screening were also tested for luminescent interference between recombinant firefly luciferase and luciferin. Initially, 40 nL of selected compounds were dispensed using a Gen 4 Plus Acoustic Transfer System (Biosero, San Diego, USA) at 1:3 in 12-point dose response format (25µM to 141.13x10^{-6} µM; final DMSO concentration 0.5% per well) in 1536-well, white, opaque-bottom plates (ref# 789173-F, Greiner Bio-One). A 24-point single

concentration series of Luciferase Inhibitor-II (9.8 µM/well) was dispensed as a positive control, while 96 wells of DMSO at 0.5%/well acted as our negative control. Separately, a solution of 20 pM recombinant luciferase (Promega cat#) was prepared on ice by successive dilutions (first 1:999 then into final solution at 20 pM) in phenol naive DMEM (Invitrogen cat# 31053-028), 5% FBS (Corning), and 5x Pen Strep Glutamine (Invitrogen). This solution was dispensed at 8 µL/well into the previously spotted plates using a MultiFlo dispenser (BioTek) and incubated at room temperature for 1 hr prior to the addition of 1 µL BrightGlo (Promega cat#). Immediately after the addition of BrightGlo, plates were read using the EnVision Microplate reader (PerkinElmer).

Robustness of HTS methods.

Assay reproducibility was measured by Z'-factor as previously described, with modifications (Zhang JH et al., 1999).

$$Z'_f = 1 - \frac{3(\sigma_p + \sigma_n)}{|\mu_p - \mu_n|}$$

(σ_p = standard deviation (SD) pos control, σ_n = SD neg control, μ_p = mean pos control, μ_n = mean neg control)

Due to the low overall infection rate and uncontrollable nature of hepatocyte invasion by sporozoites, luminescence values one standard deviation from either tail of distribution were removed prior to calculating Z'-factors. Intraerythrocytic assays were calculated normally, as their endpoints are less influenced by weekly infection rates.

Inhibitory curve calculations.

ABS, EEF, and stage V GAM single point and dose response inhibition values were calculated using custom protocol definitions on the Collaborative Drug Discovery Vault database

(www.collaborativedrug.com). Once normalized to positive and negative controls, a Levenberg-Marquardt algorithm was utilized to fit a Hill equation to the data. Fit parameters were used to constrain curves to account for run variability. Briefly, the slope was restricted to all positive numbers including zero, minimum values ranged from -5 to 5, and maximum values ranged from 80 to 120. Those compounds with inhibition below 50% at any concentration were reported as greater than the maximum tested concentration.

Cheminformatic analysis.

Fingerprints (ECFP4) for all 68,614 library compounds were generated using a custom pipeline in Knime (v3.5.2). Hierarchical clustering was then performed using these fingerprints whereby structures with a Dice similarity coefficient of 0.7 were preserved. Edges were assigned between similar scaffolds and a central parent node. Scaffolds which had no parent node at the given similarity cutoff were considered structural singletons. Clusters were visualized using Cytoscape (v3.6.0) and the Y-files organic layout (Shannon P et al., 2003). Enrichment for potent clusters was calculated using the hypergeometric distribution equation:

$$h(x, n, M, N) = \frac{\left(\frac{M}{x}\right)\left(\frac{N-M}{n-x}\right)}{\left(\frac{N}{n}\right)}$$

(x = sample successes, n = size of sample, M = population success, N = total population)

Homology modeling.

A homology model of *P. falciparum* cytochrome BC1 was constructed with SWISS-MODEL using a bovine crystal structure template (1BE3; 3Å) (Iwata S et al., 1998). Docking studies were performed by designating a search space in MGL Tools (v1.5.6) and calculating free

energy binding positions with Autodock Vina (v1.1.2). Substrate protein interactions were visualized using PyMOL (v2.0.7).

Measuring Parasite Translation using ^{35}S-Incorporation

The effect of drug treatment on parasite translation was evaluated by quantifying the incorporation of ^{35}S-labeled amino acids into newly synthesized protein using an adapted protocol (Rottmann M et al., 2010).

Synchronized trophozoite-stage parasites (5% parasitemia, 26-30 hpi) were first washed in methionine-free media three times prior to drug treatment. Parasites were then incubated in various compound concentrations in 24-well plates for 1 hour at 37^{o}C, at a final hematocrit of 5%, and a final concentration of 125 µMci/mL of EasyTag™ EXPRESS^{35}S Protein Labeling Mix (Perkin Elmer, USA). Concentrations used for incubation corresponded to 100-, 10-, 1-, 0.1- and 0.01-times the IC50 values of TCMDC-124553 (550 nM), chloroquine (85 nM) and cycloheximide (750 nM). After drug exposure, parasites were washed with 1x PBS and then lysed using ice-cold 0.1% Saponin in 1x PBS for 20 minutes. All subsequent steps were performed on ice. The saponin pellet was washed with 1x PBS, and then resuspended in 0.02% Sodium deoxycholate and supplemented with an equal volume of 16% trichloroacetic acid (TCA) to make a final concentration of 8% TCA. The suspensions were then incubated for 20 minutes on ice before vacuum filtration. To collect the radiolabeled, precipitated proteins, the samples were dispensed onto 0.7µM glass fiber filter discs (Millipore, USA) that had been presoaked in 8% TCA. The vacuum-filtered precipitates were then washed twice with 8% TCA and then, finally, with 90% acetone. The filter discs were allowed to air-dry for at least two hours, transferred into scintillation vials and resuspended in scintillation cocktail (Perkin Elmer, USA). ^{35}S counts were obtained for

1 minute using a Beckman Coulter LS 6500 Multi-purpose Scintillation Counter. Counts were normalized to data obtained from untreated parasites.

REFERENCES

WHO, R., World Malaria Report 2018.

WHO, R., World Malaria Report 2017.

Istvan, E. S.; Dharia, N. V.; Bopp, S. E.; Gluzman, I.; Winzeler, E. A.; Goldberg, D. E., Validation of isoleucine utilization targets in Plasmodium falciparum. Proceedings of the National Academy of Sciences 2011, 108 (4), 1627. DOI: 10.1073/pnas.1011560108.

Newman, D. J.; Cragg, G. M., Natural Products as Sources of New Drugs from 1981 to 2014. J Nat Prod 2016, 79 (3), 629-61. DOI: 10.1021/acs.jnatprod.5b01055.

Wells, T. N., Natural products as starting points for future anti-malarial therapies: going back to our roots? Malar J 2011, 10 Suppl 1, S3. DOI: 10.1186/1475-2875-10-s1-s3.

Achan, J.; Talisuna, A. O.; Erhart, A.; Yeka, A.; Tibenderana, J. K.; Baliraine, F. N.; Rosenthal, P. J.; D'Alessandro, U., Quinine, an old anti-malarial drug in a modern world: role in the treatment of malaria. Malar J 2011, 10, 144. DOI: 10.1186/1475-2875-10-144.

Gachelin, G.; Garner, P.; Ferroni, E.; Trohler, U.; Chalmers, I., Evaluating Cinchona bark and quinine for treating and preventing malaria. J R Soc Med 2017, 110 (1), 31-40. DOI: 10.1177/0141076816681421.

Guidelines, W. H. O. T., WHO Guidelines Approved by the Guidelines Review Committee. In Guidelines for the Treatment of Malaria, World Health Organization Copyright (c) World Health Organization 2015.: Geneva, 2015.

Faurant, C., From bark to weed: the history of artemisinin. Parasite 2011, 18 (3), 215-8. DOI: 10.1051/parasite/2011183215.

Ashley, E. A.; Dhorda, M.; Fairhurst, R. M.; Amaratunga, C.; Lim, P.; Suon, S.; Sreng, S.; Anderson, J. M.; Mao, S.; Sam, B.; Sopha, C.; Chuor, C. M.; Nguon, C.; Sovannaroth, S.; Pukrittayakamee, S.; Jittamala, P.; Chotivanich, K.; Chutasmit, K.; Suchatsoonthorn, C.; Runcharoen, R.; Hien, T. T.; Thuy-Nhien, N. T.; Thanh, N. V.; Phu, N. H.; Htut, Y.; Han, K. T.; Aye, K. H.; Mokuolu, O. A.; Olaosebikan, R. R.; Folaranmi, O. O.; Mayxay, M.; Khanthavong, M.; Hongvanthong, B.; Newton, P. N.; Onyamboko, M. A.; Fanello, C. I.; Tshefu, A. K.; Mishra, N.; Valecha, N.; Phyo, A. P.; Nosten, F.; Yi, P.; Tripura, R.; Borrmann, S.; Bashraheil, M.; Peshu, J.; Faiz, M. A.; Ghose, A.; Hossain, M. A.; Samad, R.; Rahman, M. R.; Hasan, M. M.; Islam, A.; Miotto, O.; Amato, R.; MacInnis, B.; Stalker, J.; Kwiatkowski, D. P.; Bozdech, Z.; Jeeyapant, A.; Cheah, P. Y.; Sakulthaew, T.; Chalk, J.; Intharabut, B.; Silamut, K.; Lee, S. J.; Vihokhern, B.; Kunasol, C.; Imwong, M.; Tarning, J.; Taylor, W. J.; Yeung, S.; Woodrow, C. J.; Flegg, J. A.; Das, D.; Smith, J.; Venkatesan, M.; Plowe, C. V.; Stepniewska, K.; Guerin, P. J.; Dondorp, A. M.; Day, N. P.; White, N. J., Spread of artemisinin resistance in Plasmodium falciparum malaria. N Engl J Med 2014, 371 (5), 411-23. DOI: 10.1056/NEJMoa1314981.

Hovlid, M. L.; Winzeler, E. A., Phenotypic Screens in Antimalarial Drug Discovery. Trends Parasitol 2016, 32 (9), 697-707. DOI: 10.1016/j.pt.2016.04.014.

Hooft van Huijsduijnen, R.; Wells, T. N., The antimalarial pipeline. Curr Opin Pharmacol 2018, 42, 1-6. DOI: 10.1016/j.coph.2018.05.006.

Baggish, A. L.; Hill, D. R., Antiparasitic agent atovaquone. Antimicrob Agents Chemother 2002, 46 (5), 1163-73. DOI: 10.1128/aac.46.5.1163-1173.2002.

Frevert, U.; Engelmann, S.; Zougbede, S.; Stange, J.; Ng, B.; Matuschewski, K.; Liebes, L.; Yee, H., Intravital observation of Plasmodium berghei sporozoite infection of the liver. PLoS Biol 2005, 3 (6), e192. DOI: 10.1371/journal.pbio.0030192.

Mota, M. M.; Pradel, G.; Vanderberg, J. P.; Hafalla, J. C.; Frevert, U.; Nussenzweig, R. S.; Nussenzweig, V.; Rodriguez, A., Migration of Plasmodium sporozoites through cells before infection. Science 2001, 291 (5501), 141-4. DOI: 10.1126/science.291.5501.141.

Swann, J.; Corey, V.; Scherer, C. A.; Kato, N.; Comer, E.; Maetani, M.; Antonova-Koch, Y.; Reimer, C.; Gagaring, K.; Ibanez, M.; Plouffe, D.; Zeeman, A. M.; Kocken, C. H.; McNamara, C. W.; Schreiber, S. L.; Campo, B.; Winzeler, E. A.; Meister, S., High-Throughput Luciferase-Based Assay for the Discovery of Therapeutics That Prevent Malaria. ACS Infect Dis 2016, 2 (4), 281-293. DOI: 10.1021/acsinfecdis.5b00143.

Meister, S.; Plouffe, D. M.; Kuhen, K. L.; Bonamy, G. M.; Wu, T.; Barnes, S. W.; Bopp, S. E.; Borboa, R.; Bright, A. T.; Che, J.; Cohen, S.; Dharia, N. V.; Gagaring, K.; Gettayacamin, M.; Gordon, P.; Groessl, T.; Kato, N.; Lee, M. C.; McNamara, C. W.; Fidock, D. A.; Nagle, A.; Nam, T. G.; Richmond, W.; Roland, J.; Rottmann, M.; Zhou, B.; Froissard, P.; Glynne, R. J.; Mazier, D.; Sattabongkot, J.; Schultz, P. G.; Tuntland, T.; Walker, J. R.; Zhou, Y.; Chatterjee, A.; Diagana, T. T.; Winzeler, E. A., Imaging of Plasmodium liver stages to drive next-generation antimalarial drug discovery. Science 2011, 334 (6061), 1372-7. DOI: 10.1126/science.1211936.

Zhang, H.; Zhao, Z.; Wang, H., Cytotoxic Natural Products from Marine Sponge-Derived Microorganisms. Mar Drugs 2017, 15 (3). DOI: 10.3390/md15030068.

Cutler, S.; Cutler, H.; Burger, A.; Abraham, D. J., Natural Products as Cytotoxic Agents Burger's Medicinal Chemistry and Drug Discovery, 6th ed., 6v.

Taniguchi, M.; Nunnery, J. K.; Engene, N.; Esquenazi, E.; Byrum, T.; Dorrestein, P. C.; Gerwick, W. H., Palmyramide A, a cyclic depsipeptide from a Palmyra Atoll collection of the marine cyanobacterium Lyngbya majuscula. J Nat Prod 2010, 73 (3), 393-8. DOI: 10.1021/np900428h.

Choi, H.; Pereira, A. R.; Cao, Z.; Shuman, C. F.; Engene, N.; Byrum, T.; Matainaho, T.; Murray, T. F.; Mangoni, A.; Gerwick, W. H., The hoiamides, structurally intriguing neurotoxic lipopeptides from Papua New Guinea marine cyanobacteria. J Nat Prod 2010, 73 (8), 1411-21. DOI: 10.1021/np100468n.

Marquez, B. L.; Watts, K. S.; Yokochi, A.; Roberts, M. A.; Verdier-Pinard, P.; Jimenez, J. I.; Hamel, E.; Scheuer, P. J.; Gerwick, W. H., Structure and absolute stereochemistry of hectochlorin, a potent stimulator of actin assembly. J Nat Prod 2002, 65 (6), 866-71.

Muller, P. Y.; Milton, M. N., The determination and interpretation of the therapeutic index in drug development. Nat Rev Drug Discov 2012, 11 (10), 751-61. DOI: 10.1038/nrd3801.

Cetusic, J. R.; Green, F. R., 3rd; Graupner, P. R.; Oliver, M. P., Total synthesis of hectochlorin. Org Lett 2002, 4 (8), 1307-10.

Balda, M. S.; Matter, K., Size-selective assessment of tight junction paracellular permeability using fluorescently labelled dextrans. Size-selective assessment of tight junction paracellular permeability using fluorescently labelled dextrans 2007, (1).

Stracke, M. L.; Soroush, M.; Liotta, L. A.; Schiffmann, E., Cytoskeletal agents inhibit motility and adherence of human tumor cells. Kidney international 1993, 43 (1), 151-157.

Alano, P., Plasmodium falciparum gametocytes: still many secrets of a hidden life. Molecular microbiology 2007, 66 (2), 291-302.

Plouffe, D.; Brinker, A.; McNamara, C.; Henson, K.; Kato, N.; Kuhen, K.; Nagle, A.; Adrian, F.; Matzen, J. T.; Anderson, P.; Nam, T. G.; Gray, N. S.; Chatterjee, A.; Janes, J.; Yan, S. F.; Trager, R.; Caldwell, J. S.; Schultz, P. G.; Zhou, Y.; Winzeler, E. A., In silico activity profiling reveals the mechanism of action of antimalarials discovered in a high-throughput screen. Proc Natl Acad Sci U S A 2008, 105 (26), 9059-64. DOI: 10.1073/pnas.0802982105.

Suzuki, Y.; St Onge, R. P.; Mani, R.; King, O. D.; Heilbut, A.; Labunskyy, V. M.; Chen, W.; Pham, L.; Zhang, L. V.; Tong, A. H.; Nislow, C.; Giaever, G.; Gladyshev, V. N.; Vidal, M.; Schow, P.; Lehar, J.; Roth, F. P., Knocking out multigene redundancies via cycles of sexual assortment and fluorescence selection. Nat Methods 2011, 8 (2), 159-64. DOI: 10.1038/nmeth.1550.

Corey, V. C.; Lukens, A. K.; Istvan, E. S.; Lee, M. C.; Franco, V.; Magistrado, P.; Coburn-Flynn, O.; Sakata-Kato, T.; Fuchs, O.; Gnadig, N. F.; Goldgof, G.; Linares, M.; Gomez-Lorenzo, M. G.; De Cozar, C.; Lafuente-Monasterio, M. J.; Prats, S.; Meister, S.; Tanaseichuk, O.; Wree, M.; Zhou, Y.; Willis, P. A.; Gamo, F. J.; Goldberg, D. E.; Fidock, D. A.; Wirth, D. F.; Winzeler, E. A., A broad analysis of resistance development in the malaria parasite. Nat Commun 2016, 7, 11901. DOI: 10.1038/ncomms11901.

Goldgof, G. M.; Durrant, J. D.; Ottilie, S.; Vigil, E.; Allen, K. E.; Gunawan, F.; Kostylev, M.; Henderson, K. A.; Yang, J.; Schenken, J.; LaMonte, G. M.; Manary, M. J.; Murao, A.; Nachon, M.; Stanhope, R.; Prescott, M.; McNamara, C. W.; Slayman, C. W.; Amaro, R. E.; Suzuki, Y.; Winzeler, E. A., Comparative chemical genomics reveal that the spiroindolone antimalarial KAE609 (Cipargamin) is a P-type ATPase inhibitor. Sci Rep 2016, 6, 27806. DOI: 10.1038/srep27806.

Dias, D. A.; Urban, S.; Roessner, U., A historical overview of natural products in drug discovery. Metabolites 2012, 2 (2), 303-36. DOI: 10.3390/metabo2020303.

Delves, M.; Plouffe, D.; Scheurer, C.; Meister, S.; Wittlin, S.; Winzeler, E. A.; Sinden, R. E.; Leroy, D., The activities of current antimalarial drugs on the life cycle stages of Plasmodium: a

comparative study with human and rodent parasites. PLoS Med 2012, 9 (2), e1001169. DOI: 10.1371/journal.pmed.1001169.

Schwartz, E., Prophylaxis of malaria. Mediterranean journal of hematology and infectious diseases 2012, 4 (1).

Wells, T. N.; Hooft van Huijsduijnen, R.; Van Voorhis, W. C., Malaria medicines: a glass half full? Nat Rev Drug Discov 2015, 14 (6), 424-42. DOI: 10.1038/nrd4573.

Guiguemde, W. A.; Shelat, A. A.; Bouck, D.; Duffy, S.; Crowther, G. J.; Davis, P. H.; Smithson, D. C.; Connelly, M.; Clark, J.; Zhu, F., Chemical genetics of Plasmodium falciparum. Nature 2010, 465 (7296), 311.

Avery, V. M.; Bashyam, S.; Burrows, J. N.; Duffy, S.; Papadatos, G.; Puthukkuti, S.; Sambandan, Y.; Singh, S.; Spangenberg, T.; Waterson, D., Screening and hit evaluation of a chemical library against blood-stage Plasmodium falciparum. Malaria journal 2014, 13 (1), 190.

Marris, E., Marine natural products: drugs from the deep. In Nature, England, 2006; Vol. 443, pp 904-5. DOI: 10.1038/443904a.

LaMonte, G. M.; Almaliti, J.; Bibo-Verdugo, B.; Keller, L.; Zou, B. Y.; Yang, J.; Antonova-Koch, Y.; Orjuela-Sanchez, P.; Boyle, C. A.; Vigil, E.; Wang, L.; Goldgof, G. M.; Gerwick, L.; O'Donoghue, A. J.; Winzeler, E. A.; Gerwick, W. H.; Ottilie, S., Development of a Potent Inhibitor of the Plasmodium Proteasome with Reduced Mammalian Toxicity. J Med Chem 2017, 60 (15), 6721-6732. DOI: 10.1021/acs.jmedchem.7b00671.

Looareesuwan, S.; Chulay, J. D.; Canfield, C. J.; Hutchinson, D. B., Malarone (atovaquone and proguanil hydrochloride): a review of its clinical development for treatment of malaria. Malarone Clinical Trials Study Group. The American journal of tropical medicine and hygiene 1999, 60 (4), 533-541.

Waschke, J.; Curry, F. E.; Adamson, R. H.; Drenckhahn, D., Regulation of actin dynamics is critical for endothelial barrier functions. Am J Physiol Heart Circ Physiol 2005, 288 (3), H1296-305. DOI: 10.1152/ajpheart.00687.2004.

Baum, J.; Papenfuss, A. T.; Baum, B.; Speed, T. P.; Cowman, A. F., Regulation of apicomplexan actin-based motility. Nature Reviews Microbiology 2006, 4 (8), 621-628. DOI: 10.1038/nrmicro1465.

Das, S.; Lemgruber, L.; Tay, C. L.; Baum, J.; Meissner, M., Multiple essential functions of Plasmodium falciparum actin-1 during malaria blood-stage development. BMC biology 2017, 15 (1), 70-70. DOI: 10.1186/s12915-017-0406-2.

Vahokoski, J.; Bhargav, S. P.; Desfosses, A.; Andreadaki, M.; Kumpula, E. P.; Martinez, S. M.; Ignatev, A.; Lepper, S.; Frischknecht, F.; Siden-Kiamos, I.; Sachse, C.; Kursula, I., Structural differences explain diverse functions of Plasmodium actins. PLoS Pathog 2014, 10 (4), e1004091. DOI: 10.1371/journal.ppat.1004091.

Deligianni, E.; Morgan, R. N.; Bertuccini, L.; Kooij, T. W.; Laforge, A.; Nahar, C.; Poulakakis, N.; Schuler, H.; Louis, C.; Matuschewski, K.; Siden-Kiamos, I., Critical role for a stage-specific actin in male exflagellation of the malaria parasite. Cell Microbiol 2011, 13 (11), 1714-30. DOI: 10.1111/j.1462-5822.2011.01652.x.

Shanks, G. D.; Mohrle, J. J., Treating malaria: new drugs for a new era. Lancet Infect Dis 2017, 17 (12), 1223-1224. DOI: 10.1016/s1473-3099(17)30475-9.

Killeen, G. F.; Tatarsky, A.; Diabate, A.; Chaccour, C. J.; Marshall, J. M.; Okumu, F. O.; Brunner, S.; Newby, G.; Williams, Y. A.; Malone, D.; Tusting, L. S.; Gosling, R. D., Developing an expanded vector control toolbox for malaria elimination. BMJ Glob Health 2017, 2 (2), e000211. DOI: 10.1136/bmjgh-2016-000211.

Mills, A.; Lubell, Y.; Hanson, K., Malaria eradication: the economic, financial and institutional challenge. Malar J 2008, 7 Suppl 1 (Suppl 1), S11. DOI: 10.1186/1475-2875-7-s1-s11.

Rosenberg, R.; Wirtz, R. A.; Schneider, I.; Burge, R., An estimation of the number of malaria sporozoites ejected by a feeding mosquito. Trans R Soc Trop Med Hyg 1990, 84 (2), 209-12.

Medica, D. L.; Sinnis, P., Quantitative dynamics of Plasmodium yoelii sporozoite transmission by infected anopheline mosquitoes. Infect Immun 2005, 73 (7), 4363-9. DOI: 10.1128/iai.73.7.4363-4369.2005.

Blackman, M. J., Malarial proteases and host cell egress: an 'emerging' cascade. Cell Microbiol 2008, 10 (10), 1925-34. DOI: 10.1111/j.1462-5822.2008.01176.x.

Amino, R.; Thiberge, S.; Martin, B.; Celli, S.; Shorte, S.; Frischknecht, F.; Menard, R., Quantitative imaging of Plasmodium transmission from mosquito to mammal. Nat Med 2006, 12 (2), 220-4. DOI: 10.1038/nm1350.

Eichner, M.; Diebner, H. H.; Molineaux, L.; Collins, W. E.; Jeffery, G. M.; Dietz, K., Genesis, sequestration and survival of Plasmodium falciparum gametocytes: parameter estimates from fitting a model to malariatherapy data. Trans R Soc Trop Med Hyg 2001, 95 (5), 497-501.

Talman, A. M.; Domarle, O.; McKenzie, F. E.; Ariey, F.; Robert, V., Gametocytogenesis: the puberty of Plasmodium falciparum. Malar J 2004, 3, 24. DOI: 10.1186/1475-2875-3-24.

Saliba, K. S.; Jacobs-Lorena, M., Production of Plasmodium falciparum gametocytes in vitro. Methods Mol Biol 2013, 923, 17-25. DOI: 10.1007/978-1-62703-026-7_2.

Antony, H. A.; Parija, S. C., Antimalarial drug resistance: An overview. Trop Parasitol 2016, 6 (1), 30-41. DOI: 10.4103/2229-5070.175081.

Raju, T. N., The Nobel chronicles. 1988: James Whyte Black, (b 1924), Gertrude Elion (1918-99), and George H Hitchings (1905-98). Lancet 2000, 355 (9208), 1022.

Noedl, H.; Se, Y.; Schaecher, K.; Smith, B. L.; Socheat, D.; Fukuda, M. M.; Artemisinin Resistance in Cambodia 1 Study, C., Evidence of artemisinin-resistant malaria in western

Cambodia. In N Engl J Med, United States, 2008; Vol. 359, pp 2619-20. DOI: 10.1056/NEJMc0805011.

Lu, F.; Culleton, R.; Zhang, M.; Ramaprasad, A.; von Seidlein, L.; Zhou, H.; Zhu, G.; Tang, J.; Liu, Y.; Wang, W.; Cao, Y.; Xu, S.; Gu, Y.; Li, J.; Zhang, C.; Gao, Q.; Menard, D.; Pain, A.; Yang, H.; Zhang, Q.; Cao, J., Emergence of Indigenous Artemisinin-Resistant Plasmodium falciparum in Africa. N Engl J Med 2017, 376 (10), 991-3. DOI: 10.1056/NEJMc1612765.

Diagana, T. T., Supporting malaria elimination with 21st century antimalarial agent drug discovery. Drug Discov Today 2015, 20 (10), 1265-70. DOI: 10.1016/j.drudis.2015.06.009.

Okombo, J.; Chibale, K., Correction: Recent updates in the discovery and development of novel antimalarial drug candidates. In Medchemcomm, England, 2018; Vol. 9, p 590. DOI: 10.1039/c8md90009d.

Sinha, S.; Sarma, P.; Sehgal, R.; Medhi, B., Development in Assay Methods for in Vitro Antimalarial Drug Efficacy Testing: A Systematic Review. Front Pharmacol 2017, 8, 754. DOI: 10.3389/fphar.2017.00754.

Almela, M. J.; Lozano, S.; Lelievre, J.; Colmenarejo, G.; Coteron, J. M.; Rodrigues, J.; Gonzalez, C.; Herreros, E., A New Set of Chemical Starting Points with Plasmodium falciparum Transmission-Blocking Potential for Antimalarial Drug Discovery. PLoS One 2015, 10 (8), e0135139. DOI: 10.1371/journal.pone.0135139.

Kuhen, K. L.; Chatterjee, A. K.; Rottmann, M.; Gagaring, K.; Borboa, R.; Buenviaje, J.; Chen, Z.; Francek, C.; Wu, T.; Nagle, A.; Barnes, S. W.; Plouffe, D.; Lee, M. C.; Fidock, D. A.; Graumans, W.; van de Vegte-Bolmer, M.; van Gemert, G. J.; Wirjanata, G.; Sebayang, B.; Marfurt, J.; Russell, B.; Suwanarusk, R.; Price, R. N.; Nosten, F.; Tungtaeng, A.; Gettayacamin, M.; Sattabongkot, J.; Taylor, J.; Walker, J. R.; Tully, D.; Patra, K. P.; Flannery, E. L.; Vinetz, J. M.; Renia, L.; Sauerwein, R. W.; Winzeler, E. A.; Glynne, R. J.; Diagana, T. T., KAF156 is an antimalarial clinical candidate with potential for use in prophylaxis, treatment, and prevention of disease transmission. Antimicrob Agents Chemother 2014, 58 (9), 5060-7. DOI: 10.1128/aac.02727-13.

Rottmann, M.; McNamara, C.; Yeung, B. K.; Lee, M. C.; Zou, B.; Russell, B.; Seitz, P.; Plouffe, D. M.; Dharia, N. V.; Tan, J.; Cohen, S. B.; Spencer, K. R.; Gonzalez-Paez, G. E.; Lakshminarayana, S. B.; Goh, A.; Suwanarusk, R.; Jegla, T.; Schmitt, E. K.; Beck, H. P.; Brun, R.; Nosten, F.; Renia, L.; Dartois, V.; Keller, T. H.; Fidock, D. A.; Winzeler, E. A.; Diagana, T. T., Spiroindolones, a potent compound class for the treatment of malaria. Science 2010, 329 (5996), 1175-80. DOI: 10.1126/science.1193225.

Coteron, J. M.; Marco, M.; Esquivias, J.; Deng, X.; White, K. L.; White, J.; Koltun, M.; El Mazouni, F.; Kokkonda, S.; Katneni, K.; Bhamidipati, R.; Shackleford, D. M.; Angulo-Barturen, I.; Ferrer, S. B.; Jimenez-Diaz, M. B.; Gamo, F. J.; Goldsmith, E. J.; Charman, W. N.; Bathurst, I.; Floyd, D.; Matthews, D.; Burrows, J. N.; Rathod, P. K.; Charman, S. A.; Phillips, M. A., Structure-guided lead optimization of triazolopyrimidine-ring substituents identifies potent Plasmodium falciparum dihydroorotate dehydrogenase inhibitors with clinical candidate potential. J Med Chem 2011, 54 (15), 5540-61. DOI: 10.1021/jm200592f.

Paquet, T.; Le Manach, C.; Cabrera, D. G.; Younis, Y.; Henrich, P. P.; Abraham, T. S.; Lee, M. C. S.; Basak, R.; Ghidelli-Disse, S.; Lafuente-Monasterio, M. J.; Bantscheff, M.; Ruecker, A.; Blagborough, A. M.; Zakutansky, S. E.; Zeeman, A. M.; White, K. L.; Shackleford, D. M.; Mannila, J.; Morizzi, J.; Scheurer, C.; Angulo-Barturen, I.; Martinez, M. S.; Ferrer, S.; Sanz, L. M.; Gamo, F. J.; Reader, J.; Botha, M.; Dechering, K. J.; Sauerwein, R. W.; Tungtaeng, A.; Vanachayangkul, P.; Lim, C. S.; Burrows, J.; Witty, M. J.; Marsh, K. C.; Bodenreider, C.; Rochford, R.; Solapure, S. M.; Jimenez-Diaz, M. B.; Wittlin, S.; Charman, S. A.; Donini, C.; Campo, B.; Birkholtz, L. M.; Hanson, K. K.; Drewes, G.; Kocken, C. H. M.; Delves, M. J.; Leroy, D.; Fidock, D. A.; Waterson, D.; Street, L. J.; Chibale, K., Antimalarial efficacy of MMV390048, an inhibitor of Plasmodium phosphatidylinositol 4-kinase. Sci Transl Med 2017, 9 (387). DOI: 10.1126/scitranslmed.aad9735.

Olliaro, P.; Wells, T. N., The global portfolio of new antimalarial medicines under development. Clin Pharmacol Ther 2009, 85 (6), 584-95. DOI: 10.1038/clpt.2009.51.

Lipinski, C. A.; Lombardo, F.; Dominy, B. W.; Feeney, P. J., Experimental and computational approaches to estimate solubility and permeability in drug discovery and development settings. Adv Drug Deliv Rev 2001, 46 (1-3), 3-26.

McKerrow, J. H.; Lipinski, C. A., The rule of five should not impede anti-parasitic drug development. Int J Parasitol Drugs Drug Resist 2017, 7 (2), 248-249. DOI: 10.1016/j.ijpddr.2017.05.003.

Hou, T.; Wang, J.; Zhang, W.; Xu, X., ADME evaluation in drug discovery. 7. Prediction of oral absorption by correlation and classification. J Chem Inf Model 2007, 47 (1), 208-18. DOI: 10.1021/ci600343x.

Lovering, F.; Bikker, J.; Humblet, C., Escape from flatland: increasing saturation as an approach to improving clinical success. J Med Chem 2009, 52 (21), 6752-6. DOI: 10.1021/jm901241e.

Love, M. S.; Beasley, F. C.; Jumani, R. S.; Wright, T. M.; Chatterjee, A. K.; Huston, C. D.; Schultz, P. G.; McNamara, C. W., A high-throughput phenotypic screen identifies clofazimine as a potential treatment for cryptosporidiosis. PLoS Negl Trop Dis 2017, 11 (2), e0005373. DOI: 10.1371/journal.pntd.0005373.

Burkhardt, D.; Wiesner, J.; Stoesser, N.; Ramharter, M.; Uhlemann, A. C.; Issifou, S.; Jomaa, H.; Krishna, S.; Kremsner, P. G.; Borrmann, S., Delayed parasite elimination in human infections treated with clindamycin parallels 'delayed death' of Plasmodium falciparum in vitro. Int J Parasitol 2007, 37 (7), 777-85. DOI: 10.1016/j.ijpara.2006.12.010.

Dahl, E. L.; Rosenthal, P. J., Multiple antibiotics exert delayed effects against the Plasmodium falciparum apicoplast. Antimicrob Agents Chemother 2007, 51 (10), 3485-90. DOI: 10.1128/aac.00527-07.

Gamo, F. J.; Sanz, L. M.; Vidal, J.; de Cozar, C.; Alvarez, E.; Lavandera, J. L.; Vanderwall, D. E.; Green, D. V.; Kumar, V.; Hasan, S.; Brown, J. R.; Peishoff, C. E.; Cardon, L. R.; Garcia-Bustos, J. F., Thousands of chemical starting points for antimalarial lead identification. Nature 2010, 465 (7296), 305-10. DOI: nature09107

Ekland, E. H.; Schneider, J.; Fidock, D. A., Identifying apicoplast-targeting antimalarials using high-throughput compatible approaches. Faseb j 2011, 25 (10), 3583-93. DOI: 10.1096/fj.11-187401.

Dahl, E. L.; Rosenthal, P. J., Multiple antibiotics exert delayed effects against the Plasmodium falciparum apicoplast. Antimicrobial agents and chemotherapy 2007, 51 (10), 3485-3490. DOI: 10.1128/AAC.00527-07.

Ramya, T. N.; Mishra, S.; Karmodiya, K.; Surolia, N.; Surolia, A., Inhibitors of nonhousekeeping functions of the apicoplast defy delayed death in Plasmodium falciparum. Antimicrob Agents Chemother 2007, 51 (1), 307-16. DOI: 10.1128/aac.00808-06.

Janse, C. J.; Franke-Fayard, B.; Mair, G. R.; Ramesar, J.; Thiel, C.; Engelmann, S.; Matuschewski, K.; van Gemert, G. J.; Sauerwein, R. W.; Waters, A. P., High efficiency transfection of Plasmodium berghei facilitates novel selection procedures. Mol Biochem Parasitol 2006, 145 (1), 60-70. DOI: 10.1016/j.molbiopara.2005.09.007.

Yalaoui, S.; Zougbede, S.; Charrin, S.; Silvie, O.; Arduise, C.; Farhati, K.; Boucheix, C.; Mazier, D.; Rubinstein, E.; Froissard, P., Hepatocyte permissiveness to Plasmodium infection is conveyed by a short and structurally conserved region of the CD81 large extracellular domain. PLoS Pathog 2008, 4 (2), e1000010. DOI: 10.1371/journal.ppat.1000010.

Thorne, N.; Auld, D. S.; Inglese, J., Apparent activity in high-throughput screening: origins of compound-dependent assay interference. Curr Opin Chem Biol 2010, 14 (3), 315-24. DOI: 10.1016/j.cbpa.2010.03.020.

Auld, D. S.; Thorne, N.; Maguire, W. F.; Inglese, J., Mechanism of PTC124 activity in cell-based luciferase assays of nonsense codon suppression. Proc Natl Acad Sci U S A 2009, 106 (9), 3585-90. DOI: 10.1073/pnas.0813345106.

Plouffe, D. M.; Wree, M.; Du, A. Y.; Meister, S.; Li, F.; Patra, K.; Lubar, A.; Okitsu, S. L.; Flannery, E. L.; Kato, N.; Tanaseichuk, O.; Comer, E.; Zhou, B.; Kuhen, K.; Zhou, Y.; Leroy, D.; Schreiber, S. L.; Scherer, C. A.; Vinetz, J.; Winzeler, E. A., High-Throughput Assay and Discovery of Small Molecules that Interrupt Malaria Transmission. Cell Host Microbe 2016, 19 (1), 114-26. DOI: 10.1016/j.chom.2015.12.001.

D'Alessandro, S.; Camarda, G.; Corbett, Y.; Siciliano, G.; Parapini, S.; Cevenini, L.; Michelini, E.; Roda, A.; Leroy, D.; Taramelli, D.; Alano, P., A chemical susceptibility profile of the Plasmodium falciparum transmission stages by complementary cell-based gametocyte assays. J Antimicrob Chemother 2016, 71 (5), 1148-58. DOI: 10.1093/jac/dkv493.

Pendergrass, W.; Wolf, N.; Poot, M., Efficacy of MitoTracker Green and CMXrosamine to measure changes in mitochondrial membrane potentials in living cells and tissues. Cytometry A 2004, 61 (2), 162-9. DOI: 10.1002/cyto.a.20033.

Yang, H. Y.; Tae, J.; Seo, Y. W.; Kim, Y. J.; Im, H. Y.; Choi, G. D.; Cho, H.; Park, W. K.; Kwon, O. S.; Cho, Y. S.; Ko, M.; Jang, H.; Lee, J.; Choi, K.; Kim, C. H.; Pae, A. N., Novel

pyrimidoazepine analogs as serotonin 5-HT(2A) and 5-HT(2C) receptor ligands for the treatment of obesity. Eur J Med Chem 2013, 63, 558-69. DOI: 10.1016/j.ejmech.2013.02.020.

Hain, A. U.; Bartee, D.; Sanders, N. G.; Miller, A. S.; Sullivan, D. J.; Levitskaya, J.; Meyers, C. F.; Bosch, J., Identification of an Atg8-Atg3 protein-protein interaction inhibitor from the medicines for Malaria Venture Malaria Box active in blood and liver stage Plasmodium falciparum parasites. J Med Chem 2014, 57 (11), 4521-31. DOI: 10.1021/jm401675a.

Phillips, M. A.; Rathod, P. K., Plasmodium dihydroorotate dehydrogenase: a promising target for novel anti-malarial chemotherapy. Infect Disord Drug Targets 2010, 10 (3), 226-39.

Leeza Zaidi, S.; Agarwal, S. M.; Chavalitshewinkoon-Petmitr, P.; Suksangpleng, T.; Ahmad, K.; Avecilla, F.; Azam, A. Y., - Thienopyrimidine sulphonamide hybrids: design, synthesis, antiprotozoal activity and molecular docking studies. - RSC Advances (- 93), - 90371. DOI: - 10.1039/c6ra15181g m3 - 10.1039/c6ra15181g.

Akhoon, B. A.; Singh, K. P.; Varshney, M.; Gupta, S. K.; Shukla, Y., Understanding the mechanism of atovaquone drug resistance in Plasmodium falciparum cytochrome b mutation Y268S using computational methods. PLoS One 2014, 9 (10), e110041. DOI: 10.1371/journal.pone.0110041.

Siregar, J. E.; Kurisu, G.; Kobayashi, T.; Matsuzaki, M.; Sakamoto, K.; Mi-ichi, F.; Watanabe, Y.; Hirai, M.; Matsuoka, H.; Syafruddin, D.; Marzuki, S.; Kita, K., Direct evidence for the atovaquone action on the Plasmodium cytochrome bc1 complex. Parasitol Int 2015, 64 (3), 295-300. DOI: 10.1016/j.parint.2014.09.011.

Stickles, A. M.; Ting, L. M.; Morrisey, J. M.; Li, Y.; Mather, M. W.; Meermeier, E.; Pershing, A. M.; Forquer, I. P.; Miley, G. P.; Pou, S.; Winter, R. W.; Hinrichs, D. J.; Kelly, J. X.; Kim, K.; Vaidya, A. B.; Riscoe, M. K.; Nilsen, A., Inhibition of cytochrome bc1 as a strategy for single-dose, multi-stage antimalarial therapy. Am J Trop Med Hyg 2015, 92 (6), 1195-201. DOI: 10.4269/ajtmh.14-0553.

Wu, T.; Nagle, A.; Kuhen, K.; Gagaring, K.; Borboa, R.; Francek, C.; Chen, Z.; Plouffe, D.; Goh, A.; Lakshminarayana, S. B.; Wu, J.; Ang, H. Q.; Zeng, P.; Kang, M. L.; Tan, W.; Tan, M.; Ye, N.; Lin, X.; Caldwell, C.; Ek, J.; Skolnik, S.; Liu, F.; Wang, J.; Chang, J.; Li, C.; Hollenbeck, T.; Tuntland, T.; Isbell, J.; Fischli, C.; Brun, R.; Rottmann, M.; Dartois, V.; Keller, T.; Diagana, T.; Winzeler, E.; Glynne, R.; Tully, D. C.; Chatterjee, A. K., Imidazolopiperazines: hit to lead optimization of new antimalarial agents. J Med Chem 2011, 54 (14), 5116-30. DOI: 10.1021/jm2003359.

Kato, N.; Comer, E.; Sakata-Kato, T.; Sharma, A.; Sharma, M.; Maetani, M.; Bastien, J.; Brancucci, N. M.; Bittker, J. A.; Corey, V.; Clarke, D.; Derbyshire, E. R.; Dornan, G. L.; Duffy, S.; Eckley, S.; Itoe, M. A.; Koolen, K. M.; Lewis, T. A.; Lui, P. S.; Lukens, A. K.; Lund, E.; March, S.; Meibalan, E.; Meier, B. C.; McPhail, J. A.; Mitasev, B.; Moss, E. L.; Sayes, M.; Van Gessel, Y.; Wawer, M. J.; Yoshinaga, T.; Zeeman, A. M.; Avery, V. M.; Bhatia, S. N.; Burke, J. E.; Catteruccia, F.; Clardy, J. C.; Clemons, P. A.; Dechering, K. J.; Duvall, J. R.; Foley, M. A.; Gusovsky, F.; Kocken, C. H.; Marti, M.; Morningstar, M. L.; Munoz, B.; Neafsey, D. E.; Winzeler, E. A.; Wirth, D. F.; Scherer, C. A.; Schreiber, S. L., Diversity-oriented synthesis

yields novel multistage antimalarial inhibitors. Nature 2016, 538 (7625), 344-349. DOI: 10.1038/nature19804.

Burrows, J. N.; Duparc, S.; Gutteridge, W. E.; Hooft van Huijsduijnen, R.; Kaszubska, W.; Macintyre, F.; Mazzuri, S.; Mohrle, J. J.; Wells, T. N. C., New developments in anti-malarial target candidate and product profiles. Malar J 2017, 16 (1), 26. DOI: 10.1186/s12936-016-1675-x.

Mair, G. R.; Braks, J. A.; Garver, L. S.; Wiegant, J. C.; Hall, N.; Dirks, R. W.; Khan, S. M.; Dimopoulos, G.; Janse, C. J.; Waters, A. P., Regulation of sexual development of Plasmodium by translational repression. Science 2006, 313 (5787), 667-9. DOI: 10.1126/science.1125129.

Cervantes, S.; Bunnik, E. M.; Saraf, A.; Conner, C. M.; Escalante, A.; Sardiu, M. E.; Ponts, N.; Prudhomme, J.; Florens, L.; Le Roch, K. G., The multifunctional autophagy pathway in the human malaria parasite, Plasmodium falciparum. Autophagy 2014, 10 (1), 80-92. DOI: 10.4161/auto.26743.

Delves, M. J.; Ruecker, A.; Straschil, U.; Lelièvre, J.; Marques, S.; López-Barragán, M. J.; Herreros, E.; Sinden, R. E., Male and female Plasmodium falciparum mature gametocytes show different responses to antimalarial drugs. Antimicrob Agents Chemother 2013, 57 (7), 3268-74. DOI: 10.1128/aac.00325-13.

Antonova-Koch, Y.; Meister, S.; Abraham, M.; Luth, M. R.; Ottilie, S.; Lukens, A. K.; Sakata-Kato, T.; Vanaerschot, M.; Owen, E.; Jado, J. C.; Maher, S. P.; Calla, J.; Plouffe, D.; Zhong, Y.; Chen, K.; Chaumeau, V.; Conway, A. J.; McNamara, C. W.; Ibanez, M.; Gagaring, K.; Serrano, F. N.; Eribez, K.; Taggard, C. M.; Cheung, A. L.; Lincoln, C.; Ambachew, B.; Rouillier, M.; Siegel, D.; Nosten, F.; Kyle, D. E.; Gamo, F. J.; Zhou, Y.; Llinas, M.; Fidock, D. A.; Wirth, D. F.; Burrows, J.; Campo, B.; Winzeler, E. A., Open-source discovery of chemical leads for next-generation chemoprotective antimalarials. Science 2018, 362 (6419). DOI: 10.1126/science.aat9446.

Ambroise-Thomas, P., The tragedy caused by fake antimalarial drugs. Mediterr J Hematol Infect Dis 2012, 4 (1), e2012027. DOI: 10.4084/mjhid.2012.027.

McClure, N. S.; Day, T., A theoretical examination of the relative importance of evolution management and drug development for managing resistance. Proc Biol Sci 2014, 281 (1797). DOI: 10.1098/rspb.2014.1861.

Yuthavong, Y.; Tarnchompoo, B.; Vilaivan, T.; Chitnumsub, P.; Kamchonwongpaisan, S.; Charman, S. A.; McLennan, D. N.; White, K. L.; Vivas, L.; Bongard, E.; Thongphanchang, C.; Taweechai, S.; Vanichtanankul, J.; Rattanajak, R.; Arwon, U.; Fantauzzi, P.; Yuvaniyama, J.; Charman, W. N.; Matthews, D., Malarial dihydrofolate reductase as a paradigm for drug development against a resistance-compromised target. Proceedings of the National Academy of Sciences of the United States of America 2012, 109 (42), 16823-16828. DOI: 10.1073/pnas.1204556109.

Schweitzer, B. I.; Dicker, A. P.; Bertino, J. R., Dihydrofolate reductase as a therapeutic target. Faseb j 1990, 4 (8), 2441-52.

Ittarat, I.; Asawamahasakda, W.; Meshnick, S. R., The effects of antimalarials on the Plasmodium falciparum dihydroorotate dehydrogenase. Exp Parasitol 1994, 79 (1), 50-6. DOI: 10.1006/expr.1994.1058.

Phillips, M. A.; Rathod, P. K., Plasmodium dihydroorotate dehydrogenase: a promising target for novel anti-malarial chemotherapy. Infectious disorders drug targets 2010, 10 (3), 226-239.

Abbat, S.; Jain, V.; Bharatam, P. V., Origins of the specificity of inhibitor P218 toward wild-type and mutant PfDHFR: a molecular dynamics analysis. J Biomol Struct Dyn 2015, 33 (9), 1913-28. DOI: 10.1080/07391102.2014.979231.

Phillips, M. A.; Lotharius, J.; Marsh, K.; White, J.; Dayan, A.; White, K. L.; Njoroge, J. W.; El Mazouni, F.; Lao, Y.; Kokkonda, S.; Tomchick, D. R.; Deng, X.; Laird, T.; Bhatia, S. N.; March, S.; Ng, C. L.; Fidock, D. A.; Wittlin, S.; Lafuente-Monasterio, M.; Benito, F. J.; Alonso, L. M.; Martinez, M. S.; Jimenez-Diaz, M. B.; Bazaga, S. F.; Angulo-Barturen, I.; Haselden, J. N.; Louttit, J.; Cui, Y.; Sridhar, A.; Zeeman, A. M.; Kocken, C.; Sauerwein, R.; Dechering, K.; Avery, V. M.; Duffy, S.; Delves, M.; Sinden, R.; Ruecker, A.; Wickham, K. S.; Rochford, R.; Gahagen, J.; Iyer, L.; Riccio, E.; Mirsalis, J.; Bathhurst, I.; Rueckle, T.; Ding, X.; Campo, B.; Leroy, D.; Rogers, M. J.; Rathod, P. K.; Burrows, J. N.; Charman, S. A., A long-duration dihydroorotate dehydrogenase inhibitor (DSM265) for prevention and treatment of malaria. Sci Transl Med 2015, 7 (296), 296ra111. DOI: 10.1126/scitranslmed.aaa6645.

Baragaña, B.; Forte, B.; Choi, R.; Nakazawa Hewitt, S.; Bueren-Calabuig, J. A.; Pisco, J. P.; Peet, C.; Dranow, D. M.; Robinson, D. A.; Jansen, C.; Norcross, N. R.; Vinayak, S.; Anderson, M.; Brooks, C. F.; Cooper, C. A.; Damerow, S.; Delves, M.; Dowers, K.; Duffy, J.; Edwards, T. E.; Hallyburton, I.; Horst, B. G.; Hulverson, M. A.; Ferguson, L.; Jiménez-Díaz, M. B.; Jumani, R. S.; Lorimer, D. D.; Love, M. S.; Maher, S.; Matthews, H.; McNamara, C. W.; Miller, P.; O'Neill, S.; Ojo, K. K.; Osuna-Cabello, M.; Pinto, E.; Post, J.; Riley, J.; Rottmann, M.; Sanz, L. M.; Scullion, P.; Sharma, A.; Shepherd, S. M.; Shishikura, Y.; Simeons, F. R. C.; Stebbins, E. E.; Stojanovski, L.; Straschil, U.; Tamaki, F. K.; Tamjar, J.; Torrie, L. S.; Vantaux, A.; Witkowski, B.; Wittlin, S.; Yogavel, M.; Zuccotto, F.; Angulo-Barturen, I.; Sinden, R.; Baum, J.; Gamo, F.-J.; Mäser, P.; Kyle, D. E.; Winzeler, E. A.; Myler, P. J.; Wyatt, P. G.; Floyd, D.; Matthews, D.; Sharma, A.; Striepen, B.; Huston, C. D.; Gray, D. W.; Fairlamb, A. H.; Pisliakov, A. V.; Walpole, C.; Read, K. D.; Van Voorhis, W. C.; Gilbert, I. H., Lysyl-tRNA synthetase as a drug target in malaria and cryptosporidiosis. Proceedings of the National Academy of Sciences 2019, 116 (14), 7015. DOI: 10.1073/pnas.1814685116.

Nyamai, D. W.; Tastan Bishop, O., Aminoacyl tRNA synthetases as malarial drug targets: a comparative bioinformatics study. Malar J 2019, 18 (1), 34. DOI: 10.1186/s12936-019-2665-6.

Herman, J. D.; Pepper, L. R.; Cortese, J. F.; Estiu, G.; Galinsky, K.; Zuzarte-Luis, V.; Derbyshire, E. R.; Ribacke, U.; Lukens, A. K.; Santos, S. A.; Patel, V.; Clish, C. B.; Sullivan, W. J.; Zhou, H.; Bopp, S. E.; Schimmel, P.; Lindquist, S.; Clardy, J.; Mota, M. M.; Keller, T. L.; Whitman, M.; Wiest, O.; Wirth, D. F.; Mazitschek, R., The cytoplasmic prolyl-tRNA synthetase of the malaria parasite is a dual-stage target of febrifugine and its analogs. Science Translational Medicine 2015, 7 (288), 288ra77. DOI: 10.1126/scitranslmed.aaa3575.

Nakama, T.; Nureki, O.; Yokoyama, S., Structural basis for the recognition of isoleucyl-adenylate and an antibiotic, mupirocin, by isoleucyl-tRNA synthetase. J Biol Chem 2001, 276 (50), 47387-93. DOI: 10.1074/jbc.M109089200.

McCarthy, M.; MacCulloch, D., Antibacterial activity of mupirocin (Bactroban). N Z Med J 1987, 100 (816), 26.

Koon, H. B.; Fingleton, B.; Lee, J. Y.; Geyer, J. T.; Cesarman, E.; Parise, R. A.; Egorin, M. J.; Dezube, B. J.; Aboulafia, D.; Krown, S. E., PHASE II AIDS MALIGNANCY CONSORTIUM TRIAL OF TOPICAL HALOFUGINONE IN AIDS-RELATED KAPOSI'S SARCOMA. Journal of acquired immune deficiency syndromes (1999) 2011, 56 (1), 64.

Bhatt, T. K.; Kapil, C.; Khan, S.; Jairajpuri, M. A.; Sharma, V.; Santoni, D.; Silvestrini, F.; Pizzi, E.; Sharma, A., A genomic glimpse of aminoacyl-tRNA synthetases in malaria parasite Plasmodium falciparum. BMC genomics 2009, 10, 644-644. DOI: 10.1186/1471-2164-10-644.

Vaughan, A. M.; Mikolajczak, S. A.; Wilson, E. M.; Grompe, M.; Kaushansky, A.; Camargo, N.; Bial, J.; Ploss, A.; Kappe, S. H. I., Complete Plasmodium falciparum liver-stage development in liver-chimeric mice. The Journal of clinical investigation 2012, 122 (10), 3618-3628. DOI: 10.1172/JCI62684.

Schneider-Poetsch, T.; Ju, J.; Eyler, D. E.; Dang, Y.; Bhat, S.; Merrick, W. C.; Green, R.; Shen, B.; Liu, J. O., Inhibition of eukaryotic translation elongation by cycloheximide and lactimidomycin. Nature chemical biology 2010, 6 (3), 209-217. DOI: 10.1038/nchembio.304.

Hoepfner, D.; McNamara, C. W.; Lim, C. S.; Studer, C.; Riedl, R.; Aust, T.; McCormack, S. L.; Plouffe, D. M.; Meister, S.; Schuierer, S.; Plikat, U.; Hartmann, N.; Staedtler, F.; Cotesta, S.; Schmitt, E. K.; Petersen, F.; Supek, F.; Glynne, R. J.; Tallarico, J. A.; Porter, J. A.; Fishman, M. C.; Bodenreider, C.; Diagana, T. T.; Movva, N. R.; Winzeler, E. A., Selective and specific inhibition of the plasmodium falciparum lysyl-tRNA synthetase by the fungal secondary metabolite cladosporin. Cell Host Microbe 2012, 11 (6), 654-63. DOI: 10.1016/j.chom.2012.04.015.

Almela, M. J.; Lozano, S.; Lelièvre, J.; Colmenarejo, G.; Coterón, J. M.; Rodrigues, J.; Gonzalez, C.; Herreros, E., A New Set of Chemical Starting Points with Plasmodium falciparum Transmission-Blocking Potential for Antimalarial Drug Discovery. PLOS ONE 2015, 10 (8), e0135139. DOI: 10.1371/journal.pone.0135139.

Lavazec, C.; Sanyal, S.; Templeton, T. J., Hypervariability within the Rifin, Stevor and Pfmc-2TM superfamilies in Plasmodium falciparum. Nucleic acids research 2006, 34 (22), 6696-6707. DOI: 10.1093/nar/gkl942.

Rao, S. T.; Rossmann, M. G., Comparison of super-secondary structures in proteins. J Mol Biol 1973, 76 (2), 241-56.

Vondenhoff, G. H. M.; Van Aerschot, A., Aminoacyl-tRNA synthetase inhibitors as potential antibiotics. European Journal of Medicinal Chemistry 2011, 46 (11), 5227-5236. DOI: https://doi.org/10.1016/j.ejmech.2011.08.049.

Caro, F.; Ahyong, V.; Betegon, M.; DeRisi, J. L., Genome-wide regulatory dynamics of translation in the Plasmodium falciparum asexual blood stages. eLife 2014, 3, e04106. DOI: 10.7554/eLife.04106.

Bopp, S. E.; Manary, M. J.; Bright, A. T.; Johnston, G. L.; Dharia, N. V.; Luna, F. L.; McCormack, S.; Plouffe, D.; McNamara, C. W.; Walker, J. R.; Fidock, D. A.; Denchi, E. L.; Winzeler, E. A., Mitotic evolution of Plasmodium falciparum shows a stable core genome but recombination in antigen families. PLoS Genet 2013, 9 (2), e1003293. DOI: 10.1371/journal.pgen.1003293.

Gardner, M. J.; Hall, N.; Fung, E.; White, O.; Berriman, M.; Hyman, R. W.; Carlton, J. M.; Pain, A.; Nelson, K. E.; Bowman, S.; Paulsen, I. T.; James, K.; Eisen, J. A.; Rutherford, K.; Salzberg, S. L.; Craig, A.; Kyes, S.; Chan, M. S.; Nene, V.; Shallom, S. J.; Suh, B.; Peterson, J.; Angiuoli, S.; Pertea, M.; Allen, J.; Selengut, J.; Haft, D.; Mather, M. W.; Vaidya, A. B.; Martin, D. M.; Fairlamb, A. H.; Fraunholz, M. J.; Roos, D. S.; Ralph, S. A.; McFadden, G. I.; Cummings, L. M.; Subramanian, G. M.; Mungall, C.; Venter, J. C.; Carucci, D. J.; Hoffman, S. L.; Newbold, C.; Davis, R. W.; Fraser, C. M.; Barrell, B., Genome sequence of the human malaria parasite Plasmodium falciparum. Nature 2002, 419 (6906), 498-511. DOI: 10.1038/nature01097.

Fukunaga, R.; Yokoyama, S., Structural basis for substrate recognition by the editing domain of isoleucyl-tRNA synthetase. J Mol Biol 2006, 359 (4), 901-12. DOI: 10.1016/j.jmb.2006.04.025.

Baell, J. B.; Holloway, G. A., New substructure filters for removal of pan assay interference compounds (PAINS) from screening libraries and for their exclusion in bioassays. J Med Chem 2010, 53 (7), 2719-40. DOI: 10.1021/jm901137j.

Bruns, R. F.; Watson, I. A., Rules for identifying potentially reactive or promiscuous compounds. J Med Chem 2012, 55 (22), 9763-72. DOI: 10.1021/jm301008n.

Manary, M. J.; Singhakul, S. S.; Flannery, E. L.; Bopp, S. E.; Corey, V. C.; Bright, A. T.; McNamara, C. W.; Walker, J. R.; Winzeler, E. A., Identification of pathogen genomic variants through an integrated pipeline. BMC Bioinformatics 2014, 15, 63. DOI: 10.1186/1471-2105-15-63.

Zhang, J. H.; Chung, T. D.; Oldenburg, K. R., A Simple Statistical Parameter for Use in Evaluation and Validation of High Throughput Screening Assays. J Biomol Screen 1999, 4 (2), 67-73. DOI: 10.1177/108705719900400206.

Shannon, P.; Markiel, A.; Ozier, O.; Baliga, N. S.; Wang, J. T.; Ramage, D.; Amin, N.; Schwikowski, B.; Ideker, T., Cytoscape: a software environment for integrated models of biomolecular interaction networks. Genome Res 2003, 13 (11), 2498-504. DOI: 10.1101/gr.1239303.

Iwata, S.; Lee, J. W.; Okada, K.; Lee, J. K.; Iwata, M.; Rasmussen, B.; Link, T. A.; Ramaswamy, S.; Jap, B. K., Complete structure of the 11-subunit bovine mitochondrial cytochrome bc1 complex. Science 1998, 281 (5373), 64-71.